**FOREIGN
BROADCAST
INFORMATION
SERVICE**

JPRS Report

Science &
Technology

China

DTIC QUALITY INSPECTED 3

19981203 142

10
125
A06

18 November 1987

NOTICE

Effective December 1987, JPRS will issue a new serial entitled SCIENCE &
TECHNOLOGY: FOREIGN DATA BASES. This new serial will be FOR OFFICIAL USE
ONLY.

This serial, with the trigraph FDB, will contain material from foreign data
bases currently published in SCIENCE & TECHNOLOGY: EUROPE/LATIN AMERICA and
in SCIENCE & TECHNOLOGY: JAPAN. These reports will continue to be published.

Subscribers who receive the SCIENCE & TECHNOLOGY: EUROPE/LATIN AMERICA and
the SCIENCE & TECHNOLOGY: JAPAN reports will automatically receive the new
SCIENCE & TECHNOLOGY: FOREIGN DATA BASES report.

If any subscription changes are desired, subscribers should notify their
distribution contact point.

SCIENCE & TECHNOLOGY

CHINA

CONTENTS

APPLIED SCIENCES

/7310

COMPUTER APPLICATION TO ARMED POLICE WORK

[Article by Li Guowei [2621 0948 1218] and Zheng Youming [6774 0645 2494] of the Central China Academy of Engineering: "Application of Microcomputers to Armed Police Combat Command"]

[Text] 1. Foreword

The Central China Academy of Engineering and the Hubei People's Armed Police Headquarters have used the mission and characteristics of armed police units as the basis for their joint research and development of an armed police combat command system for the purpose of increasing units' command effectiveness and quick reaction capabilities. This system is made up of microcomputer, display, communications and early warning equipment. A block diagram showing the system appears in Figure 1. Computers are able to control slide projectors, microfiche readers, and large screen projectors, and are able to retrieve and display all kinds of maps and textual materials. Slide projectors are used primarily to display detailed terrain maps; microfiche readers are used to display detailed maps of partial areas or targets; and large screen projectors are used to display combat command diagrams. The three are used in conjunction with each other as circumstances warrant and to help commanders make quick decisions.

This system can handle the situation at several trouble spots. During combat, the location of all trouble spots, the location of all mobile units, troop deployments and distances to trouble spots, and time needed to reach them are posted on a combat command map for direct observation. In addition, all movable targets are set up, shifted or erased from the screen in real time by the computer. Once fighting is over, a chart showing the course of the fighting may be readily printed out.

This system may be used for real time command during wartime. During peacetime, it may be used to analyze and study battles that have taken place, assisting staff in a vivid way to become familiar with cases, and for the conduct of training in previous battles.
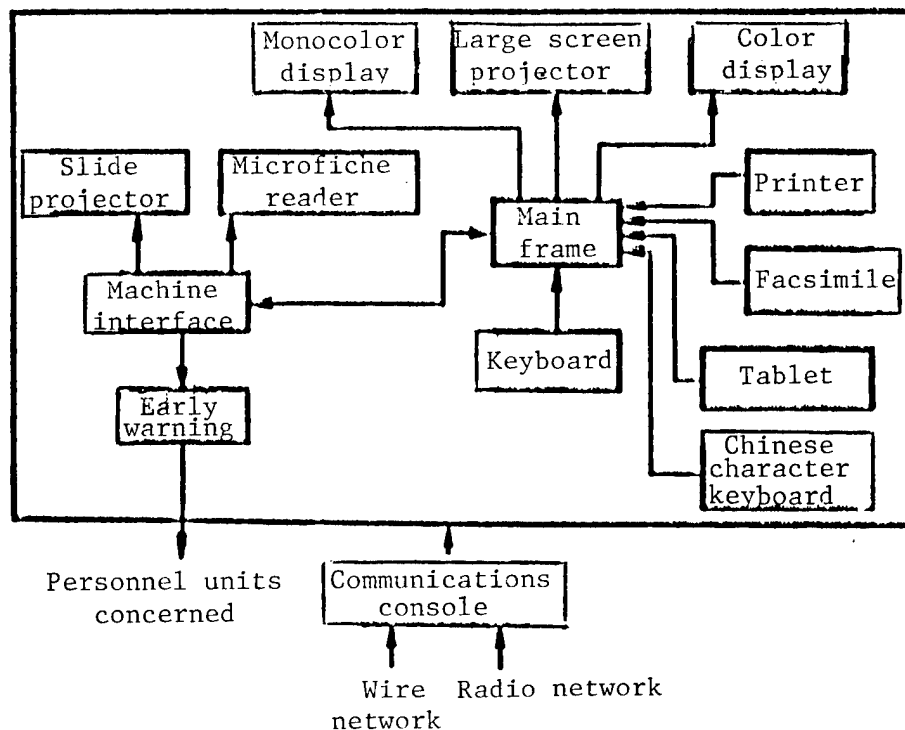
Figure 1.   Communications Block Diagram

This system may be divided into two major parts, namely the microcomputer control system and the communications control system. This article deals primarily with the former.

2.   System Hardware Configuration and Interfacing

The ZD-2600 microcomputer is the mainframe used by the system. It is connected to a facsimile machine, a tablet, and a Chinese character keyboard. All graphics and textual material may be readily inputted into the mainframe through these externals, and the keyboard may be used to control direct manual drawing. Graphics or text may be stored either in monochrome or in color, and it may be accessed at any time for revision, supplementation, or deletion. The mainframe is equipped with two display devices, the color display device possessing rather high resolution (600 x 800) and being able to display 32 different colors simultaneously. This is of extremely great importance in the drawing of clear combat command maps. The large screen projection device may be connected directly to the mainframe.

We developed interface equipment to enable the computer to control the slide projector and the selection of fiches for display on the microfiche reader. This interface makes possible the remote regulation of the focal length of the projector, control of the forward and backward movement of individual frames as well as the line-by-line movement of the microfiche reader, and fine adjustments to it.

3. System Program Design

The graphics handling function of the ZD-2600 microcomputer is fairly complete, and it comes equipped with various kinds of graphics software suited to customers' needs that makes for convenience in the fashioning of systems programs. FORTRAN is the primary language used for systems programming, but some programs are made with assembler languages. Figure 2 provides a work flow chart. The complete programming may be divided into four parts in terms of functions as follows: document scheduling, computing, accessing of software packages, and control. Each of these actions is explained briefly below.

```
        ┌─────────────────────────┐      ┌──────────────────┐
        │ Communications network  │◄─────│  Trouble report  │
        └─────────────────────────┘      └──────────────────┘
                    │
                    ▼
        ┌─────────────────────────┐
        │   Booting of equipment  │
        └─────────────────────────┘
                    │
                    ▼
        ┌─────────────────────────┐
        │      Early warning      │
        └─────────────────────────┘
                    │
                    ▼
      ┌───────────────────────────┐
      │ Slide directory first level│
      └───────────────────────────┘
                    │
                    ▼
      ┌────────────────────────────┐
      │ Slide directory second level│
      └────────────────────────────┘
                    │
                    ▼
    ┌──────────────────────────────┐
    │  Slide maps control, display │
    └──────────────────────────────┘
                    │
  ┌─────────────────┤
  │                 ▼
  │  ┌──────────────────────────────────┐
  │  │ Microfiche reader control, display│
  │  └──────────────────────────────────┘
  │                 │
  │                 ▼
  │  ┌──────────────────────────────────┐
  │  │   Display of command maps and    │
  │  │      relevant textual data       │
  │  └──────────────────────────────────┘
  │                 │                        ┌──────────────────┐
  │◄───────────────┤◄───────────────────────│ Decision by leader│
  │                 ▼                        └──────────────────┘
  │  ┌──────────────────────────────────┐
  │  │  Setting up, moving, and deleting │
  │  │          trouble spots            │
  │  └──────────────────────────────────┘
  │                 │
  │                 ▼
  │  ┌──────────────────────────────────┐
  │  │     Card control and display     │
  │  └──────────────────────────────────┘
  │                 │
  │                 ▼
  │  ┌──────────────────────────────────┐
  │  │  Setting up, moving, and deleting │
  │  │          combat units             │
  │  └──────────────────────────────────┘
  │                 │
  │◄───────────────┤
                    ▼
      ┌──────────────────────────────┐
      │  Print out of combat events  │
      └──────────────────────────────┘
                    │
                    ▼
                Conclusion
```
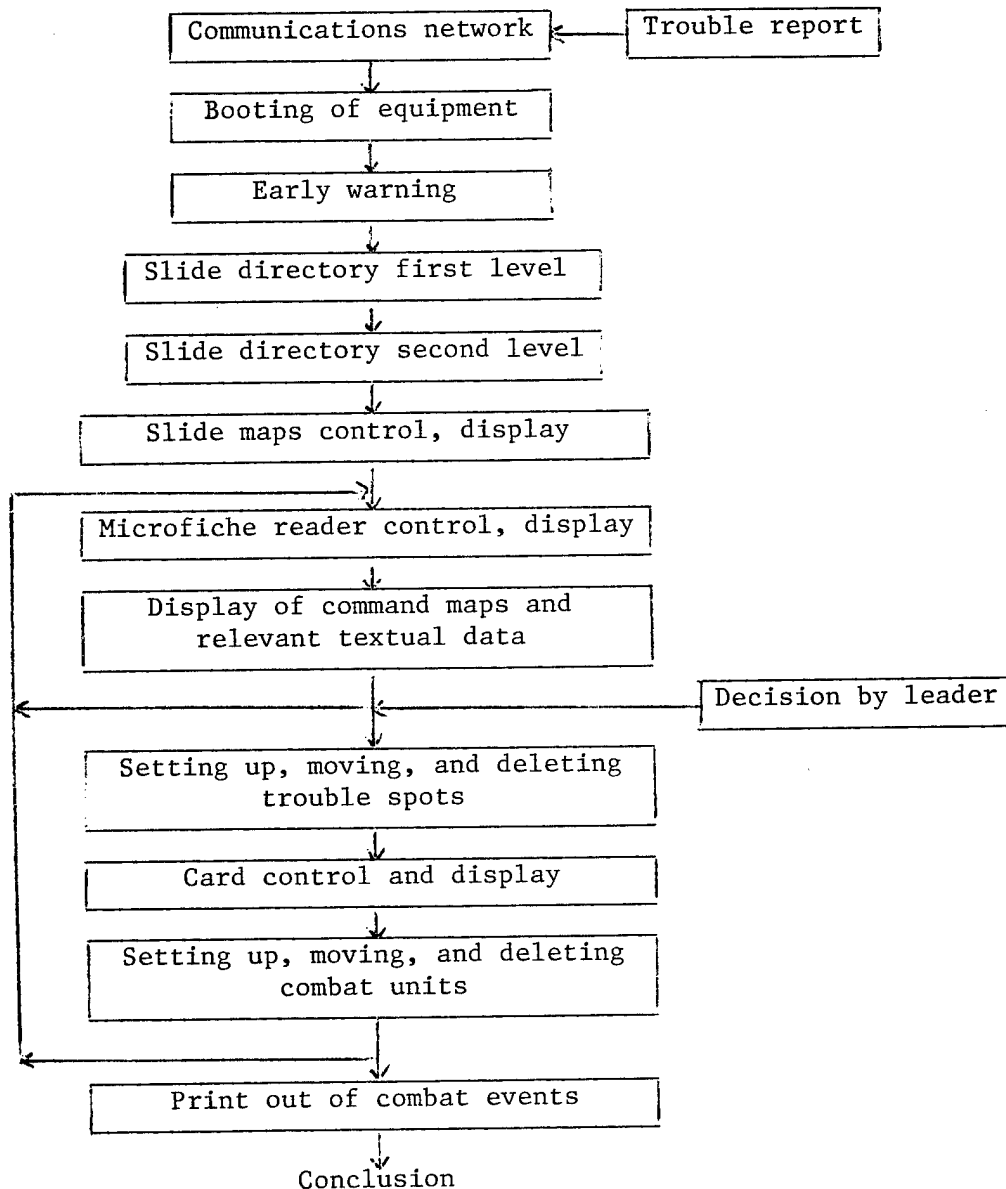
Figure 2.   System Work Flow Chart

3

a. Document Scheduling

As soon as a situation arises in the armed police combat command, the various maps and textual materials related to the site of the trouble or the scene of the crime are called up at once. Thus, once this system's early warning equipment provides personnel concerned with information about an incident that has taken place, the slide map retrieval program stage begins immediately. Retrieval employs a two level cataloging (Chinese character text) method that accesses relevant terrain maps by slide sequence number. Since each of the combat command maps in this system correspond to the detailed terrain maps, once the slides display the detailed terrain maps, the system automatically accesses the corresponding command maps and pertinent textual data. Depending on the circumstances, retrieval and display of maps and data stored in the microfiche projector is done only as needed. Though the projector contains 1,000 fiches, thanks to the two level catalogue retrieval, it is extremely easy to call up any single fiche. For convenience in operation, whenever an operator inputs data, a Chinese language prompt appears on the color monitor. All of the aforestated combat command maps, retrieval menus, and operating prompts are stored and controlled in textual form.

b. Computing

The computing part of the program is used mostly for changing coordinates. Display on the screen of our own and the enemy's deployments, and all changes in movable targets (including trouble spots, mobile forces, and the erection of obstacles) requires real time setting up, changes, or deletions by operators. We know that the base coordinates and scale of maps are not completely identical. When the geographic coordinates of a movable target are known, they have to be converted into screen coordinates in order to be displayed at the appropriate position. When the geographic coordinates of a target cannot be precisely determined, and only the general location is known, the target may be set up at an arbitrary position on the screen and later moved (in eight directions) to the necessary location. Once target location has been determined, the computer will convert the screen coordinates to actual geographic coordinates and display them on the monocolor monitor for the operator. Additionally, the distances involved and times that have been noted on the command map have to be first converted from the screen coordinates to actual coordinates before the computation of actual data.

Since there is need for changes and revisions to command maps during use, coordinate conversion parameters should not be directly built into the program, but rather should be stored in a designated part of data storage. When command maps are being revised, the DDT debugging program is used to place the system program into memory and to change the parameters of the proper storage location. Then it can be written to a disc.

c. Use of the Graphics Software Package

It was mentioned earlier than the ZD-2600 is equipped with various software packages, and that this system uses FORTRAN to work with them. Examples

include setting up, changing, and deleting movable target patterns; changes in screen displays of the English alphabet and numbers; and the accessing of storage disc documents and the temporary full color compressed storage disc for command maps.

d. Control

Selection of slides and fiches by the slide projector and the microfiche projector is controlled by a program. Changing projector slides is done by pulse triggering. A reply system together with a software time delay system is used to detect pulses sent back by the slide projector in order to effect coordination with the hardware so as to avoid sudden projector stoppages and interruption of the main program. Selection of fiches by the microfiche reader employs two methods. One is the direct inputting from the keyboard of the fiche number, which the program converts to the appropriate code and sends to the interface circuit, and driving of the microfiche reader. The second is a step-by-step method whereby a single tape on the proper key causes the microfiche to move a single frame forward or backward.

Research and development of this system was a one-time effort. It was done with the needs of real combat in mind, and quite a few problems remain that require further solution and improvement. The system's microcomputer control portion has already been entered in a national exhibition of computer application achievements.

We believe that with slight modifications, this system may also be used by aviation, navigation, railroad and communications units.

Support and assistance during the process of research and development of this system was received from leaders concerned in the People's Army Police Headquarters, the Hubei People's Armed Police Headquarters, and the Central China Academy of Engineering. Other participants in this work were Comrades Li Cunyan [2621 1317 1750] and Ding Jing [0002 7234] of the Hubei People's Armed Police Headquarters.

9432/6091

THEORETICAL STUDY OF COLLIDING PULSE MODE-LOCKING IN DYE LASERS

[Article by Chen Jutao [7115 6830 3447], Liu Yupu [0491 3768 3877], and Wang Zhijiang [3769 0037 3068] of the Shanghai Institute of Optics and Fine Mechanics, Chinese Academy of Sciences; received 16 Dec 1985]

[Text] Abstract: This paper provides a new theory of colliding pulse mode-locking of dye lasers which has a clear physical image and is able to better explain the properties of mode-locked pulses, particularly in the area of frequency.

I. Introduction

Colliding pulse mode-locking lasers are an important means of producing ultra-short pulses on which there have been many articles containing refined experiments and theoretical research.(1-4) However, these theoretical analyses have mostly been constructed on the foundations of speed-frequency equation approximations, believing that ultrashort pulses are formed by the absorption effects of the saturated absorber and the gain medium on the clipped wave of the front and back edges of the pulse and on the pulse DODCI colliding mode-locking, the interaction between the light field and the medium is a coherence effect and to use speed-frequency equation approximations to describe it cannot satisfy anyone. In fact, even the speed-frequency equation approximations require the

introduction of a phenomenological filter $F(\omega)=\left[1+i\left(\dfrac{\omega-\omega_0}{\Delta\omega/2}\right)\right]^{-1}$ to represent

the total result of the coherence effects.(4) Recently, some have attempted to use (Buluohe) [1580 3157 6378] equations with a two energy level system to describe the interaction of light and the medium so as to compute the mode-locking properties. However, neither the theory nor the results have been convincing. We closely considered the details of the interaction between the mode-locking process and the medium and, using self consistent field methods, computed the properties of colliding pulse mode-locking. The predicted results tallied with experiments.
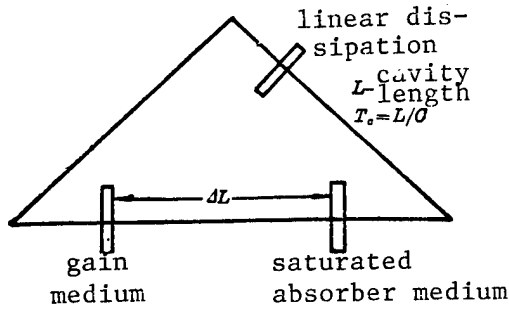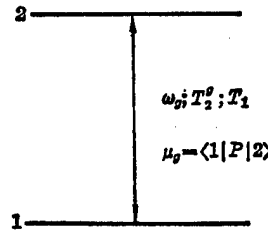
II. Basic Equations

Fig. 1. Colliding Pulse Mode-Locking Laser

Fig. 2. Gain Medium Energy Levels
T_2, T_1 are the horizontal and vertical
relaxation intervals; ω_g = 3.208 X $10^{15}s^{-1}$
corresponding to a wavelength λ_g = 588nm

A colliding pulse mode-locking laser is as shown in Figure 1. The gain medium is supposed to be a two energy level system, like that of Figure 2. The central frequency is ω_g; the polarization constant μ_g = <1|ρ|2>; T_2^g is the phase resolving interval. Its interaction with light is described by the density array equation:(5)

$$\begin{cases} \dot{n} = \dfrac{i\mu_g}{\hbar}(E_0\sigma_{21}^* - E_0^*\sigma_{21}) \\ \dot{\sigma}_{21} = i(\omega - \omega_g)\sigma_{21} - \sigma_{21}/T_2^g \\ \qquad - \dfrac{i\mu_g}{2\hbar}E_0 n \end{cases} \tag{1}$$

E_0 is the slowly changing amplitude of the light field $\quad E = \dfrac{E_0}{2}(e^{i(kz-\omega t)} + c \cdot c)\quad$,

n = $\rho_{22} - \rho_{11}$ is the population inversion; σ_{21} is the slowly changing amplitude of the density array with respect to the angle element. From Maxwell's equations the light field equations give:

$$\frac{\partial \epsilon}{\partial z} - \frac{n}{c}\frac{\partial \epsilon}{\partial t} = -K_g\sigma_{21} \tag{2}$$

in which $\epsilon = \dfrac{\mu_g}{\hbar}E_0$; $K_g = \dfrac{\omega N_g\mu_g^2}{2c\epsilon\hbar}$, N_g is the gain medium concentration (populations per unit volume).

7

Because the mode-locking pulse is far smaller than the population damping interval, T_1, the longitudinal relaxation drops out of the equation and serves as a factor influencing the initial conditions. The dynamic initial population inversions each time a pulse reaches the gain medium are:

$$n_i = n_0 + (n_f - n_0)\exp\left(-\frac{\Delta t}{T_1}\right) \qquad (3)$$

$\Delta t = 2\Delta L/c$ or $(L-2\Delta L)/c$ is the interval from the previous pulse passing through to this pulse arriving; n_f is residual population inversions after the previous pulse passed through; n_0 represents the pumping strength; this is the steady state value of the population inversion caused by the pumping source when laser oscillation is not happening.

Since the interaction between the absorber and the light is coherent, for conditions when the light is strong enough, within the interval $\Delta t \sim T_2^a$ to make the absorption interaction able to transport ground level particles to the highest level, (i.e. satisfy the condition that

$$\frac{\frac{1}{2}E_{max}\mu_0}{\hbar}T_{min} \gtrsim \pi,$$

$$T_{min} = \text{minimum}(\Delta T, T_2^a),$$

where ΔT is the pulse width and E_{max} is the maximum value of the light field), then during the interaction period, the saturated absorber not only absorbs light, it also radiates light. In this way, the saturated absorber is not only an absorber but is also a laser medium. The locking mechanism is this: the gain medium amplifies the pulse leading edge and due to gain saturation it has a smaller effect on the pulse trailing edge. The saturated absorber thus absorbs light at the pulse's leading edge but emits light at its trailing edge so that the absorption-emission process of the absorber and the amplification-saturation process of the gain medium form pulse mode-locking and maintain stable operation. The absorption-emission process of the absorber also determines that the mode-locking light wave length is red-shifted from the gain center, λ_g, to the vicinity of the absorber emission wave length, λ_e and the collision process then accelerates the development of the absorption-emission process. Consequently, narrower pulses can be obtained. (It can be shown that for a thin sample approximation, if the two light fields of the collisions are identical, the effect of collisions is equivalent to converting the E_0 of the medium to $\sqrt{2}E_0$.) Under mode-locking conditions, the processes of absorption-emission, amplification-saturation, and linear dissipation are complementary and balanced. At the same time, the self consistent field equations of the mode-locking system have a stable, periodic solution; i.e. the pulse. When the gain medium is sufficiently concentrated and the pumping is large enough, the operating state can change to non-mode-locking and the cavity's light field becomes quasi-continuous. The action of the saturated absorber and the light field is no longer coherent. This way, the absorber only serves for common absorption dissipation and is not a laser medium.

8

The characteristics of the laser also will suddenly change ($\lambda \sim \lambda_e = 615$nm changes to $\lambda \sim \lambda_g = 588$nm and $\Delta T \sim T_2$ goes to $\Delta T \sim \infty$.) At the same time, for the self consistent field equations, there exists a stable steady state solution.

Using simplified density array equations to describe the interaction of the saturated absorber and the light, and introducing a relaxation term:

$$
\begin{cases}
\dot{\rho}_a = -i\omega_a\rho_a - \rho_a/T_2^a - \dfrac{i\mu_a}{\hbar} E(\rho_{22} - \rho_{11}) \\[2mm]
\dot{\rho}_e = -i\omega_e\rho_e - \rho_e/T_2^e - \dfrac{i\mu_e}{\hbar} E(\rho_{44} - \rho_{33}) \\[2mm]
\dot{\rho}_{11} = -\dfrac{i\mu_a}{\hbar}(\rho_a^* E - \rho_a E^*) + \rho_{33}/\tau_1' \\[2mm]
\dot{\rho}_2 = \dfrac{i\mu_a}{\hbar}(\rho_a^* E - \rho_a E^*) - \rho_{22}/\tau_1 \\[2mm]
\dot{\rho}_{33} = -\dfrac{i\mu_e}{\hbar}(\rho_e^* E - \rho_e E^*) - \rho_{33}/\tau_1' \\[2mm]
\dot{\rho}_{44} = \dfrac{i\mu_e}{\hbar}(\rho_e^* E - \rho_e E^*) + \rho_{22}/\tau_1
\end{cases}
\tag{4}
$$

in which, $\rho_a = \langle 2|\Psi|1\rangle$; $\rho_e = \langle 4|\Psi|3\rangle$; and r_{11}, ρ_{22}, ρ_{33}, and ρ_{44} are the number of particles occupying each energy level. Note that in the absorber, two oppositely propagating pulses produce a collision and the expansion of each quantity into a Fourier series gives:

$$
\begin{cases}
E = \dfrac{1}{2}(E + e^{i(kz-\omega t)} + E - e^{i(-kz-\omega t)} + c \cdot c) \\[2mm]
\rho_\nu = \left(\displaystyle\sum_{p=0}^{\infty} \sigma_p^{\nu+} e^{2ipkz}\right)e^{i(kz-\omega t)} \\[2mm]
\qquad + \left(\displaystyle\sum_{p=0}^{\infty} \sigma_p^{\nu-} e^{-2ipkz}\right)e^{i(-kz-\omega t)} \\[2mm]
\rho_{jj} = n_0^j + \displaystyle\sum_{p=1}^{\infty}(n_p^j e^{2ipkz} + n_p^{j*} e^{-2ipkz}) \\[2mm]
\nu = a, e; \quad j = 1, 2, 3, 4.
\end{cases}
\tag{5}
$$

After substituting (5) into formula (4) and simplifying, we can get a system of infinite dimension differential equations like below, which when computing are truncated at $p = 0, 1$. That is, only considering the average population inversion and the population transient grating, this represents E_+ and E_- through direct coupling and direct mutual coupling of the population.

9

$$
\begin{cases}
\dot{n}_0^3 = -\frac{i\mu_e}{2\hbar}(E_+\sigma_0^{e+*} + E_-\sigma_0^{e-*} \\
\qquad - E_+^*\sigma_0^{e+} - E_-^*\sigma_0^{e-}) - n_0^3/\tau_1' \\[2mm]
\dot{n}_0^4 = \frac{i\mu_e}{2\hbar}(E_+\sigma_0^{e+*} + E_-\sigma_0^{e-*} \\
\qquad - E_+^*\sigma_0^{e+} - E_-^*\sigma_0^{e-}) + n_0^2/\tau_1 \\[2mm]
\dot{n}_p^1 = -\frac{i\mu_a}{2\hbar}(E_+\sigma_{p-1}^{a-} + E_-\sigma_p^{a-*} \\
\qquad - E_+^*\sigma_p^{a+} - E_-^*\sigma_{p-1}^{a+}) + n_p^3/\tau_1'; \quad p \neq 0 \\[2mm]
\dot{n}_p^2 = \frac{i\mu_a}{2\hbar}(E_+\sigma_{p-1}^{a-*} + E_-\sigma_p^{a-*} \\
\qquad - E_+^*\sigma_p^{a+} - E_-^*\sigma_{p-1}^{a+}) - n_p^2/\tau_1; \quad p \neq 0 \\[2mm]
\dot{n}_p^3 = -\frac{i\mu_e}{2\hbar}(E_+\sigma_{p-1}^{e-*} + E_-\sigma_p^{e-*} \\
\qquad - E_+^*\sigma_p^{e+} - E_-^*\sigma_{p-1}^{e+}) - n_p^3/\tau_1'; \quad p \neq 0 \\[2mm]
\dot{n}_p^4 = \frac{i\mu_e}{2\hbar}(E_+\sigma_{p-1}^{e-*} + E_-\sigma_p^{e-*} \\
\qquad - E_+^*\sigma_p^{e+} - E_-^*\sigma_{p-1}^{e+}) + n_p^2/\tau_1; \quad p \neq 0 \\[2mm]
p = 0, 1, 2, \cdots, \infty
\end{cases}
\qquad
\begin{cases}
\dot{\sigma}_p^{a+} = -i(\omega_a - \omega)\sigma_p^{a+} - \sigma_p^{a+}/T_2^a \\
\qquad -\frac{i\mu_a}{2\hbar}((n_p^2 - n_p^1)E_+ + (n_{p+1}^2 - n_{p+1}^1)E_-) \\[2mm]
\dot{\sigma}_p^{a-} = -i(\omega_a - \omega)\sigma_p^{a-} - \sigma_p^{a-}/T_2^a \\
\qquad -\frac{i\mu_a}{2\hbar}(n_p^{2*} - n_p^{1*})E_- + (n_{p+1}^{2*} - n_{p+1}^{1*})E_+) \\[2mm]
\dot{\sigma}_p^{e+} = -i(\omega_e - \omega)\sigma_p^{e+} - \sigma_{p+}^e/T_2^e \\
\qquad -\frac{i\mu_e}{2\hbar}((n_p^4 - h_p^3)E_+ + (n_{p+1}^4 - n_{p+1}^3)E_-) \\[2mm]
\dot{\sigma}_p^{e-} = -i(\omega_e - \omega)\sigma_p^{e-} - \sigma_p^{e-}/T_2^e \\
\qquad -\frac{i\mu_e}{2\hbar}((n_p^{4*} - n_p^{3*})E_- + (n_{p+1}^{4*} - n_{p+1}^{3*})E_+) \\[2mm]
\dot{n}_0^1 = -\frac{i\mu_a}{2\hbar}(E_+\sigma_0^{a+*} + E_-\sigma_0^{a-*} \\
\qquad - E_+^*\sigma_0^{a+} - E_-^*\sigma_0^{a-}) + n_0^3/\tau_1' \\[2mm]
\dot{n}_0^2 = \frac{i\mu_a}{2\hbar}(E_+\sigma_0^{a+*} + E_-\sigma_0^{a-*} \\
\qquad - E_+^*\sigma_0^{a+} - E_-^*\sigma_0^{a-}) - n_0^2/\tau_1
\end{cases}
$$

$$\tag{6}$$

The light field equation, simplified by Maxwell's equations gives:

$$
\frac{\partial \epsilon_\pm}{\partial z} \mp \frac{n}{c}\frac{\partial \epsilon_\pm}{\partial t} = -\beta_a K_a \sigma_0^{a\pm} - \beta_e K_e \sigma_0^{e\pm}
\tag{7}
$$

in which,

$$
\epsilon_\pm = \frac{\mu_a}{\hbar}E_\pm; \quad K_a = \frac{\omega N_a \mu_a^2}{2c\varepsilon\hbar}; \quad K_e = \frac{\omega N_a \mu_a \mu_e}{2c\varepsilon\hbar} = \left(\frac{\mu_e}{\mu_a}\right)K_a; \quad \beta_a = \frac{n_0^1 + n_0^2}{n_0^1 + n_0^2 + n_0^3 + n_0^4}; \quad \beta_e = 1 - \beta_{a0}
$$

Here, β_a represents the ratio of population at a two energy level subsystem to the entire population and N_a is the saturated absorber concentration (population per unit volume).

III. Computation Results

We used the model described by the parameters below and the self consistent field method to analyze the characteristics of colliding pulse mode-locking.

$$
\alpha_a = K_a l_a; \quad \alpha_g = K_g l_g
$$

in which l_a and l_g are the thicknesses of the two media. α_a and α_g are small signal absorption and gain.

$$
m = \frac{\mu_a}{\mu_g}\sqrt{\frac{S_g}{S_a}}; \quad R = \frac{\mu_e}{\mu_a},
$$

10

in which S_a, and S_g are the spot areas on the two media. γ is the linear dissipation.

$$\mathscr{E} = \int_{-\infty}^{\infty} \left(\frac{\mu_g}{\hbar} E_+ \right)^2 dt$$

is the pulse energy.

(1) Effect of the parameters on the characteristics of colliding pulse mode-locking
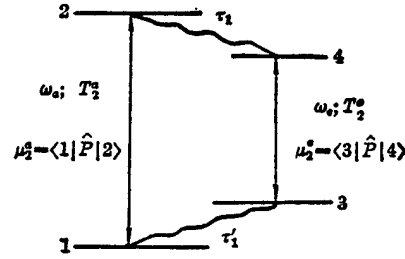

Fig. 3. Saturated Absorber Energy Level Diagram

T_2^a, T_2^g are the respective transverse relaxation times; $\omega_a = 3.250 \times 10^{15} s^{-1}$ ($\lambda_a = 580nm$); $\omega_e = 3.065 \times 10^{15} s^{-1}$ ($\lambda_e = 615nm$); τ_1, τ_1 are the fast relaxation times

Figure 4 and Figure 5 show the effect of the small signal absorption, α_a. With increasing α_a, the central wavelength of the mode-locking pulse is red-shifted with the stable zone ranging from 959 to 624nm, close to the experimental results of 600 to 630nm.(7) This phenomenon can be explained thusly: As the small signal absorption gets larger, the shortwave absorption, which takes $\lambda_a = 580nm$, increases. Then the population inversion formed by the absorbed light quickly relax to a 3-4 subsystem (see Figure 3), making the population inversion increase so the emitted light with central wavelength of $\lambda_e = 615nm$, correspondingly increases, shortwave absorption increases, and longwave emission increases sufficiently to red-shift the mode-locking pulse wave length. From the figure we can also see that in the curve there is one minimum in which vicinity the pulse width and the autocorrelation width are not sensitive with respect to small signal absorption.
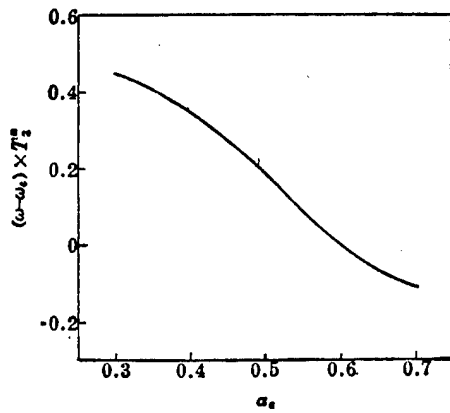
Fig. 4. Variation of Frequency with α_a

parameters:

$T_2^a = 4.44 \times 10^{-15}$s; $m = 4.5$; $B = 0.8$;
$\tau_1 = \tau_1' = 0.08 T_2^a$; $T_2^g = 1.1 T_2^a$; $\alpha_g = 0.9$;
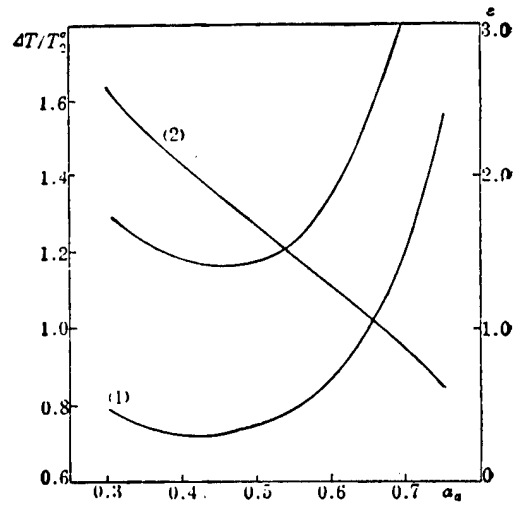$T_2^g = 1.0 T_2^a$; $\hat{T}_1 = 0.8 T_c$; $n_0 = 0.95$; $\gamma = 0.1$, $\Delta L/L = 0.25$

Fig. 5. Variation of Pulse(1) and energy(2) with α_a

(parameters are the same as for Fig. 4; the additional curve is the autocorrelation width)

Figures 6 and 7 indicate the influence of pumping on mode-locking characteristics. Within the stable zone, as pumping strength increases, the mode-locking pulse energy gets larger, and the pulse width narrows, the frequency changes all first red-shift then tend to shift to shortwaves. Generally, as the pumping strength intensifies, the laser will tend toward the gain center, λ_g = 588nm, i.e. shift toward shortwaves. But, on the other hand, pumping strength increase will lead to pulse energy increase, causing the absorber to increase absorption and the emission of light near wavelength λ_e = 615nm with which it is related increases correspondingly. This is the red-shift factor.

Fig. 6. Variation of Frequency with n_0
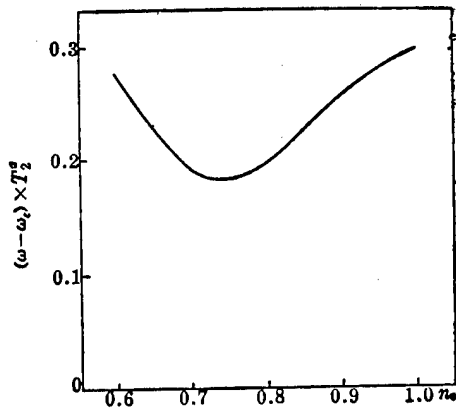
parameters:

$T_2^a = 4.44 \times 10^{-15}$s; $m = 3.5$; $B = 0.8$;
$\alpha_a = 0.45$; $\tau_1 = \tau_1' = 0.08 T_2^a$;
$T_2^g = 1.1 T_2^a$; $\alpha_g = 0.9$; $T_2^g = 1.0 T_2^a$;
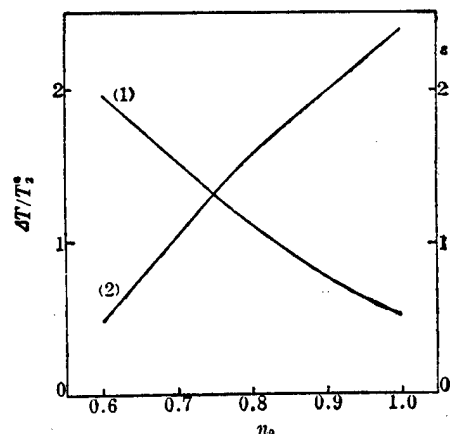$T_1 = 0.8 T_c$; $\gamma = 0.1$; $\Delta L/L = 0.25$

Fig. 7. Variation of Pulse width(1) and energy (2) with n_0

(parameters identical to Fig. 6)

(2) Chirp and wave form

Computational results show that the transient frequency of the pulse is not purely negative chirp but rather that the leading and trailing edge of the pulse has a rather large positive chirp and the pulse centers have a smaller negative chirp. This can be written approximately as $\omega(t) = \omega_0 - \alpha t + \beta t^2 +$

γt^3. Figure 8 is the change of $\frac{d\omega}{dt}\Big|_{I_{max}}$ at the pulse intensity maximum when

saturated absorber small signal absorption increases. It approximates the small chirp of the central portion of the pulse. Figure 9 is a typical wave-form and transient frequency near the central part of the stability zone. It is evident that about 70 percent of the total energy of the central part of the pulse is negative chirp and that within a half width the frequency sweep is about 3.2nm, which is roughly the same as the experimental result of 1nm.(8) The negative chirp of the pulse is the result of the combined effects of the saturated absorber and the gain medium. The saturated absorber must absorb shortwave components at the front part of the pulse while at the rear part emitting longwave components. Due to the relationship of the saturation effect, the stimulated emission of the gain medium at the front part of the pulse is always more than at the rear portion. This requires that, under most conditions, the steady state pulse has negative chirp.
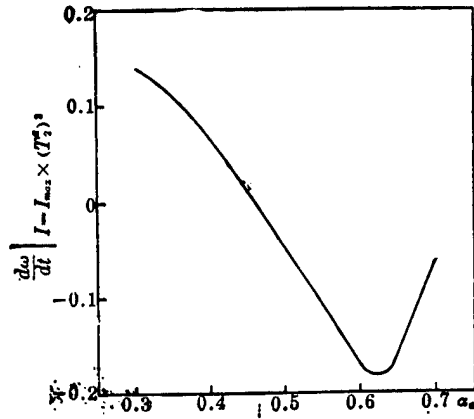
13

Fig. 8. Saturated Absorber Concentration Increase Causing Negative Chirp Increase
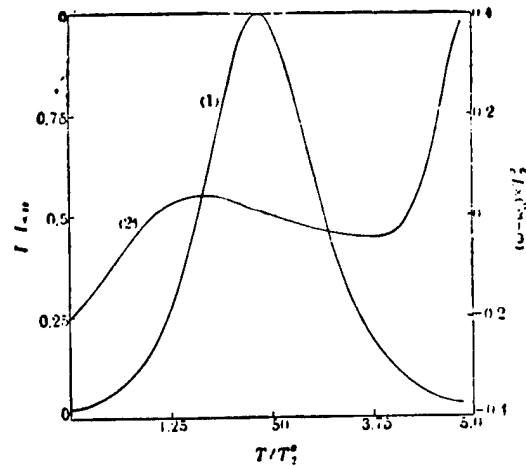
(parameters same as Fig. 4)

Fig. 9. Typical Pulse Waveform(1) and Transient Frequency(2)

Except for $\alpha_a = 0.55$, parameters are the same as Fig. 4

Using Gaussian and hyperbolic secant wave forms to approximate computational results, it was discovered that under conditions where the pulse was narrower ($\Delta T < 0.8T_2^a$), the hyperbolic secant waveform fit rather well, while for wider conditions ($\Delta T > 1.2T_2^a$), the Gaussian waveform fit better, and the waveform of the middle range width pulse came at the transition from the hyperbolic secant to the Gaussian wave form.

We wish to express our appreciation to Zhang Yinghua [1728 1758 5478] and Zhang Guoxuan [1728 0948 6513], for beneficial discussions and to Qian Jiajun [6929 1367 6874] and Shen Huijuan [3088 1979 1227] for providing computer assistance.

REFERENCES

1. R.L. Fork, et al., IEEE J. Quant. Electr., 1983, QE-19, No 4, 500.

2. D. Kuhlke, et al., IEEE J. Quant. Electr., 1983, QE-19, No 4, 526.

3. Masayuki, et al., IEEE J. Quant. Electr., 1984, QE-20, No 7, 197.

4. D. Kuhlke, et al., Opt. and Quant. Electr., 1985, 16, No 1, 57.

5. A. Yariv, Quant. Electr. (New York/London/Sydney/Toronto: John Wiley & Sons, 1967), p 152.

6. Paul Mandel, Opt. Commun. 1984, 51, No 2, 87.

7. J.-C. Diels, et al., ZHONGGUO JIGUANG [CHINESE JOURNAL OF LASERS], in Chinese, 1983, 10, No 8-9, 582.

8. W. Dietel, et al., Opt. Commun. 1982, 43, No 10, 433.

12966/7358

PULSED MAGNET FIELDS FOR FREE-ELECTRON LASERS

[Article by Shi Jiabiao [2457 0857 2871], Pan Yinnian [3382 1714 1628], and
Wang Wei [3769 0251] of the Strong Magnetic Field Research Group, Plasma
Physics Research Institute, Chinese Academy of Sciences; received 24 Jan 1986]

[Text] Abstract: This paper presents developments of and experiments with
pulsed FEL magnets. The magnet can provide a 0-20kG magnetic field with a
very long lifetime. Experiments have shown that its field uniformity is
0.011 percent in an area of diameter 14 mm along the z axis from +400 to
-400mm (center point is zero).

I. Introduction

Free-electron lasers at present face the very important problem of how to in-
crease energy conversion efficiency. Although theoretical predictions of their
energy conversion efficiency reach as high as 50 percent, experiments have only
been able to attain efficiencies nearly one magnitude lower. For this reason
current researchers have been doing work largely around this goal. Besides
selecting suitable Wiggler structure parameters, adding another appropriate
uniform magnetic field under the space periodic magnetic field can also in-
crease the laser gain. This is due to the uniform magnetic field being able
to induce rotational resonance.(1)

II. Magnetic Body Structure

According to the requirements of a FEL total body, the inner diameter is 149mm
and the length is 1120mm. Figure 1 shows a transverse profile of the magnetic
body. This magnetic body is formed by QXY/QZY 1.6 X 9, enameled flat copper
wound wire in four layers of 122 turns each. We used a large cross section
flat wire mainly in consideration of ensuring a relatively small resistance
for a fixed inductance to facilitate the magnetic body having good thermal
stability operating at laboratory temperature. In order to reduce effects on
the uniformity of the magnetic body from technical defects in the element con-
ductors or electromotive force displacement during discharge, we used an
appropriate number of turns and added a belt of heat-holding solid epoxied
crushed mica between each layer. Due to the small number of layers, the

potential between layers is rather high. So to prevent arcing between layers, in addition to the 594 mica, a strong insulator is required and the space between turns was filled with a special kind of high powered glued polyimide film. The transition helical angle crevice at the two ends of the magnetic body is another factor which effects the mechanical stability of the magnetic body. This problem can be resolved by the method of using suitable epoxy polyester fiber material during the wrapping affixed after preparation and heating.
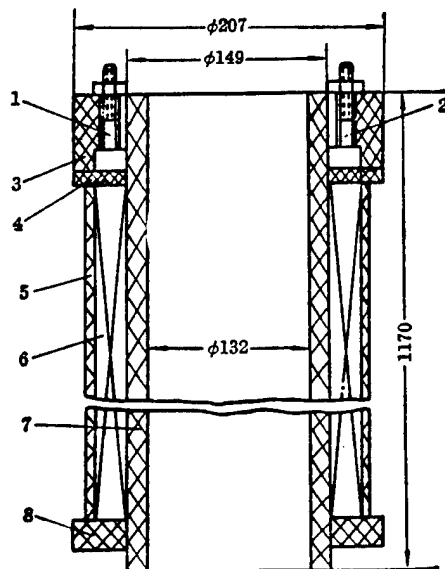
Fig. 1. Transverse Profile of the Magnetic Body

1 - inner lead column; 2 - outer lead column;
3 - back and plate; 4 - clamp plate; 5 - winding insulator; 6 - winding; 7 - liner cylinder;
8 - front end plate

The mechanical performance of the magnetic body's ejection section is the key part of the magnetic body structure. The failure of many magnetic bodies frequently begins from the processing of the ejection section being improper. Any movement in the pulse period of the ejection section, if slight effects the configuration of the magnetic field of the two ends, and if heavy will influence the experimental lifetime of the magnetic body.

The winding of the magnetic body is carried out under a fixed, calculated stress. The arrangement of the insulator material and the element conductors is very fine such that the structure tightly matches the design optimized space plan. In the processing of the body insulator, besides the consideration of being able to withstand the pulse voltage, we used high-strength glass silk ribbon for reinforcement.(2)

The fundamental parameters of the magnetic body were as follows:

magnetic body inner diameter: 149
magnetic body outer diameter: 167.6
magnetic body length: 1120
packing factor: 0.75
number of turns: 122 x 4
wire gauge: 1.6 X 9 QXY/QZY
resistance: 0.29 ohms
inductance: 4.36mh
uniformity: within 14mm $\varepsilon_{max} < 0.011\%$

　　　　　in $-400~400$mm $\varepsilon_{max} < 4.4\%$
maximum magnetic field: 2Toe, continuously adjustable pulse sustaining time: 29ms (when C = 19.2mF)

III. Magnetic Body Experiments

The schematic of the FEL pulse magnetic body was as below.
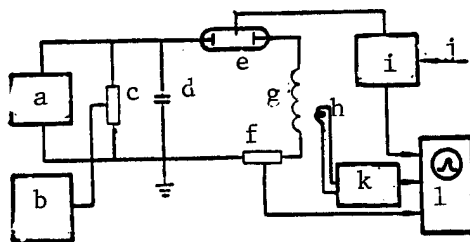
Fig. 2. Free-Electron Laser Pulse Magnetic Body Experiment Schematic

a – constant current charging apparatus; b – PZ-8 digital voltmeter;
c – voltage divider; d – capacitor network; e – ignitron;
f – current divider; g – magnetic body; h – magnetic probe;
i – pulse generator; j – trigger button; k – RC integrator;
l – memory oscilloscope

The total capacitance of the capacitor network used in the experiment was 19.2mF equivalent to the maximum magnetic field voltage being 3640V, and, when the magnetic field was maximum, corresponding to a storage energy of 4.22×10^4 in the magnetic body. By appropriate selection of the electromagnetic parameters of the main return circuit

$$\left[2\sqrt{\frac{C}{L}} \gg r \right]$$

we can make the main current in the return circuit and the magnetic field wave form display a sine wave shape. The major point of this entire technical conception is that we can use a pulsed field to replace a steady state field thereby greatly simplifying the equipment, shortening the manufacturing period, and saving a large amount of money.

The experimental return circuit current was measured by an inductionless current divider with its resistance standardized to 15 X 10^{-6} ohms. The precision was 1 percent. The magnetic field peak value was obtained by a magnetic probe. This probe was an accessory to the strong magnetic field meter manufactured by the Harbin Electrical Instrument Institute. Its precision was 1 percent and its Ns value was 500cm2. The magnetic field signal through an integrator was input to a memory oscilloscope (7623A) and photographed. The discharge voltage of the high voltage capacitor was monitored by a digital voltmeter after going through a voltage divider.

To check the axial and radial uniformity of the magnetic body, first we placed a probe on the axis and moved it ± 10cm and ± 40cm. Then we moved the probe radially from the magnetic body axis to the inner wall of the glass steel corner of the coil (10mm from the inner wall of the magnetic body, i.e. at a position 50-60mm from the central axis of the magnetic body) and observed the magnetic field values of the magnetic body. On the memory oscilloscope, there was no obvious variation, showing that the magnetic uniformity was very good.

This magnetic body has been successfully used by Wang Zhijiang [3769 0037 3068] of the Shanghai Institute of Optics and Fine Mechanics in China's first Raman free electron laser.

REFERENCES

1. Lei Shizhan [7191 0099 3277], et al., JIGUANG KEXUE YU JISHU [LASER SCIENCE AND TECHNOLOGY] in Chinese, 1984, No 3.

2. Shi Jiabiao [2457 0857 2871], et al., HEKEXUE YU GONGCHENG [CHINESE JOURNAL OF NUCLEAR SCIENCE AND ENGINEERING] in Chinese, 1984, 4, No 2, 163.

12966/7358

PARTICLE SIMULATION RESEARCH BY PLASMA PARAMETRIC HEATING CAUSED BY STRONG LASER

[Article by Liu Chenghai [0491 2052 3189], of the Institute of Atomic Energy and Zhang Jiatai [1728 1367 3141], Zhang Shugui [1728 2579 6311], Yu Shuzhen [0151 3219 3791], Liang Huaxiang [4731 5478 3276], and Xu Linbao [6079 2651 1405] of the Institute of Applied Physics and Computational Mathematics]

[Text] Abstract: We used a one and a half dimensional ion cloud (CIC) method as a numerical simulation to study the parametric heating caused by the electric field of a strong laser with a frequency ($\omega = 1.1\ \omega_p$) slightly higher than the plasma. The results show that the ion acoustic decay instability and oscillation two-stream instability are stimulated simultaneously, the nonlinear saturation demonstrated rather fine structure, the plasma was severely heated, and, after saturation, the Langmuir turbulence spectrum followed a typical power law.

I. Introduction

When a strong laser (electromagnetic waves) is propagated in a plasma, under the action of the high frequency electric field of light waves, the electrons undergo a severe, high velocity flutter. The flutter shows a regular oscillation and its energy is a portion of the light wave energy in the medium. The electron flutter is capable of serving as an energy source which stimulates plasma instability. Since this instability is developed against the background of the plasma's periodic oscillation and usually occurs in the form of parametric resonance so it is commonly called parametric instability.

The presence of this sort of parametric interaction means that there exists a vast and very important area of plasma physics. In the last ten or more years, with the progress in laser fusion research, a large amount of theoretical and experimental work has been done on the lasing threshold, linear growth rate, and linear expansion of parametric instabilities. Correspondingly numerical simulation methods for collective phenomena in plasmas have also seen rapid growth.

On the linear behavior of parametric instabilities, Nishikawa has provided a general theory(1) which has served as the foundation for most subsequent

discussions. For a more complete theoretical treatment of parametric insta-
bilities see reference (2).

In laser fusion research one of the important topics is the absorption
mechanism of a laser targeted plasma. Because the classical collision fre-
quency in a hot plasma is very small, Joule heating is usually exceedingly
insigificant. In the process of parametric stimulation, nonlinear coupling
between different modes occurs and causes energy transfer from a pump field
(laser) to another mode. In the vicinity of the laser plasma critical sur-
face, the laser frequency approaches the plasma frequency, $\omega_0 \simeq \omega_p$. Para-
metric instability leads to laser light wave decay into an electron plasma
wave and ion wave coupled pair. The stimulated static electric wave is
absorbed by the plasma forming an "abnormal heating" mechanism. Many
researchers have done numerical simulations of high frequency electric field
driven parametric instabilities and abnormal plasma heating with lasing
frequencies close to plasma frequencies within different parametric ranges.(3-6)
These simulations can be divided into two types according to the pump field
strength. One type has a weak pump strength(3-5) with normalized field
strength $\eta_0 = E_0/4\pi nkT_{e0})^{1/2} \leq 1$. Here E_0 is the pump field amplitude, n is
the electron density, T_{e0} is the initial electron temperature, and k is the
Boltzmann constant. The simulated pump field frequency is in the range of
$\omega_0 = (1.0 - 1.05)\omega_p$. The other type has a very strong pump field(6) with a
normalized field strength $\nu_0 > 1$. The simulated pump field frequency is
$\omega_0 = \omega_p$. The simulation reported in this paper uses a strong pump field, with
the pump field frequency slightly higher than the laser frequency, $\omega_0 = 1.1\omega_p$.

Below, Section II roughly introduces parametric instability theory, Section
III outlines the simulation model, and Section IV to VII present the results
and analysis of major simulations.

II. Stimulation of Parametric Instabilities

When the pump field frequency approaches that of the plasma, there is a direct-
ly perceivable physical explanation for the growth mechanism of parametric
instabilities. Assuming that in the plasma there is one ion fluctuation
σn_{ik} with known wave number k and its level is very low, i.e. at the level
of thermal noise, then due to the quasi electrical neutrality of plasmas in
slow motion, there will be present correspondingly an electron density fluc-
tuation at the same low frequency, i.e. the plasma density exhibits a low
frequency fluctuation, σ. In an electric field $E_L = E_0(\omega_0 t)$, the electrons
flutter along the electric field direction according to the spatial amplitude
$\chi_0 = eE/m\omega_o^2$. Therefore the action of the pump field is to shift the electron
density with low frequency quickly through a given point thereupon causing a
supplementary high frequency contribution with respect to electron density,
that is, producing a high frequency electron density fluctuation, σn_{ek}, a
high frequency electric field, E_p is made. The difference flip between this
high frequency electric field, E_p and the high frequency electric field of the
pump wave form a spatially heterogeneous field pressure strength. It is
exactly the same as if there was a force causing a plasma thermal pressure
strength gradient and also a force causing a field pressure strength gradient.

20

This is called a pendro-motive force. The pendro-motive force also impells electrons and drives ions to a new low frequency motion. This further intensifies the original plasma low frequency density fluctuation, σn. Therefore a feedback mechanism is present as shown in Figure 1.
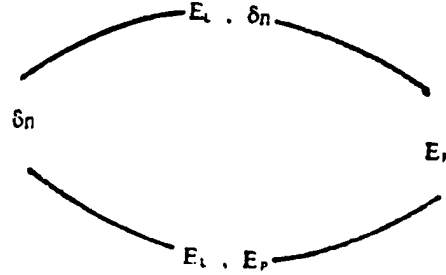

Fig. 1. Parametric Instabilities Feedback Mechanism

Description of the definite quantities of parametric instabilities can be done using the two stream-coupling equations:

$$\frac{\partial^2 n_{e\vec{k}}}{\partial t^2} + \omega^2_{e\vec{k}} n_{e\vec{k}} + \nu_{e\vec{k}} \frac{\partial n_{e\vec{k}}}{\partial t} = -\frac{ie\vec{k} E_0}{m} n_{i\vec{k}} \tag{1}$$

$$\frac{\partial^2 n_{i\vec{k}}}{\partial t} + \omega^2_{i\vec{k}} n_{i\vec{k}} + \nu_{i\vec{k}} \frac{\partial n_{i\vec{k}}}{\partial t} = -\frac{ie\vec{k} E_0}{M} n_{e\vec{k}} \tag{2}$$

in which $n_{e\vec{k}}$ is the electron high frequency density fluctuation and $n_{i\vec{k}}$ is the ion low frequency density fluctuation. $(\omega_{e\vec{k}}, \nu_{e\vec{k}})$ and $(\omega_{i\vec{k}}, \nu_{i\vec{k}})$ are respectively the frequency and damping rate of the electron high frequency oscillation and ion low frequency oscillation when there is no coupling, m and M are the mass of an electron and an ion, and E_0 is the amplitude of an infinitely long wave pump field.

Three wave parametric interaction requires satisfaction of the phase matching conditions

$$\omega_0 = \omega_1 + \omega_2 \tag{3}$$

$$\vec{k}_0 = \vec{k}_1 + \vec{k}_2 \tag{4}$$

in which $(\omega_0, \vec{k}_0)$, $(\omega_1, \vec{k}_1)$ and $(\omega_2, \vec{k}_2)$ are respectively the pump wave, ion acoustic wave, and electron plasma wave frequencies and wave vectors. Using quantum language, we can say that formulae (3) and (4) are the energy and momentum conservation conditions of three wave interaction, also called the Manley-Rowe relations.

Under the conditions (3) and (4), Fourier analysis with respect to the coupling equations shows that when the pump field frequency approaches the plasma frequency, there are two classes of instabilities. When $\omega_0 \leq \omega_p$, it stimulates an oscillating two-stream instability. At this time, the high frequency

oscillation of electrons occurs at the pump frequency while the low frequency oscillation of ions occurs at zero frequency. The simulations done by DeGroot and Katz(6) belong to this sort of condition. When $\omega_0 < \omega_p$, it stimulates simultaneously oscillating two-stream instability and ion acoustic decay instability. The later high frequency oscillation occurs near the Bohm-Gross frequency, $\omega_{ek} = \omega_p(1 + 2/3 \, k^2\lambda^2_{De})$, in which $\lambda_{De} = (KT_0/4\pi ne^2)$ is the electron debye length. The simulation presented in this paper belongs to the condition where $\omega_0 > \omega_p$.

III. Simulation Model

Our simulation was carried out using a one and a half dimensional particle cloud grid method numerical coding (called CIC for short).(7-12)
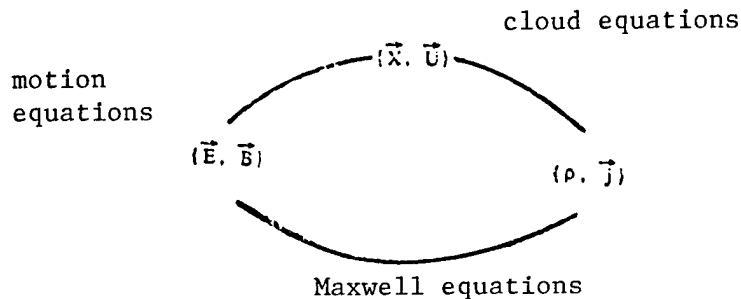

Fig. 2. Fundamental Cycle of the Particle Simulation

The period length of the plasma system we simulated was $L = 512\lambda_D$. Here λ_{Do} is the initial debye length. In an externally applied pump field with $E_L = E_0\cos(\omega_0 t)$ and self consistent, we traced the motion of 8192 giant electrons and giant ions. In continuous coordinates and velocity phase space, we solved for the particle motion equations and in discretized coordinate space solved for self consistent equations.(9) The spatial descretized grid length $\Delta = \lambda_{Do}$. The traced giant electrons and giant ions were both finitely large small particles called the particle cloud. The electron and ion cloud width, $R_e = R_i = \lambda_{Do}$. We selected a time step of $\Delta t = 0.2\omega_p^{-1}$ which was both economical and sufficient to resolve the fastest collective behavior in the system. A leap frog algorithm was used for solving, see Figure 2.

Initially the electron and ion temperatures were $T_{eo} = T_{io} = 1$ kev. When forming the initial velocity distribution, the Maxwell distributions of the electrons and ions were separately taken at u_{em} and u_{im} cross sections with $u_{em} = 4.8 \, u_{eT}$, $u_{im} = 4.8_{iT}$. In which u_{eT} and u_{iT} were the initial thermal velocities of the electrons and ions. In order to save computing time and be sufficient to make the temporal length of the electrons and ions be clearly distinguished, as in common simulations, the ion-electron mass ratio was taken as $M/m = 100$.

In order to simulate thermal noise, at the initial time a random turbulence was applied to the electron and ion densities and velocities. The level of this turbulence was very low.

In the simulation, the pump field frequency was $\omega_0 = 1.1\omega_p$ and the normalized pump field strengths were $\eta_0 = 5$ and 7.

IV. Growth Static Oscillation Field Energy Density
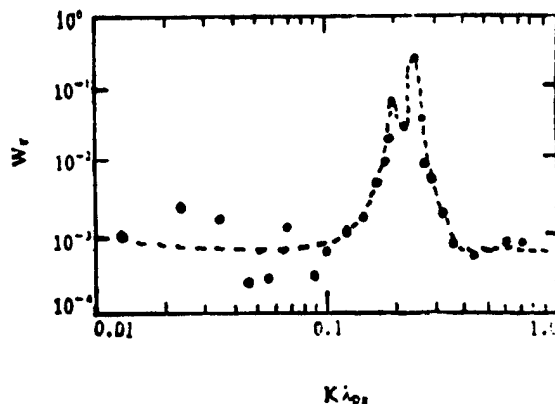
Fig. 3. Linear Growth State ($\omega_p t = 75$) Static Electric Oscillation Field Energy Density Spectrum

Figure 3 gives a typical normalized static electric oscillation energy density spectrum $W_k = |E_k|^2/4\pi n T_{eo} \sim k\lambda_{D_0}$ for the instability growth stage ($\omega_p t = 75$). The principle growth mode is concentrated in $k\lambda_{D_0} = 0.15$ to 0.3. The Langmuir waves to which they respond are weakly damped long waves. There are two maximum growth modes. One is at $k\lambda_D = 0.2$ and corresponds to ion acoustic decay instability. The other is at $k\lambda_D = 0.25$ and corresponds to oscillation two-stream instability.

Figure 4 gives the time expansion of normalized self consistent energy density $W_T = E_T^2/(4\pi n T_{eo})$ (corresponding to a normalized pump field strength $\eta_0 = 5$).

In the interval $\omega_p t = 0$ to 80, the self consistent field energy density very closely follows a linear rule of growth with time with a linear growth rate $\nu \cong 0.075\omega_p$. This and a linear theory offer straight forward reasonable agreement.

23

Fig. 4.   Static Electric Oscillation Field Energy Density Time Expansion

V.   Field Energy Saturation

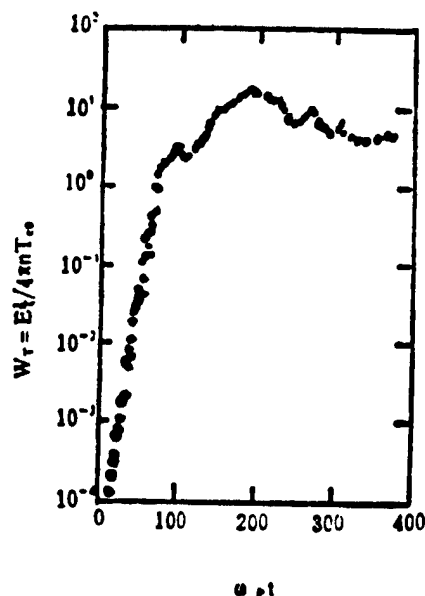The saturation of the self consistent field energy density exhibits a fine structure.   From Figure 4 we see that when $\omega_p t \simeq 90$, the linear growth stage stops and nonlinear saturation of the energy density field occurs.   Its saturation level is about $W_T = E^2/(4\pi nTe_0) = 3.16$.   Subsequently the saturation field energy density falls slightly then slowly rises reaching a maximum, $W_{max} \simeq 16$ at about $\omega_p t = 180$.

The physical explanation of the appearance of this saturation structure is as follows: After the maximum growth mode saturation of the linear growth stage, the plasma has already begun heating and the plasma temperature T_e rises so the electron debye length λ_D changes greatly.   The unstable mode will drift toward a wave number k zone and even longer waves continue to grow.   However, after the plasma temperature rose the pump field normalized strength $\eta = E_0/(4\pi nT_e)^{1/2}$ fell and became a weak pump field so the growth velocity of these longer waves is slower.

In the laser plasma interaction, the saturation level reached by the static electric waves stimulated resonately or parametrically is a very important and significant physics question.   This problem involves the abnormal absorption efficiency of the plasma with respect to the laser and the production of super heated electrons.

The physic of parametric instability nonlinear saturation is extremely rich and has many different areas related to pump field intensity.   Many authors have studied saturation behavior in cold or hot and spatially homogeneous or heterogeneous plasmas.(13-18)   Generally it is recognized that when the pump field is weak the process that predominates is simply electron capture in the

24

most unstable Langmuir waves. Large amplitude static waves capture electrons in large number causing wave breaking. Here we use two methods to estimate the saturation level from theory.

1. Simple Estimate(6)

When the phase velocity of the most unstable Langmuir waves is far greater than the electron thermal velocity, i.e. $V_p = o_k/k >> u_{eT}$, we can consider the electron kinetic energy in wave coordinates to be:

$$\frac{1}{2}mv^2 = \frac{1}{2}m\left(\frac{o_k}{k}\right)^2 \approx \frac{1}{2}mu_{oT}^2/(k^2\lambda_D^2)$$ (5)

When the peak thermal energy difference $2e\phi_n$ of the most unstable Langmuir waves is equal to the electron kinetic energy in wave coordinates, i.e. when

$$\phi_m = \frac{mu_{oT}^2}{4e}\frac{1}{k^2\lambda_D^2}$$ (6)

then electron capture occurs. In the formula, ϕ_m is the electric potential amplitude. The maximum field strength estimate is:

$$\left|E_k\right| = \left|\frac{\partial\phi}{\partial x}\right| \approx k\phi_m$$ (7)

The rightward and leftward propagated waves are stimulated at the same time so when saturated the total field energy is:

$$W_T = 2E_m^2$$ (8)

From this we estimate the normalized self consistent field energy density when saturated to be:

$$W_\infty \approx (8k^2\lambda_D^2)^{-1}$$ (9)

2. Waterbag Model

Coffey used a waterbag model to study the wave breaking of large amplitude plasma.(13) He assumed the ions to be an immobile electrically neutral background and used a constant electron velocity distribution between $\pm\sqrt{3}u_{eT}$ in place of the Maxwell velocity distribution. Then from the one dimensional Vlasov equations for an infinite space plasma he derived a super elliptical integral representing the oscillation structure. When the wave oscillation structure was not present it was the predicted breaking of waves occurring. According to wave breaking theory during saturation the self consistent field normalized field energy density is:

$$W_\infty = \frac{6}{\beta}\left[1 - \frac{8}{3}\beta^{\frac{1}{4}} + 2\beta^{\frac{1}{2}} - \frac{1}{3}\beta\right]$$ (10)

in

$$\beta \equiv 3u^2_{eT}/V^2_p \approx 3(k\lambda_D)^2$$

A comparison of the results of our simulation with those of the two theories discussed above is given in Table 1.

Table 1

Pump field strength	$k\lambda_p$	Self consistent field normalized energy density saturation value W		
		CIC	Simple	Waterbag
5	0.25	3.16	2	1.56
7	0.173	7.08	4.18	7.32

From the Table we see that the CIC computed value agrees with the theoretical estimates within a factor of 2.

VI. Plasma Heating

Figure 5(a) gives the variation of plasma electron temperature over time T_e/T_{eo} to t. At about $\omega_p t = 50$, the electrons slowly begin heating. When $\omega_p t \simeq 120$, the speed of electron heating increases. After $\omega_p t = 200$, the speed of heating again slows down.

The energy transfer rate in the laser-plasma determines the absorption length of electromagnetic waves. It is common to introduce a phenomenological collision frequency ν^* to represent this abnormal energy transfer rate, i.e.:

$$m\frac{du_e}{dt} = -eE_L - \nu^* m v_e \qquad (11)$$

Obviously the pump field power input with respect to the plasma is

$$\langle J \cdot E \rangle = \frac{1}{T_L} \int_t^{T_L+t} JE dt \qquad (12)$$

in which $J = ienv_e$ is the electric current of $T_L \simeq 2\pi/\omega_0$ is the pump field oscillation period. Obviously, $\langle J \cdot E_L \rangle$ is equal to the plasma energy time growth rate $n_0 dT_e/dt$. Thereupon we get the abnormal collision frequency to be

$$\nu^* = \frac{\omega_0^2}{\omega_p^2} \cdot \frac{8\pi n_0}{E^2}\frac{dT_e}{dt} = -\frac{\omega_v}{\omega_p}\Big) \eta_0^{-2}\frac{d}{dt}\Big(\frac{\cdots}{T_{eo}}\Big) \qquad (13)$$

in which η_0 is the pump normalized strength. Computing by this formula for a pump strength of $\eta_0 = 5$, $\nu^* = 0.04\omega_p$. Clearly this abnormal collision frequency is far greater than the classical collision frequency.
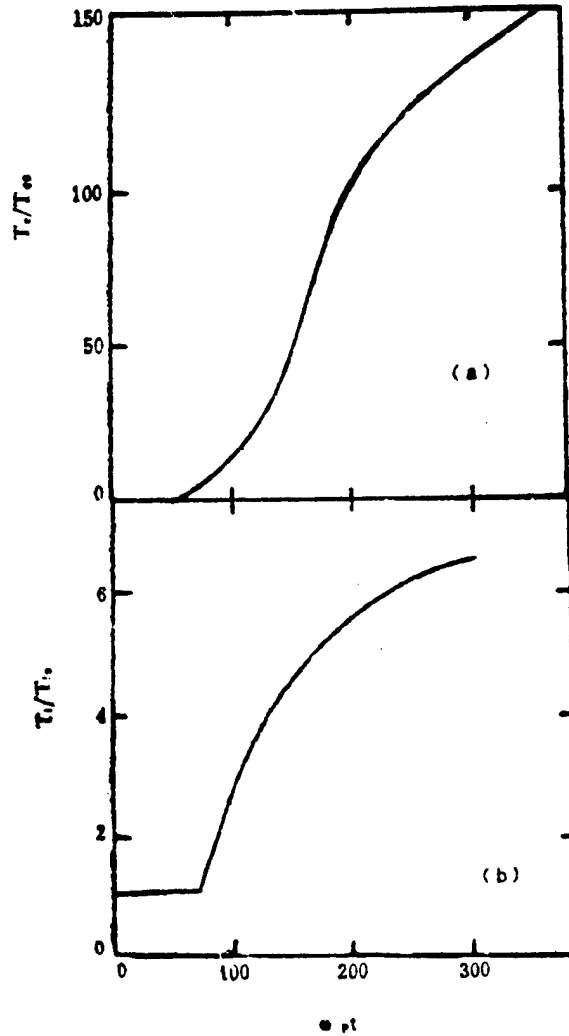
Fig. 5. Plasma Heating (a) by electron temperature-time development
and (b) by ion temperature-time development

Because the ion velocities are much less than the electron velocities, the ions
are heated by the low frequency portion of the static electric field. The
simulation results illustrated a lower ion heating level.

Figure 6 gives the turbulence spectrum after static electric wave energy
saturation. W_k is proportional to $k\lambda_{po}$. This spectrum is the average result
for $\omega_p t$ = 300 to 360. In the region from $k\lambda_p$ = 0.1 to 0.25, a "trace" of the
maximum growth mode of the linear growth stage is preserved. Viewed in total,
the static electric wave turbulent spectrum here approximately satisfies a
power relation

$$W_k = a(k\lambda_{D_0})^{-b} \tag{14}$$

in which a = 0.93 x 10^{-3}, b = 2.0.

27

Fig. 6. Post Saturation Static Electric Turbulence Spectrum
(average spectrum at $\omega_p t = 300$ to 350)

With plasma heating, the electron temperature increases and the electron debye
length gets larger making even smaller wave number (longer wave length) waves
be stimulated parametrically by the pump field. Obviously, with electron
temperature increase, the ratio of pump field strength to plasma thermal energy
gets smaller and smaller like the pump field getting weaker and weaker and the
rate of stimulated static electric waves in the long wavelength area also will
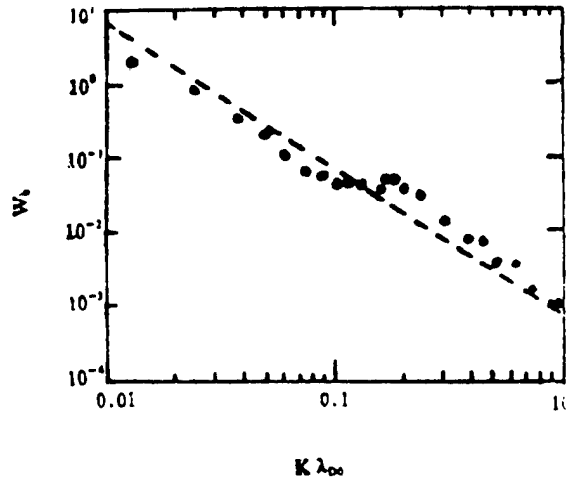fall lower and lower.

Langmuir waves on plasma particles are induction scattered.(19) The induction
scattering of waves on the particles satisfy resonance conditions:

$$(\omega_{\vec{k}} - \omega_{\vec{k}'}) - (\vec{k} - \vec{k}') \cdot \vec{V} = 0. \tag{15}$$

in which $\vec{V}$ is the particle velocity. AT long wavelengths the result of induced
scattering is to transfer wave energy to even longer wavelengths.

Langmuir waves are induction scattered on ion waves.(19) The result of scat-
tering leads to "relay" type energy transfer in wave number space from high
wave numbers toward low wave numbers.

It can be expected that with time the "trace" of linear growth stage maximum
growth mode will gradually disappear and the wave energy will concentrate at
an even lower wave number.

VII. Conclusion

The numerical simulation we made shows that a strong laser electric field with
a frequency slightly higher than the plasma frequency strongly stimulates
parametric instability. The parametric instability saturation manifests a
rather fine structure, the plasma is severely heated, and after saturation the
turbulent spectrum approximately satisfies a negative quadratic power relation
of the wave number.

28

BIBLIOGRAPHY

1. K. Nishikawa, J. Phys. Soc. Jap., 24(1968), 916.

2. P. Kaw, W.L. Kruer, C.S. Liu, and K. Nishikawa, in Advances in Plasma
    Physics, Vol 6, Edited by A. Simon and W.B. Thoson (New York: 1976).

3. W.L. Kruer and J.M. Dawson, Phys. Fluids, 15(1972), 446.

4. J.J. Thomson, R.J. Faehi, and W.L. Kruer, Phys. Rev. Lett., 31(1973), 918.

5. J. Denavit, Phys. Fluids, 19(1976), 972.

6. J.S. DeGroot and J.I. Katz, Phys. Fluids, 16(1973), 401.

7. Yu Min [0060 2404], "Ion Cloud Methods with Plasmas," in Chinese,
    (1975 [as printed], forthcoming.)

8. Xu Linbao [6079 2651 1405], Liang Huaxiang [4731 5478 3276] et al.,
    HEJUBIAN YU DENGLIZITI WULI [NUCLEAR FUSION AND PLASMA PHYSICS] in
    Chinese, 2(1982), 92.

9. Liu Chenghai [0491 2052 3189] and Zhang Jiatai [1728 1367 3141],
    HEJUBIAN YU DENGLIZITI WULI [NUCLEAR FUSION AND PLASMA PHYSICS] in
    Chinese, 2(1982), 39.

10. Liu Chenghai [0491 2052 3189], HEJUBIAN YU DENGLIZITI WULI [NUCLEAR
    FUSION AND PLASMA PHYSICS] in Chinese, 3(1983), 119.

11. Liu Chenghai [0491 2052 3189] and Xu Linbao [6079 2651 1405], JISUAN
    WULI [CHINESE JOURNAL OF COMPUTATIONAL PHYSICS] in Chinese, 1(1984), 102.

12. Liu Chenghai [0491 0252 3189], Wang Min [3769 7044], JISUAN WULI [CHINESE
    JOURNAL OF COMPUTATIONAL PHYSICS] in Chinese, 1(1984), 200.

13. T.P. Coffey, Phys. Fluids, 14(1971), 1402.

14. J.M. Dawson, Phys. Rev. Lett., 112(1959), 383.

15. E. Valeo, C. Oberman, and F.W. Perkins, Phys. Rev. Lett., 28(1972), 340.

16. B. Bezzerlides and J. Weinstock, Phys. Rev. Lett., 28(1972), 481.

17. W.L. Kruer, Phys. Fluids, 22(1979), 1111.

18. T. Spezlale et al., Phys. Fluids, 24(1981), 883.

19. B.B. Kadomtsev, KOLLEKTIVNYYE YAVLENIYA V PLASME [COLLECTIVE PHENOMENA IN
    PLASMA] in Russian (Moscow: Nauka Publishing House, 1976). Translated by
    Liu Chenghai [0491 2052 3189], DENGLIZITI ZHONG DE JITIXIANXIANG [COLLEC-
    TIVE PHENOMENA IN PLASMA] in Chinese, (n.p.: Atomic Energy Publishers,
    1983).

12966/7358

ANALYSIS, SUPPRESSION OF LAND CLUTTER CHARACTERISTICS REPORTED

[Article by Wang Fengzhen [3769 7364 2182] and Zhang Xinbo [1728 2450 3134] of East China Institute of Technology, Nanjing; manuscript received March 1985 and revised March 1986: "Analysis and Suppression of Ground Clutter Characteristics"]

[Text] Abstract: The properties of land clutter and target echo of the ground combat surveillance radar are presented. The mathematical model for the clutter power spectrum and the relationship between the cutoff frequency of the clutter spectrum and the wind speed are obtained. Experimental results showed that strongly cluttered echoes from slow moving targets could be detected by long time integration of positive and negative Doppler signals which were converted into positive and negative voltage, respectively. The paper also includes an investigation of the statistical characteristics of the echo amplitude of the CW radar.

The early warning ability of a ground combat surveillance radar operating in wooded and hilly areas is greatly reduced, or completely lost, under gusty wind conditions due to clutter. The frequency spectrum distribution and amplitude probability distribution of this type of clutter has been studied. [1-3, 5,6] However, the frequency spectrum model was based on pulse radar technology. As we know, a non-coherent pulse radar signal is displayed by amplifying the signal output from a sampler-holder. The reference signal is unstable. The frequency measured is not the absolute Doppler frequency of the target with respect to the radar. As for the tree clutter frequency distribution which serves as an internal reference of the CW radar, it will be a topic to be discussed in this paper. The paper will also explore ways to raise the improvement factor of the MTI system which has the problem of lowering the gain of the slow moving target echo as it suppresses clutter.

Measurement of Clutter Frequency Spectrum

A radar echo is composed of many points of target echoes. At the receiving end, the resultant vector is:

$$u(t) = A(t) \cos [\omega_0 t + \phi(t)]$$

where u(t) is the instantaneous input voltage at the receiver, A(t) is the clutter amplitude, ϕ(t) is the clutter phase fluctuation, and ω_0 is the radar carrier frequency. The clutter fluctuation caused by A(t) and ϕ(t) can be considered as a random angular and amplitude modulation signal. In order to improve accuracy in measuring the clutter and to avoid other incident wave, we used a pseudo-random coding, phase modulating, internally correlating CW radar as the test equipment. Its primary operating parameters are: carrier f_0 = 9100 MHz, antenna gain G >, 600, wave lobe width $\theta < 6°$, $\theta < 8°$, side lobe θ= side = -18dB, θ side = 15dB feeder stationary wave index $\rho < 1.2$, transmission power p = 40 mW, code length 511 bits, and resolution 50 m. The sequence m is generated by the linear shift register. The carrier wave is modulated in the phase modulator. The echo code is correlated to the local reference code. The signal in the range element can be made the strongest. Other response side lobes can be lowered to 1/N of the range element. As long as the code length N is sufficiently long, factors other than range can essentially be omitted.

The experiment was conducted with radar beam scanning the forest under windy conditions. The echo received by the receiver goes through the correlator and is dc amplified before being entered into a MDR-Z80 computer. The A/D converted data is input into the memory by remote control. A specially designed software is used for direct analysis. The data can also be stored in a special magnetic tape for later use. Figure 1 shows the original signal wave form, autocorrelation function and power spectrum as plotted by the WX4671 microprocessor based plotter. In the experiment, the sampling frequency was 1 kHz, sampling points 1024 (2048) and electromagnetic wave perpendicularly polarized.

In order to provide a good video frequency processing scheme, we concentrated on the study of the mean power spectra under identical conditions. The work lasted over spring, summer and fall. Based on the vast amount of experiments done, the normalized tree clutter power spectrum of the CW radar can be approximately expressed by the following equation:

$$P_1(f) = \frac{1}{1 + (f/f_c)^3} \qquad (1)$$

where f_c is the frequency at half power in Hz. Figure 2 shows the approximation at 9.2 m/s wind speed and f_c = 10 Hz.

The span of the clutter spectrum varies with wind condition, i.e. f_c is a function of wind speed. By fitting the f_c versus wind speed v(m/s) data using the least square method, we find that the average wind speed and the 3dB cutoff frequency in the tree clutter power spectrum have the following relationship:

$$f_c = 1.2336 e^{0.2317 v} \qquad (2)$$

Figure 3 shows the f_c versus wind speed curve.

tree echo
voltage (mV)

time t(s)

autocorrelation
function R (τ)
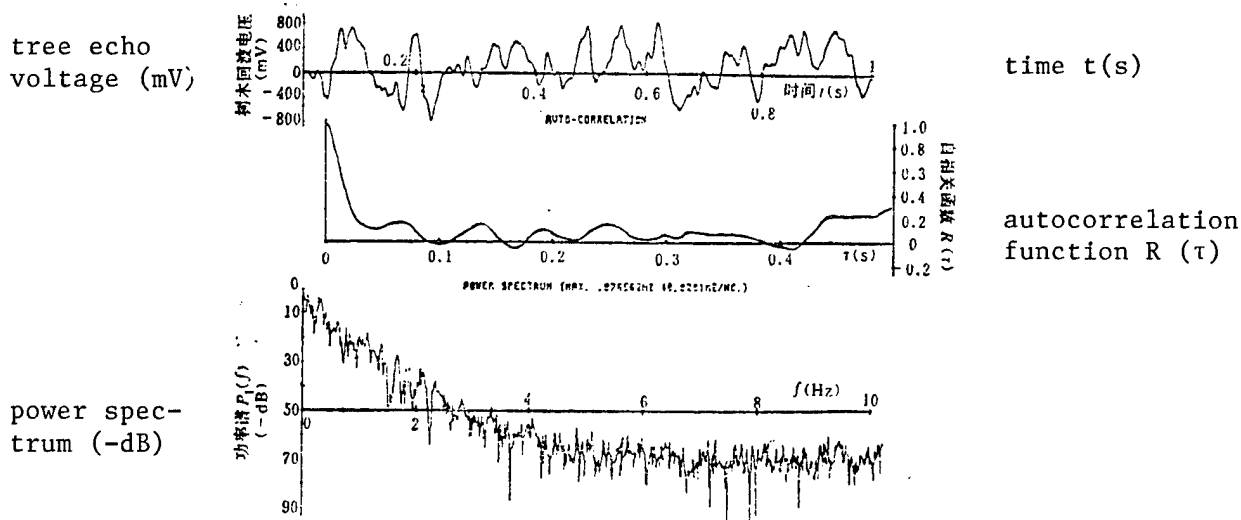
power spec-
trum (-dB)

Fig. 1. Tree Echo, Its Autocorrelation Function and Power Spectrum

実验值 experimental
——近似值 approximation

experimental

実验值
——近似值

approximation
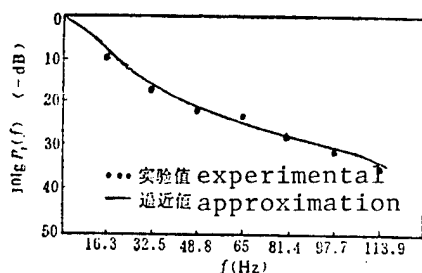
Fig. 2. Mean Tree Clutter at Wind
Speed Level 5
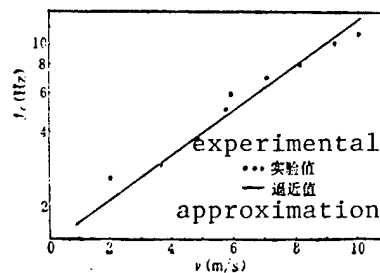
Fig. 3. f_c vs. Wind
Speed

The above study concentrates on the average energy distribution and neglects
minute differences. The clutter power spectrum above 200 Hz has been omitted.
This does not have any effect on video frequency processing. Our experiments
showed that the mean spectrum can still be expressed by equations (1) and (2)
with horizontally polarized transmission and receiving. The forest we tested
is heavily leaved. There will be some discrepancy with sparsely leaved forest.
In order not to saturate the amplifier in the measurement, the dc component
was removed. The bandwidth of the amplifier is 1 ~ 750 Hz.

Measurement of Frequency Spectrum of Individual Person

A person is not an ideal point target. Different parts are moving at different
speeds with respect to the body. The power spectrum covers a band. Figure 4
shows the power spectrum of a person as the upper body bends (vertical polari-
zation). We can see that the frequency spectrum of a slow moving target

overlaps with the ground clutter totally. It is impossible to detect a slow moving target with a simple filter.

Correlation Detection of Bi-orthogonal Channels

Based on the above we know that the improvement factor for a slow moving ground target cannot be raised by a simple filter because the target gain is lowered as the clutter is suppressed. If we treat the positive and negative Doppler signals corresponding to the back and forth motion of the wind driven trees as positive (or negative) and negative (or positive) voltage, respectively, the clutter can then be suppressed by the long time integration of the Doppler signals. The scheme is shown in Figure 5.
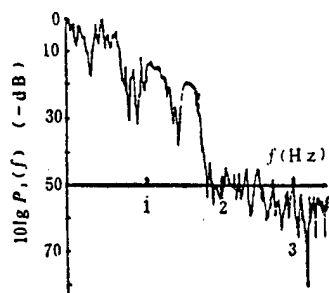

Fig. 4. Power Spectrum of Echo from Upper Body Movement (Each grid is 58.5338 Hz on the Horizontal axis.)
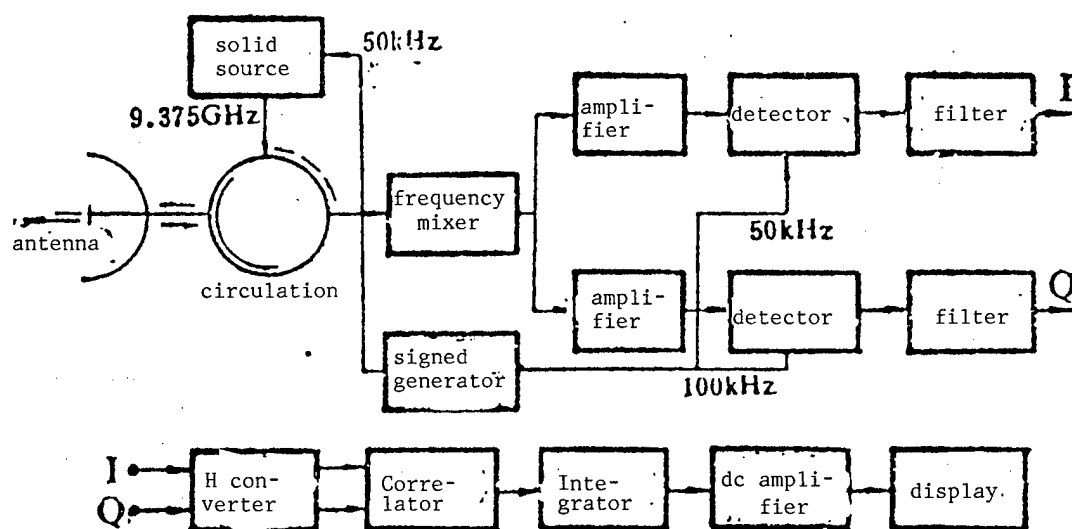

Fig. 5. Block Diagram of the Sinusoidal Frequency Modulation MTI Scheme

33

Since the weight and volume of a field surveillance radar must be low, this scheme employs a simple sinusoidal signal to modulate the carrier. The results are that: (1) Doppler signals are treated at the modulating frequency or on the harmonic wave, and (2) when the leakage is used as the reference signal in a radar, the power spectrum of the signal is a function of range after frequency mixing. Both features are favorable to reducing the internal noise of the receiver and suppressing clutter in the neighborhood. [7,8]

The sinusoidal frequency modulating signal has the following complex form:

$$e(t) = A_0 \exp(j m_f \cos \omega_m t) \cdot \exp(j \omega_0 t)$$

where m_f is the frequency modulation index, ω_m is the modulating angular frequency and ω_0 is the carrier frequency. When the target can be approximated by a point, the resultant signal of the echo of the moving target and the leakage after zero beat frequency mixing and high frequency component filtering is [8]:

$$S(t) = K J_0(M_f) \cos(\omega_d t + \varphi_0) - K_1 \sum_{n=odd} J_n(M_f) \sin(\omega_d t + \varphi_0) \cdot \sin\left[n\omega_m \left(t - \frac{R}{c}\right) \right]$$

$$+ K_1 \sum_{n=even} J_n(M_f) \cos(\omega_d t + \varphi_0) \cdot \cos\left[n\omega_m\left(t - \frac{R}{c}\right) \right] \qquad (3)$$

where

$$\varphi_0 = -\omega_d \tau - \omega_0 \tau, \quad M_f = 2m_f \sin(\omega_m \tau \ /2),$$

$J_n(M_f)$ is a Bessel function of order n, τ is a fixed time delay, c is the speed of light, R is the starting target range, ω_d is the Doppler frequency, and K and K_1 are constants. The first and second harmonics of S(t) are selected by the amplifier. The reference signals $\sin\omega_m t$ and $\cos 2\omega_m t$ are input into the dual channel coherent detector to obtain two orthogonal signals. (If $\sin\omega_m t$ is used for phase modulation, then the input reference signals are $\cos\omega_m t$ and $\cos 2\omega_m t$).

First channel: $x_1(t) = x(t) = -K_3 \sin(\omega_d t + \varphi_1)$

Second channel: $x_2(t) = C\hat{x}(t) \operatorname{sgn}(f_d)$

where K_3, . , and C are constants. $\hat{x}(t)$ is the Hilbert transform of x(t).

Based on equation (3), we can see that sinusoidal frequency modulation can provide positive and negative Doppler information. The complex linear combination of x(t) and $\hat{x}(t)$ is the pre-envelop of x(t) (without spectrum mixing). In order to derive the positive and negative voltages, we employed a dual orthogonal channel scheme. Both signals are input into the Hilbert converter,

and the second channel signal is transformed according to Hilbert transformation: $\hat{x}(t)=-x(t)$ [9]. After both signals are correlated, the frequency spectrum of the output signal $u(t)$ is:

$$\mathscr{F}[u(t)]=U(\omega)=\frac{c}{2\pi}\mathscr{F}[x(t)]\otimes\mathscr{F}[\mathrm{sgn}(-f_d)\cdot x(t)]$$

$$=\frac{\pi}{2}K_3^2\,c\,\mathrm{sgn}(f_d)\left\{e^{j2\varphi_1}\delta(\omega-2\omega_d)-2\delta(\omega)+e^{-j2\varphi_1}\cdot\delta(\omega+2\omega_d)\right\}$$

The integrator (equivalent filter) behind the correlator only accumulates the

dc components. Its frequency spectrum is $U_0(\omega)=K_3^2 c\pi\cdot\mathrm{sgn}(-f_d)\delta(\omega)$.

Because $\mathscr{F}^{-1}[2\pi\delta(\omega)]=1$, then $U_0(t)=-K_3^2 c\cdot\mathrm{sgn}(f_d)/2$.

The above equation shows that the output of a nearby target is positive (or negative) while that of a far away target is positive (or negative). For a non-ideal target, two signals are obtained after coherence treatment of the vector space of the echo.

$$x_1(t)=K_1 a(t)\sin[\omega_d t+\varphi(t)],\quad x_2(t)=K_2 a(t)\cos[\omega_d t+\varphi(t)]\cdot\mathrm{sgn}(f_d)$$

where $a(t)$ and $\varphi(t)$ are slow varying functions. Their output signals from the dual orthogonal channel coherence treatment are still positive and negative voltages proportional to the square of the amplitude of the echo.

The positive and negative Doppler signals generated by the movement of the trees are shown as positive and negative voltages at the output end of the correlator. They are cancelled after integration. If there is a moving target in the clutter, because of the superposition nature of the correlator, different target points will be shown as different dc components after filtering. However, because this linear integrator only integrates the voltage of the point of the highest regularity in the signal vector space, other components are cancelled. Therefore, it is possible to detect moving targets from the clutter.

Figure 6 shows the echo power spectrum of a slow moving pedestrian (approximately v = 0.5 m/s). The target spectrum is completely overlapped in the clutter. Figure 7 is the power spectrum of the target shown in Figure 6 after the dual orthogonal channel correlation treatment. The target is near the radar.

This demonstrates that the dual orthogonal channel detection system can effectively suppress clutter, while maintaining the signal gain. This is equivalent to an increase of the improvement factor. The following is an analysis of an unfavorable situation where the echo from a target which moves back and forth dominates. Let ω_e be the cutoff frequency of the low pass filter after correlation and τ_1 be the duration over which the positive (or negative) voltage lasts. $\omega_c\tau_1$ is used as a variable to calculate A_c, the clutter attenuation, as shown in Figure 8. If the positive (or negative) voltage lasts 0.1 s, the integration constant is 1 s. Then, the improvement factor of the system may

be raised by 42dB. Nevertheless, the price to pay for such improvement in performance is long time integration. It is not difficult to prove that in a scanning system the scan rate ω_{sp} ought to satisfy:

$$\omega_{sp} \leqslant \frac{\theta_{\pi}(\text{rad})}{t_r(\text{s})} = 2K_0 f_c \theta_{\pi}$$

Otherwise, information may be missed. In the equation, θ = the width of the horizontal beam, t_r is the step response time of the filter (s), f_c is the cut-off frequency of the filter, and K_0 is the gain.
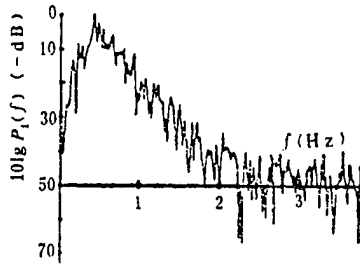
Fig. 6. Spectrum of Echo from a Slow Moving Pedestrian in Clutter (frequency axis: 73.24 Hz/block)
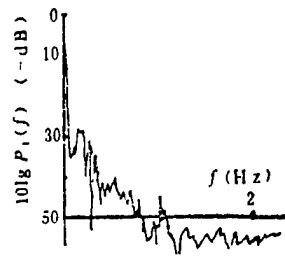
Fig. 7. Spectrum of Echo from a Slow Moving Target in Clutter After Correlation Treatment (frequency axis: 4.8828 Hz/block)
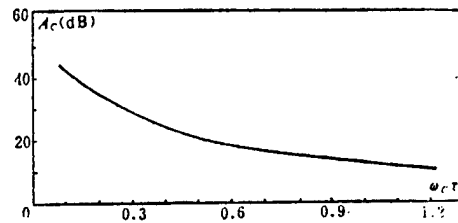
Fig. 8. Clutter Attenuation A_c vs. $\omega_c\tau$

Investigation on the Amplitude Characteristics of Tree Echo

Theoretically, the echo amplitude from a fixed scatterer and another scatterer whose amplitude obeys Rayleigh distribution is a Rice distribution. [5,11] If there is more than one scatterer, as long as the echo frequency remains constant, the resultant vector is equivalent to a fixed scatterer. However, a radar usually operates with scatterers and trees in the background. If we assume that the echo is the combination of fixed scatterers and other scatterers that obey the Rayleigh distribution, it will be incompatible with the central limit theory. This is because we cannot consider the echo from a swinging leaf and that from a swinging trunk to be comparably small. The echo must be divided as the sum of the leaf echo U_F (t), trunk (random) and fixed scatterer (not random) echo U_T (t):

36

$$U_s(t) = U_F(t) + U_T(t) \qquad\qquad (4)$$

If the instantaneous voltage of the echo from the leave is a stable normal process and the mean is zero, its frequency will be evenly distributed symmetrically on either side of f_o. Then, $U_F(t)$ can be expressed as: [11]

$$U_F(t) = \eta_c(t) \cos \omega_0 t - \eta_s(t) \sin \omega_0 t \qquad\qquad (5)$$

where ω_0 is the carrier frequency, and $\eta_c(t)$ and $\eta_s(t)$ are the statistically independent random processes corresponding to zero mean value and normal stable conditions.

The echo from the trunk can be treated based on the central limit theory. The two amplitude components of $U_T(t)$ obeys Rice distribution [11]

$$U_T(t) = a \cos(\omega_0 t + \theta) \qquad\qquad (6)$$

where the probability density of the random variable a is

$$p(a) = \frac{a}{\sigma_1^2} \exp\left(-\frac{a^2 + m^2}{2\sigma_1^2}\right) I_0\left(\frac{am}{\sigma_1^2}\right)$$

where σ_1 is the echo – component exchange power, m is a fixed component, and $I_0(\cdot)$ is the zero order modified Bessel function. Because Doppler effect will create angular modulation, let us assume that θ follows a uniform distribution (which does not affect the result).

By substituting equations (5) and (6) into (4), we get

$$U_s(t) = A_c(t) \cos \omega_0 t - A_s(t) \sin \omega_0 t$$

where

$$A_c(t) = a \cos \theta + \eta_c(t), \quad A_s(t) = a \sin \theta + \eta_s(t);$$

Under the condition that a and θ are given, $A_c(t)$ and $A_s(t)$ are statistically independent normal processes. In addition, because $\eta_c(t)$ and $\eta_s(t)$ have the same correlation function,

$$E_{a,\theta}[A_c(t)] = a \cos \theta, \qquad E_{a,\theta}[A_s(t)] = a \sin \theta$$
$$D_{a,\theta}[A_c(t)] = D_{a,\theta}[A_s(t)] \triangleq \delta^2$$

where E is the symbol for determining the expectation value, D is the symbol for determining the variance, and σ^2 is the power exchange of the echo from the leaves.

Using a and θ, we get

$$p\left(\frac{A_c(t), A_s(t)}{a, \theta}\right) = \frac{1}{2\pi\sigma^2} \exp\left\{-\frac{1}{2\sigma^2}\left[(A_c(t) - a\cos\theta)^2 + (A_s(t) - a\sin\theta)^2\right]\right\}$$

Let

$$A_c(t) = A(t)\cos\psi(t), \qquad A(t) \geqslant 0, \ \forall t$$
$$A_s(t) = A(t)\sin\psi(t), \qquad -\pi < \psi(t) \leqslant \pi, \ \forall t$$

We get

$$p\left(\frac{A(t), \psi(t)}{a, \theta}\right) = \frac{A(t)}{2\pi\sigma^2}\exp\left\{-\frac{1}{2\sigma^2}\left[A^2(t) + a^2 - 2aA(t)\cos(\theta - \psi(t))\right]\right\}$$

Integrate $\psi(t)$ in the above equation from $-\pi$ to $+\pi$ and note that

$$I_0(x) = \int_{-\pi}^{\pi} \frac{1}{2\pi} e^{x\cos\psi} \, d\psi,$$

We get

$$p\left(\frac{A(t)}{a, \ \theta}\right) = \frac{A(t)}{\sigma^2}\exp\left\{-\frac{1}{2\sigma^2}\left[A^2(t) + a^2\right]\right\} \cdot I_0\left[\frac{aA(t)}{\sigma^2}\right] \qquad (7)$$

The right side of equation (7) is independent of θ. Therefore

$$p[A(t)/a] = p[A(t)/a, \theta],$$

After simplifying it with

$$p[A(t), a] = p(a) \cdot p[A(t)/a],$$

$$I_0(x) = \sum_{n=0}^{\infty} x^{2n}/2^{2n}(n!)^2,$$

We get

$$p[A(t)] = \frac{A(t)}{\sigma_1^2 + \sigma^2}\exp\left[-\left(\frac{A^2(t)}{2\sigma^2} + \frac{m^2}{2\sigma_1^2}\right)\right]\sum_{n=0}^{\infty}\sum_{K=0}^{\infty}\frac{(K+n)!}{2^{2(k+n)}(K! \cdot n!)}$$

$$\times \left(\frac{2\sigma_1^2\sigma^2}{\sigma_1^2 + \sigma^2}\right)^{K+n} \cdot \left(\frac{m}{\sigma_1^2}\right)^{2K} \cdot \left(\frac{A(t)}{\sigma^2}\right)^{2n} \qquad (8)$$

If a is not a random variable, from equation (7) we know that A(t) obeys the Rice distribution. If the radar beam is totally blocked of thick leaves, $U_t = 0$, from equation (5) A(t) follows a Rayleigh distribution. When the echo from fixed target is strong, i.e. $aA(t)/\sigma^2 \gg 1$, $ma/\sigma_1^2 \gg 1$, based on

$$I_0(x) = e^x/\sqrt{2\pi x} \ (x \gg 1) \quad \text{we get}$$

$$p(A(t)) = \frac{\sqrt{A(t)}}{B} \exp\left\{-\frac{[A(t)-m]^2}{2(\sigma_1^2+\sigma^2)}\right\}$$

where B is related to m, σ_1^2 and σ^2.

Conclusions

When designing an internal reference CW MTI system, it is feasible to use the cubic clutter frequency spectrum to estimate its bandwidth based on clutter attenuation and slow moving target detection requirements. A ground MTI system can use a dual orthogonal channel correlation method to raise the improvement factor of the system. The price to pay is an increase in the effective observation time. Therefore, it is only suited for slow scanning, such as a fixed spot surveillance system.

Equation (8) can be used to estimate the false alarm probability based on the tree clutter amplitude distribution. The effect of different trees on δ_1, δ and m still must be further studied.

REFERENCES

1. M.W. Long: Radar Reflectivity of Land and Sea, Lexington, Health Inc., pp 40-47, 143-168, 1975.

2. M.P. Warden, B.A. Wyndham: A Study of Ground Clutter Using a 10cm Surveillance Radar, AD-704874, 1969.

3. W. Fishbein et al.: Clutter Attenuation Analysis, MTI Radar, pp 331-354, Artech House, Inc., 1978.

4. M.I. Skolnick(?): Radar Handbook, Defense Publishing Co., Vol 7, 1978.

5. Northwest Institute of Electrical Communications, Editing Group for [Radar handbook], Radar Systems, Defense Publishing Co., 1980.

6. N.C. Currie: AD-A012709, 1975.

7. David K. Barton: CW and Doppler Radar, Artech House, pp 83-87, 1978.

8. Zhang Xinbo [1728 2450 3134]: Analysis of Field Surveillance Radar Systems, Foreign Electronics, 1979.

9. Lin Maoyong [2651 5399 1661] and Ke Youan [2688 2589 1344]: Radar Signal Theory, pp 13-29, Defense Publishing Co., 1981.

10. A.V. Oppenheim: Digital Signal Processing, Prentice-Hall, Inc., 1975.

11. Wu Xinyao [0702 2450 5069] et al: Statistical Radio Technology, Defense Publishing Co., 1980.

SECONDARY ELECTRON EMISSION CHARACTERISTICS IMPROVED BY ION IMPLANTATION

[Article by Liu Xianghuai [2692 5980 2037] and Zou Shichang [6760 0013 2490], both of Shanghai Institute of Metallurgy, Chinese Academy of Sciences, and Tu Yushan [1458 5124 0810] of Institute of Electronics, Chinese Academy of Sciences, manuscript received Nov 84, revised Jun 86: "Improvement of Secondary Electron Emission by Ion Implantation"]

[Text] Abstract: Chromium ion implantation is used to improve the oxidation resistance and the secondary electron emission characteristics of the copper grid in a television camera tube. Compared to the graphite evaporation technique, this method is superior and more practical.

The grid in front of a television camera tube must have a low secondary electron emission coefficient. At 300°C in vacuum, it must have good oxidation resistance and adequate mechanical integrity. It is a key component which ensures the clarity and uniformity of the picture. The cathode grid of a travelling wave tube and the collectors of other vacuum devices also ought to be made of low electron emission materials. Usually, a high melting point metal is used as the substrate of the grid. It is then covered with a coating. Thus, the grid has not only the desired mechanical strength but also improved surface characteristics, including large radiation coefficient, high escape energy and low secondary emission coefficient. However, the coating process involves many steps and the yield is poor. It peels off at high temperatures. We successfully investigated a method to improve the secondary electron emission coefficient and the oxidation resistance of the grid by ion implantation. This is the first in China. To date, we have not seen any such work reported abroad.

Oxide-free copper grids and mechanically mirror polished oxide-free 10 mm diameter copper rods were used in the experiment. The natural surface oxide film was removed by a 1 percent chromic acid solution. After rinsing with deionized water and alcohol, the specimens were dried. They were implanted with Cr+ ions at 50 kV and $1 \times 10^{17}/cm^2$ in energy and dose, respectively. The beam density is limited to within $1 \ \mu A/cm^2$ to avoid overheating the target. The copper rod looked bright gold in color after Cr+ ion implantation. The copper grid appeared light gray.

Pure and Cr+ ion implanted copper specimens were placed in a glove box at 20-22°C and 80-90 percent humidity for a month and a half to allow natural oxidation to occur. The surface of the bright pure copper specimen was seen to gradually cloud up by an oxide film. The surface of the Cr+ ion implanted specimen still remained bright as before. In a high temperature oxidizing furnace with a quartz scale, the specimens were oxidized at 300°C. The oxide film peeled off the surface of the unimplanted specimen, while the Cr+ ion implanted specimen did not show such a phenomenon. Figures 1 and 2 [Fig. 2 not reproduced] show the reflectance curves and the metallographs of the polished pure and Cr+ ion implanted specimens after 4 hours of oxidation at 450°C. In the visible light range, the reflectance of the unimplanted specimen is only 2-6 percent of its original value after thermal oxidation. The oxide film is dark. It bulges and peels off easily. The reflectance of the Cr+ ion implanted copper specimen remained at 20-30 percent of its original value after thermal oxidation. The oxide film is light gray. The surface is clean and homogeneous.
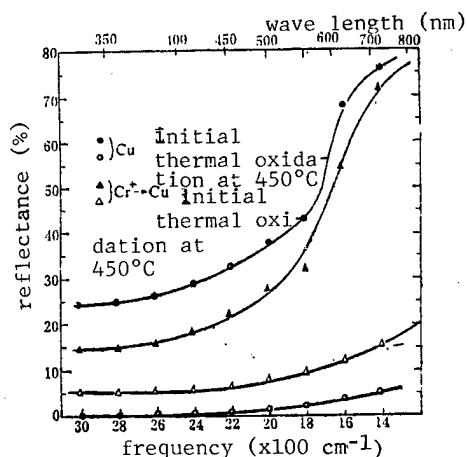
Fig. 1. Reflectance Change after 4 Hours of Oxidation at 450°C

Our measurements showed that the secondary electron emission coefficients of Cr+ ion implanted copper specimen are generally lower than those of the unimplanted specimen over the entire voltage range. At the normal operating voltage of the copper grid, 750 V, the secondary emission coefficient of the Cr+ implanted grid is lowered to 1.1 from 1.3 (see Figure 3). It is already at the normal operating requirement level and is close to that of a graphite evaporated grid.

Considering the complexity of the graphite process, the low yield and the peeling of the coating in use, it is both academically and practically worthwhile to pursue the improvement of the secondary emission of the copper grid in a television camera by ion implantation.
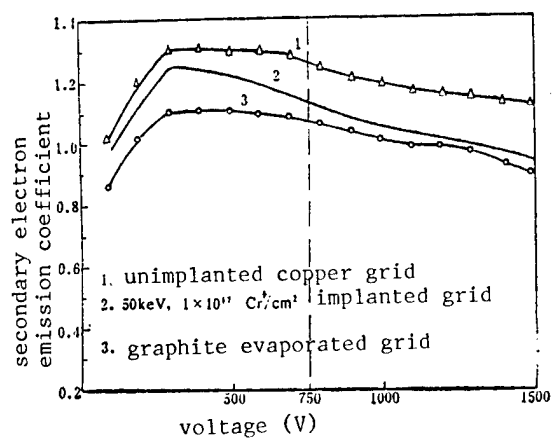
Fig. 3.   Secondary Electron Emission Coefficient vs. Voltage

The change in the secondary electron emission characteristics after ion
implantation is related to the change in its escape energy.   The introduction
of carbon, which has a high escape energy, to the specimen by ion implantation
will further lower the secondary electron emission coefficient.   Further study
will continue.

12553/7358

42

METHOD FOR CHARACTERIZING END-PLATE SURFACE RESISTANCE OF DIELECTRIC RESONATOR

[Article by Xu Deming [1776 1779 0682] and Li Zhaonian [2621 0340 1628] of Shanghai University of Science and Technology, manuscript received Feb 85, revised Apr 86: "A Novel Method for Characterizing End-Plate Surface Resistance of a Dielectric Resonator"]

[Text] Abstract: A novel method for characterizing the surface resistance of two conducting plates shorted at both ends of a dielectric resonator is given in this paper. It utilizes only one dielectric resonator that can resonate in both $TE_{012}$ and TE_{021} mode at the same frequency. The theoretical relations and experimental results are also given. The described method, when compared to the dual resonator method, has been proven to be convenient, relatively accurate and of practical usefulness.

1. Introduction

In 1977, the International Electrical Committee (IEC standard d377-2) recommended that materials with dielectric constant $\varepsilon_r > 5$ and operating at above 3 GHz be tested by using an open cavity method [1]. But, we often run into problems when measuring the loss characteristics of a low loss material. The primary problem is the accurate determination of the surface resistance of the two end plates of the cavity. Although it would be straight forward if a material of known loss is used to make the cavity so that the surface resistance can be determined, yet this material is difficult to obtain. In 1976, reference [2] reported that a material was used to fabricate two resonators with identical frequency in TE_{011} and TE_{012} or TE_{013} mode to determine the surface resistance. However, it is not easy to guarantee that both resonators are identical in material and size. The described method is a novel approach which employs a single dielectric resonator that can operate in both TE_{012} and TE_{021} mode to determine the end-plate surface resistance. (The authors named it the single cavity dual mode method.) It can avoid or alleviate the problems described above. The method was proven to be correct and feasible experimentally.

2. Principle

Figure 1 shows the mode patterns for a resonator with both ends shorted. In the diagram we can see that TE_{012} and TE_{021} have similar resonance frequencies at $(D/L) = 3.8$ (where D is the diameter of the resonator and L is its height). According to the following equations [3]:

$$\mathrm{tg}\,\delta = \frac{A}{Q_0} - B \qquad (1)$$

$$A = 1 + \frac{1}{\varepsilon_r} F(a) \cdot G(\beta) \qquad (2)$$

$$B = \frac{R_s l^2}{2\pi f^\delta \mu \varepsilon_0 \varepsilon_r L^3}[1 + F(a) \cdot G(\beta)]$$

$$= R_s B' \qquad (3)$$
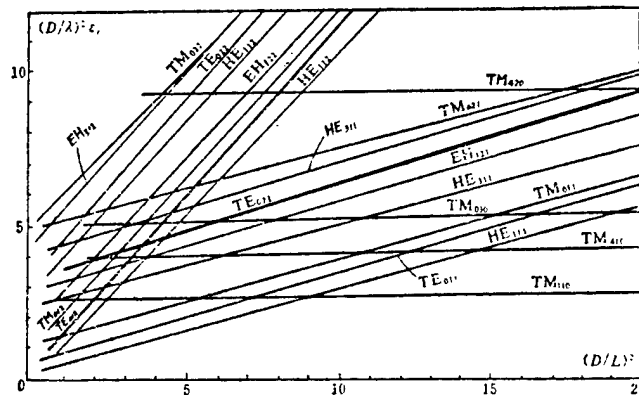
Fig. 1.   Mode Patterns for Resonator with Both Ends Shorted

$$F(a) = \frac{J_1{}^2(a_n)}{[J_1{}^2(a_n) - J_0(a_n) \cdot J_2(a_n)]} \quad (4)$$

$$G(\beta) = \frac{[K_0(\beta_l) \cdot K_2(\beta_l) - K_1{}^2(\beta_l)]}{K_1{}^2(\beta_l)}$$

$$(5)$$

a_n and β_l are the solution to the transcendental equation

$$a\frac{J_0(a)}{J_1(a)} = -\beta\frac{K_0(\beta)}{K_1(\beta)}$$

a_1 and β_1 correspond to the TE_{011} mode, and a_2 and β_2 to the TE_{021} mode. The equations for TE_{012} and TE_{021} mode are

$$\mathrm{tg}\,\delta = \frac{A_{01}}{Q_{01}} - R_s B_{01}' \qquad (6)$$

$$\mathrm{tg}\,\delta = \frac{A_{02}}{Q_{02}} - R_s B_{02}' \qquad (7)$$

44

Since the resonance frequencies of the two modes are almost identical, their dielectric loss characteristics are also the same. The surface resistance expression can be obtained by simultaneously solving equations (6) and (7):

$$R_s = \frac{A_{02}/Q_{02} - A_{01}/Q_{01}}{B'_{02} - B'_{01}} \qquad (8)$$

Where Q_{01} and Q_{02} are the load free quality factors in the TE_{012} and TE_{021} mode, respectively. A_{01}, A_{02} and B'_{01}, B'_{02} are the values of equations (2) and (3) corresponding to mode TE_{012} and TE_{021}, respectively. The value of ε_r can be calculated by the TE_{012} or TE_{021} mode field equation [3]. Or, we can take the mean value.

However, it is not only difficult to design and fabricate the resonator but also hard to measure Q (to be discussed in detail later) to make the two resonance frequencies identical. To this end, the two frequencies are designed to be very close, such as several dozens to 100 MHz different. In this narrow frequency range, in most cases, the loss is considered identical or very close. Therefore, equation (8) is still applicable.

One of the reasons why modes TE_{012} and TE_{021} are chosen is because they both belong to TE_{on1} mode. There is only electric field in the ϕ direction (in cylindrical coordinate r, ϕ, z). Hence, it is not necessary to consider the capacitive load at the end plate gap. Thus, a source of error is eliminated. Another advantage is that although TE_{012} and TE_{021} belong to higher order modes, the quality factor Q_o is around 4000 – 6000. The Q is at a medium level which is easier to measure. If higher order modes such as TE_{022} and TE_{031} are chosen, it will be more difficult to determine the mode and the Q value.

3. Experimental Method and Results

We used an alumina ceramic cavity in the measurement. It is designed that (D/L) is slightly larger or smaller than 3.8. As described before, if the two resonance frequencies overlap or are very close, the modes will interfere with each other and affect the accuracy of measuring Q. Therefore, it is more appropriate to separate them by several dozens to 100 MHz. The test system is equipped with frequency and amplitude stabilizing devices to raise accuracy. The requirements in specimen fabrication are the same as those stated in reference [4].

Mode Determination: Based on the known resonance frequency, the resonance peaks for modes TE_{012} and TE_{021} can be found. Then, excitation or detection rings can be placed simultaneously at half height and quarter height. It is possible to distinguish the TE_{012} mode from the TE_{021} mode based on how the resonance peak amplitude varies.

All measurements were made on a delicate test rack. The method and error analysis can be found in references [2] and [5]. The surface resistance values of brass and red copper were measured. The surface finish is ∇10 and ∇9 for red copper as shown in Table 1. The surface resistance for red

45

copper is higher compared to the values published elsewhere. This is because the finish on the red copper end plate is not satisfactory. It is not as easy to machine as the brass end plate. Nevertheless, when using the open cavity method, if the actual surface resistance of the end plate is determined, the accuracy in measuring the dielectric loss can be improved. Therefore, although the measured R_S value for red copper is high, yet the dielectric parameter measured is still consistent with that obtained with brass. Table 2 shows the results on other materials with the two types of end plates.

Table 1. Determination of Surface Resistance with Two End Plates

End plate material	Operating mode	Resonance frequency (MHz)	Surface resistance (Ω)
brass	TE_{012}	9683.55	5.53×10^{-2}
	TE_{021}	9525.84	
red copper	TE_{012}	9686.14	3.14×10^{-2}
	TE_{021}	9531.23	

Table 2. Results on Materials Measured with Two Types of End Plates

Specimen	Operating mode	Resonance frequency (MHz)	ε_r	ε_r ref.[6,7]	$tg\delta$	$tg\delta$ ref.[6,7]	Remark
single crystal quartz (E optical axis)	TE_{012}	9824.50	4.53	4.55	1.07×10^{-4}	$<2 \times 10^{-4}$	brass
95% alumina	TE_{021}	9526.87	9.01	9.00	2.19×10^{-4}	$(2\sim5) \times 10^{-4}$	
pure alumina	TE_{012}	9296.20	10.03	9.90	2.07×10^{-4}	$(1\sim2) \times 10^{-4}$	
zirconium tin titanate	TE_{012}	8933.83	$37.2\sim39.8$	$36.8\sim38.9$	2.02×10^{-4}	1.6×10^{-4}	
single crystal quartz (E optical axis)	TE_{012}	9821.61	4.53	4.55	9.6×10^{-5}	$<2 \times 10^{-4}$	red copper
95% alumina	TE_{021}	9531.23	9.01	9.00	2.14×10^{-4}	$(2\sim5) \times 10^{-4}$	
pure alumina	TE_{011}	9286.7	10.05	9.90	2.3×10^{-4}	$(1\sim2) \times 10^{-4}$	
zirconium tin titanate	TE_{012}	8934.51	$37.2\sim39.8$	$36.8\sim38.9$	2.11×10^{-4}	1.6×10^{-4}	

REFERENCES

1. IEC standard publication 377-2, 1977.

2. Yoshio Kobayashi and Shuzo Tanaka: Journal of Japanese Society of Electronic Communications, J59-B, pp 223-230, No 4, 1976.

3. B.W. Hakki and P.D. Coleman: IRE Trans.; Vol MTT-8, pp 402-410, July 1960.

4. W.E. Courtney: IEEE, Trans.; Vol MTT-18, pp 476-485, August 1970.

5. Xu Deming and Li Zhaonian: Chinese Journal of Instrumentation, Vol 5, No 4, pp 416-419, 1984.

6. "Development of Electronic Ceramics in Other Nations", 1973, 12.

7. MARTIN, STIGLITZ: Microwave Journal, Vol 24, pp 19-26.

12553/7358

FIRST REPORT ON InGaAs HALL DEVICE

[Article by Zheng Yiyang [6774 0001 7122], Zheng Jinchang [1728 6651 2490], Liu Yanfang [0492 5888 5364], Peng Shaojin [1756 1421 6602] and Lu Wenhong [4151 2429 1347] of the Institute of Semiconductors, Chinese Academy of Sciences, and Shen Guixian [3088 2710 6343], Zhang Yingzhu [1728 4481 4554], Su Guixiang [5685 2710 4382] and Jia Kuiyou [6328 1145 0645] of Xuanhua Factory No. 701, Hebei; manuscript received in July 1985 and revised in March 1986: "A Highly Sensitive In0.53Ga0.47As Hall Device"]

[Text] Abstract: This paper reports for the first time that a Hall device has been prepared with InGaAs by planar technology. At the same carrier concentration, the sensitivity of InGaAs is 50 percent higher than that of a GaAs Hall device. Its energy consumption is low and its ohmic contact is good. It can operate in a wide temperature range (4 to 480 K or -50 to 200 C) because of its high carrier mobility and low temperature dependence characteristics. Although it has a narrower bandgap, it has a lower contact potential barrier. At 4 K, the device can operate in a strong magnetic field of up to 80 kG. The magnetic density of such a InGaAs Hall device was determined to be up to 80 kG at 4.2 K.

Because of its high electron mobility and high electron saturation rate, GaAs is widely used in high speed logic devices, microwave devices and Hall devices [1-3]. On high resistance InP substrate, epitaxial InGaAs layer of matched lattice grown from the liquid phase has higher electron mobility and saturation rate than GaAs at room temperature over a wide doping range. Therefore, it has already been used to make high performance MESFET and transferred electron devices [4,5]. Its advantages have been demonstrated.

This is the first report of using InGaAs to make a Hall device. At the same concentration, its sensitivity is 40-50 percent higher than that of GaAs. In addition, it can operate at above 80 kG at 4 K.

I. Device Fabrication

InGaAs is grown epitaxially from the liquid phase onto a high resistance InP substrate. Thus, lattice matching is more difficult than the epitaxial growth

48

of GaAs on Cr doped high resistance GaAs substrate. If the high resistance
InP substrate is not properly chosen, the performance of the device will be
adversely affected. Figure 1 shows the leakage current versus voltage curves
at 300 K and 520 K. We can see that the GaAs substrate is better than InP.
Because the lattice was mismatched in the growing process of InGaAs, there-
fore, we must choose high quality InP substrates.

The Schottky barrier height of InGaAs, which is 0.28 eV, is lower than that of
GaAs. Therefore, it is easier to make the ohmic contact. The metallic
AuGe/Au system is still used in making the ohmic contact. It is metallized
at 450°C in a closed H_z atmosphere for 30 seconds to 1 minute. The alloying
time is slightly less than that for GaAs. Its contact resistance is approxi-
mately 50 percent lower than that of GaAs at the same concentration, which
improves the performance of the device.

leakage
current
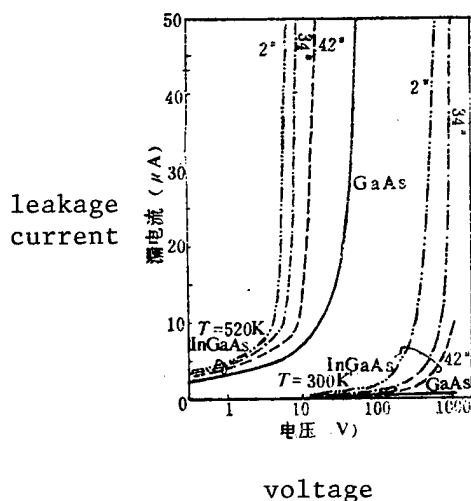
voltage

Fig. 1. Leakage Current vs. Voltage Curves for GaAs and InP Substrates

II. Test Results

1. Sensitivity

At the same concentration, the mobility of InGaAs is 40-50 percent higher than
that of GaAs. As a result, the Hall device thus prepared has a higher sensi-
tivity.

Sensitivity is an important indicator for Hall devices. Among GaAs materials,
only $10^{15} cm^{-3}$ materials can have mobility of 8000 $cm^2/V \cdot s$. The sensitivity
of a 1 kΩ internal resistance device can be as high as 30 mV/mA·kG. The
epitaxial layer is usually more than 10 μm.

The mobility of 10^{16} cm^{-3} inGaAs materials can reach 8000 cm^2/V·s. When the internal resistance is 1 kΩ , the sensitivity is 30 mV/mA kG. In this case, the concentration is higher and the film may be thinner, approximately 305 m. Thus, the potential difference is lower after etching. It is easier to form the ohmic contact. Moreover, it is less affected by light which is better for the stability of the device.

Figure 2 shows a comparison of the sensitivity of an InGaAs Hall device to that of a GaAs device. We can see that in the range from 10^{16} cm^{-3} to 10^{17} cm^{-3}, the sensitivity of InGaAs is 40-50 percent higher than that of GaAs. Hence, at the same Hall output, the former consumes less energy and generates less noise.

sensitivity
(mV/mA kG)

carrier concentration (cm^{-3})
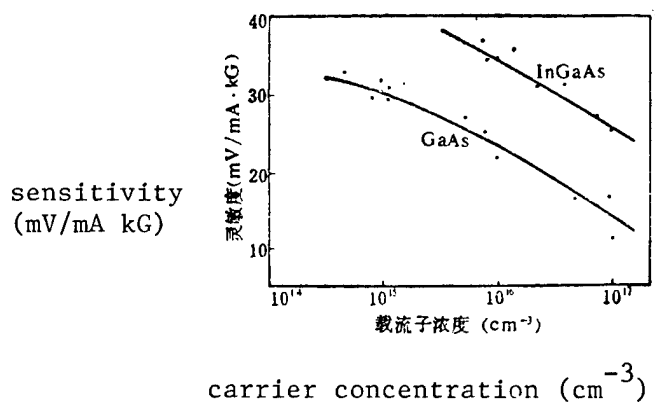
Fig. 2. Comparison of Sensitivities of InGaAs and GaAs Hall Devices

2. Temperature

GaAs Hall devices have better temperature characteristics [3]. InGaAs devices are slightly inferior. Figure 3 shows the relations between the output of the Hall device, anisotropic potential and internal resistance versus temperature. The device can usually operate within 200°C. Because mobility decreases as the temperature drops, its resistance has a positive temperature coefficient. The resistance drop at over 200°C is due to the thermal excitation of the carrier. The increase in internal resistance causes the bias of the device to go up, and the absolute value of the anisotropic potential to increase as well. At above 200°C the anisopotential also declines as a result of decreasing internal resistance. The temperature coefficient for internal resistance is 0.17%/°C.
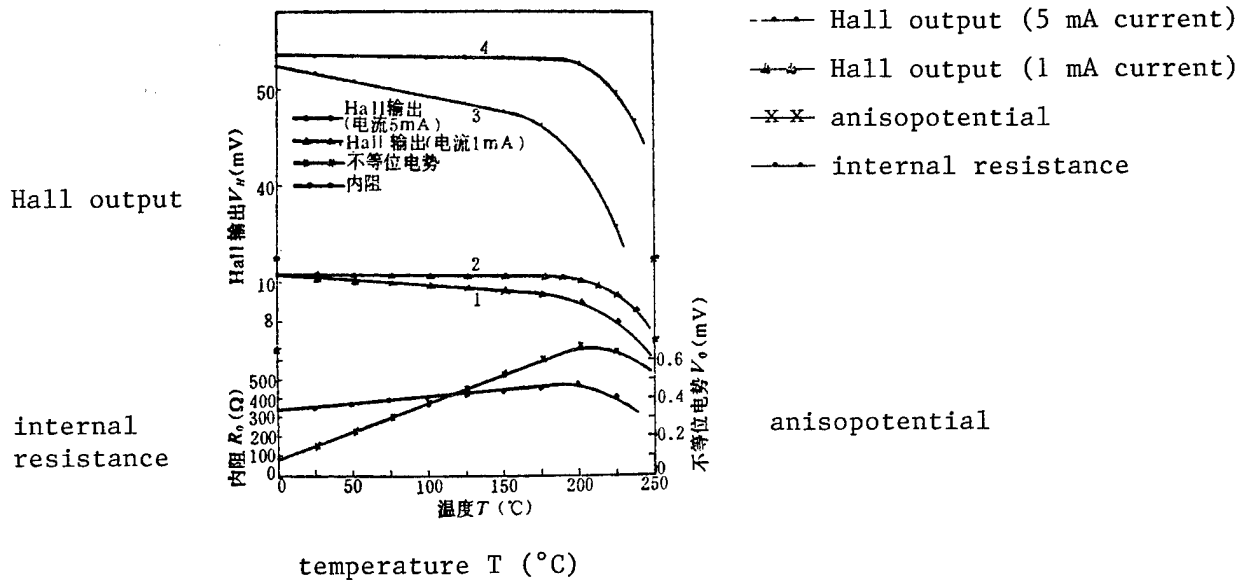
Fig. 3. Temperature Dependence of the Output, Internal Resistance and
Anisopotential of the InGaAs Hall Device

The temperature coefficient of the Hall output is also an important parameter,
which includes its sensitivity and anisopotential.

$$V_H = \pm K_H (I \times B) \sin \varphi \pm V_c$$

where the sign of the term $K_H(I \times B) \sin \varphi$ is determined by the direction of
the magnetic field. The sign of the anisopotential V_0 is determined by the
asymmetry of the device itself and the direction of the current. Usually,
when the current direction is defined, the sign of V_0 is also relatively
determined. Thus, the Hall output is either the sum or difference of its
sensitivity and anisopotential. When the anisopotential is large, the Hall
output varies significantly in different magnetic field directions. Hence,
we must separately discuss the temperature coefficient of the Hall output and
that of sensitivity. As we analyze the characteristics of the device, we
often discuss the temperature coefficient of sensitivity. In this case, we
do not take anisopotential into consideration. Therefore, the sensitivity
temperature coefficient is usually negative. In actual practice, we cannot
avoid anisopotential. When the negative temperature coefficient of sensi-
tivity is offset by the positive temperature of anisopotential, a positive
temperature may result. We measured the temperature coefficient of the Hall
output V_H of an InGaAs Hall device with a very small anisopotential and found
it to be $-(2 - 3) \times 10^4$ /°C. Because of the low anisopotential, the tempera-
ture coefficient of the Hall output is close to the temperature of coefficient
of sensitivity K_H.

Figure 3 shows the temperature coefficient of an InGaAs Hall device with a larger anisopotential. It plots out the relationship between Hall output and temperature at two current levels: 1 mA and 5 mA. When the operating current is 1 mA, there are two Hall outputs. When the sign of anisopotential coincides with the Hall output and the temperature change patterns are similar, the temperature coefficient is poor, i.e. $-5.2 \times 10^{-4}/°C$, as shown in Figure 1. When the temperature variation patterns differ, a smaller temperature coefficient results due to the offset. For instance, sensitivity decreases, anisopotential increases, with increasing temperature. They have opposite signs. As a result of the offset, the temperature coefficient may be very small. As shown in Figure 2, it is $-0.53 \times 10^{-4}/°C$ at below 180°C. Let us take the mean value as $-2.86 \times 10 /°C$ to represent the temperature coefficient of sensitivity.

The temperature coefficient of the Hall output becomes less desirable when the current increases. Curves 3 and 4 in the figure correspond to an operating current at 5 mA. The temperature coefficients are $-6.2 \times 10^{-4}/°C$ and $-0.6 \times 10^{-4} /°C$, respectively. The mean value is $-3.4 \times 10^{-4}/°C$. This indicates that the power consumption of the device at a higher current causes the internal temperature to rise.

3. Magnetic Linearity and Current Linearity

The ambient temperature magnetic and current linearity characteristics of the InGaAs Hall device are comparable to those of the GaAs device. Figure 4(a) shows the magnetic linearity of device 85-2# at 300 K. It is less than 0.5 percent within 100 kG. The current linearity is less than 0.3 percent under 10 mA. At 78 K, both internal resistance and anisopotential are small. Therefore, the linearity is even better.

Figure 4(b) shows the magnetic linearity at 4.2 K. Limited by the low temperature superconducting magnetic field, we only measured up to 80 kG which is the maximum attainable. Although it was reported in reference [6] that an ion implanted GaAs Hall device could operate up to 90 kG at 4.2 K, however, the actual data measured was 68 kG. It is very convenient to measure in a superconducting low temperature magnetic field. Between 10 kG to 30 kG, the plot shows some deviation from linearity. The cause is still yet to be investigated.
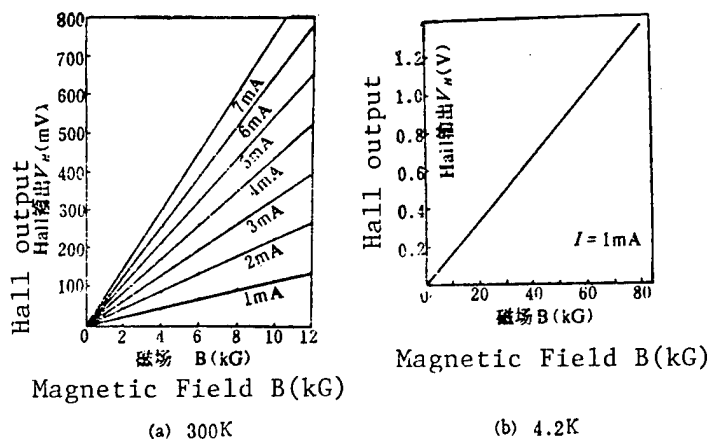

(a) 300K   (b) 4.2K

Fig. 4. Magnetic Linearity of the Device

4. Anisotropic Potential

In an epitaxial layer of identical thickness, the internal resistance of a device made of a lower carrier concentration material is higher. Correspondingly, its anisopotential is also larger. High concentration, low resistance devices, however, have smaller anisopotentials. Anisopotential is primarily due to geometrical asymmetry of the device and its ohmic contact. For the same device, anisopotential and internal resistance are also rigorously related. When temperature varies, the change in internal resistance will directly affect the change in anisopotential.

The equivalent circuit of a Hall device is a bridge circuit. An imbalance of the bridge causes an anisopotential. As the current passing through the device increases, the anisopotential also rises. It approximately obeys Ohm's law. However, it is also sensitive to other physical parameters such as light and heat. Especially when the anisopotential is very low, it is particularly susceptible to outside interference.

When measuring the anisopotential, the device must be shielded from magnetism and light. Figure 5 shows the relation between anisopotential and current. It is usually linear in devices with larger anisopotentials (such as specimens 3#, 4#, and 5#). It deviates from linearity only when the operating current is high.

anisopotential V (mV)

operating current I (mA)
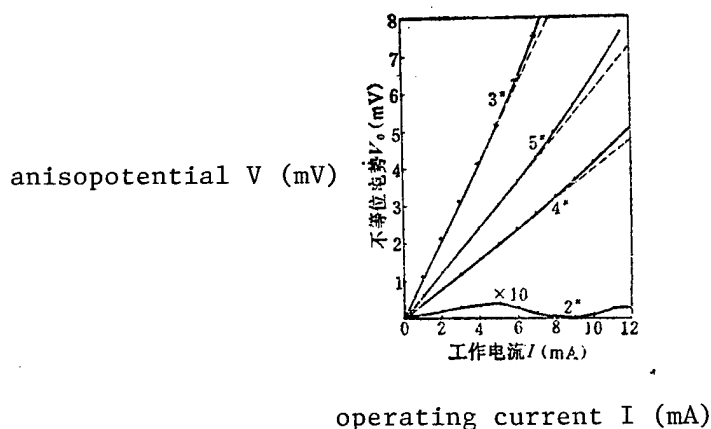
Fig. 5. Anisopotential vs. Current

When the anisopotential of the device is very low, such as specimen 2#, its anisopotential reaches a maximum at 4 mA. This is determined by various factors in the device. There are no specific laws to follow.

At below ambient temperature, because of increasing mobility, decreasing internal resistance and decreasing applied bias, anisopotential also declines. However, InGaAs is different from GaAs. GaAs has a minimum at around 100 K - 120. Beyond this point, the resistance begins to rise gradually again because electron mobility decreases and resistance increases with decreasing temperature until liquid helium temperature is reached. The minimum for InGaAs occurs at approximately 50 - 60 K. Therefore, it remains monotonic up to 77 K.

Table 1 shows the anisopotential, sensitivity, internal resistance and unit impedance sensitivity data of 2×10^{16} cm^{-3} GaAs and InGaAs devices, at 300 K, 77 K and 4.2 K.

Table 1

specimen no.	temperature (K)	sensitivity (mV/mA·kG)	ansio-potential (mV)	output resistance (Ω)	unit impendance sensitivity (mV/mA·kG·kΩ)
GaAs Hall	300	8.35	0.27	450.6	18.17
85-1*	77	10.38	0.03	187.8	55.27
InGaAs Hall	300	10.36	0.38	355.7	29.13
	77	11.32	0.13	131.9	85.82
85-4*	4.2	17.1	0.30	300.0	51.3
InGaAs Hall	300	11.08	0.87	432.6	27.01
	77	12.79	0.31	161.5	79.23
85-5*	4.2	16.7	0.05	352.0	58.78

From the table we find that although the internal resistance of the device is much smaller at 77 K than at 300 K, yet its sensitivity is still higher than at 300K. It also shows that sensitivity increases with decreasing temperature up to 4.2 K. However, unit impendance sensitivity does not peak at 4.2 K because the internal resistance of the device is not the lowest at 4.2 K. Correspondingly, at 4.2 K the anisopotential is not the minimum.

The InGaAs material used in this work was supplied by Li Jinshu [2621 6855 3219] of Institute 46 of Tianjin Electronic Industry Department. Devices were fabricated by the 6th workshop in the 701 Factory in Xuanhua, Hebei, Giving assistance in low temperature measurements was Jiang Peichuan [3068 0160 3883]. The authors wish to acknowledge their contribution and express their gratitude.

REFERENCES

1. N. Matsuda, N. Akigama, T. Konno: JEE, No. 149, p 38, 1979.

2. A. Hojo, S. Tanaka, I. Fujui: Proceedings of the 7th Conference on Solid State Devices, Tokyo 1975. Supplement to Japanese Journal of Applied Physics, Vol 15, p 261, 1976.

3. Zhenh Yiyang, Zhang Jinchang and Liu Yanfang, [Journal of Semiconductors], Vol 6, No 4, p 413, 1985.

4. W. Kowalsky, A. Schlachetzki: Electron Lett., Vol 27, p 187, 1984.

5. W. Kowalsky, A. Schlachetzki, H.H. Wehmann: Solid-State Electron, Vol 27, No 2, p 187, 1984.

6. T. Hara, Minorn Mihara, N. Toyoda, M. Zama: IEEE Trans., Vol ED-29, No 1, pp 78-82, 1982.

12553/7358

NUMERICAL MODELING OF DIVERGENT DETONATION WAVE

[Article by Li Zhiwei [2621 2535 0251] and Liu Bangdi [0491 6721 1717] of the Institute of Applied Physics and Computational Mathematics; received 6 June 1984; revised manuscript received 10 October 1984]

[Text] Abstract: This paper briefly describes the indefinite nature of divergent detonations under the assumption of instantaneous stable detonation. In the numerical modeling method for divergent detonation we have improved the artificial cohesiveness and used the Cochran reaction rate and the JWL equations of state to describe the ignition process of the explosion. Several typical divergent detonation problems were computed obtaining rather satisfying results.

I. Introduction

In practical work, the process of divergent detonations and their interactions is encountered frequently. In recent years, many foreign detonation physics researchers have carried out a large amount of numerical modeling work on divergent detonation processes.[1] Our previous numerical modeling of divergent detonation processes was based on the C-J theory. When making concrete computations we adopt an artificially controlled initiation function and equations of state of the form p = Aρ together with artificial cohesiveness to process steep detonation wavefronts into the more gradual adjoining exoergic process transition zone. This sort of processing method can give rather good computation results for one dimensional detonation processes. However, for divergent detonation processes, especially two dimensional divergent detonation processes, it cannot provide correct results. In order to compute divergent detonation processes, this paper introduces a numerical modeling method, improving the artificial cohesiveness as well as using the chemical reaction rate provided by Cochran et al.[2] and the JWL equations of state to model the explosion volume exoergic process. The paper emphasizes accounts of the tests we have made of numerical modeling work on the divergent detonation process.

II. The Indefinite Nature of Divergent Detonation Waves

For conditions of a plane explosion, the detonation propagation after the explosion ignition is primarily manifested in explosion pressure and the explosion rate propagation is smaller.[7] Unlike a plane explosion, the explosion propagation of a divergent detonation wave or curved divergent detonation wave produced from a point initiation as manifested after ignition, when the radius of curvature of the wavefront is small, is such that the explosion speed and the explosion pressure will both increase with the radius of wavefront curvature.[3,5] We know from a qualitative analysis that because the divergent detonation wavefront has a certain size radius of curvature, there must therefore be area effects apparent in its propagation process. Comparable to a plane detonation, in the conservation relationship, there is one extra area term. This leads to a difference between the chemical reaction processes in a divergent detonation wavefront and plane conditions: the combustion process of a plane detonation wave takes place in a Rayleigh straight line while the combustion process for a divergent detonation takes place along the line $Z_1 L$ in Figure 1. From the conservation relationships satisfied by a divergent detonation process we can get that the slope of $Z_1 L$ must be less than the slope of the corresponding Rayleigh line, that is

$$- \frac{dP}{dV} \Big|_{\text{along } Z_1 L} \leqslant \rho_0^2 D^2 \Big|_{\text{along } Z_1 O}$$

(As the radius of curvature of the wavefront tends to infinity, this becomes an equality.) The area effect of a divergent detonation wave causes the explosion pressure and explosion rates to fall. With increasing propagated distance, the wavefront radius of curvature increases, the area effect correspondingly decreases, the explosion pressure and rate gradually increase and approach that of a plane detonation wave. K.E. Gubkin of the Soviet Union considered the effect of chemical reaction breadth on the explosion rate, obtaining from theory the relationship between the explosion rate and the wavefront's radius of curvature, R.[3]

$$D(R) = D_j \left(1 - \frac{8 \gamma^2}{\gamma^2 - 1} \frac{l_0}{R} \right). \tag{2.1}$$

in which D_J is the plane C-J explosion rate, γ is the explosion product multiple index, l_0 is the chemical reaction breadth of the explosive, and R is the wavefront's radius of curvature.

Based on the Z-N-D model, we can take this sort of low pressure, slower explosion rate detonation wave and view it approximately as a Rayleigh process corresponding to a certain degree of reaction $F = \beta$, with a combustion process proceeding along $Z_1 O$, and incomplete combustion. That is, we use a series of instantaneous stable detonation processes to describe approximately the entire unstable process of a divergent detonation.
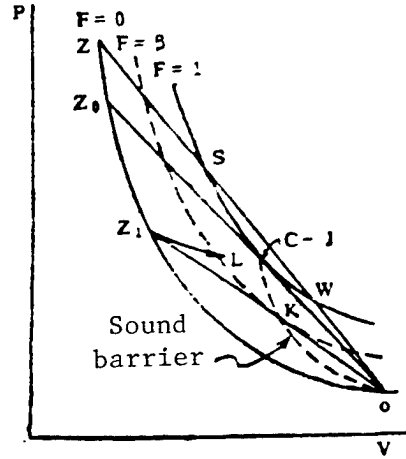
Figure 1.   Combustion process with a divergent detonation wave

In order to establish the relationship between explosion rate and explosion pressure in a divergent detonation process, we simply discuss the relationship between the various state parameters within the reaction zone and the degree of reaction F.   Consequently, we can better understand the physical meaning of the above approximation process.   Because the chemical reaction zone breadth of the detonation wave is larger than the average free path of a molecule, in any plane within the reaction zone we can apply three conservation relationships to study the question.   Letting the explosive degree of reaction $F = \beta$ at a certain cross section within the reaction zone, ignoring the initial explosive pressure, P_0, and internal energy, e_0, then for the two sides of the area between the leading edge of the wavefront and the said cross section, we have

$$D/V_0 = \frac{1}{V}(D - u),$$ (2.2)

$$p = \frac{1}{V_0}Du,$$ (2.3)

$$e = \tfrac{1}{2}p(V_0 - V) + FQ.$$ (2.4)

Supposing that the mix of the explosive and the product satisfies the equation of state

$$p = (\gamma - 1)\rho e_\circ$$ (2.5)

in which D is the explosion rate, V is the specific volume of the mix, u is the particle speed, p is the explosion pressure, e is the specific internal energy, F is the degree of reaction, and Q is the chemical energy of a unit mass explosive.   From this we get

$$p = \frac{1}{\gamma + 1}\frac{D^2}{V_0}\left[1 \pm \sqrt{1 - \frac{2(\gamma^2 - 1)FQ}{D^2}}\right]_\circ$$ (2.6)

58

If we let
$$2(\gamma^2 - 1)FQ = D^2, \tag{2.7}$$

then we obtain
$$p = \frac{1}{\gamma+1}\frac{D^2}{V_0}。 \tag{2.8}$$

Formula (2.6) gives the relationship between the explosion pressure with the explosion rate, D, as a parameter and the degree of reaction, F. It is actually just the Hugoniot curve on a p - F plane. From Figure 2 it is evident that when the explosion rate, D < D_J, the chemical reaction cannot be completely performed and a certain explosion rate, D, can only attain a maximum degree of reaction, F_{max} which is determined by formula (2.7)

$$F_{max} = \frac{D^2}{2(\gamma^2-1)Q}。 \tag{2.7}$$

Formula (2.8) is the relationship between explosion rate and explosion pressure. From this, with the aid of formula (2.1) after it gives the explosion rate D(R) corresponding with a certain wavefront radius, R, we can solve for F(R) from formula (2.7), that is

$$F(R) = \frac{D^2(R)}{2(\gamma^2-1)Q}, \tag{2.9}$$

and from formula (2.8) we get the corresponding explosion pressure

$$p(R) = \frac{1}{\gamma+1}\frac{D^2(R)}{V_0} \tag{2.10}$$

In form, formula (2.10) and the stable C-J detonation process relation are entirely identical, however, its physical significance is different. Formula (2.10) is the relationship between explosion rate and explosion pressure in a divergent detonation process when the degree of reaction corresponding to a wavefront radius R reaches F(R). We will make comparisons of results estimated using the above relationship and precise numerical results.
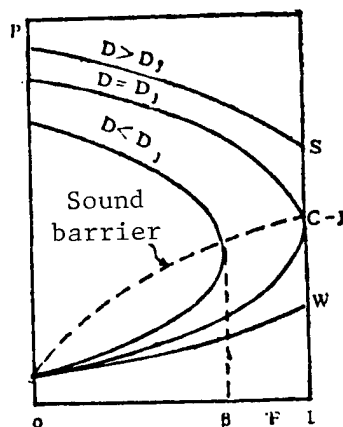

Figure 2. Hugoniot curve in the p - F plane

III. Basic Equations and Differencing Scheme

The longitudinal structure of a detonation wave still adopts the Z-N-D model where the detonation wave is composed from a leading impact wave and a closely following reaction zone. It is assumed that the chemical reactions within the reaction zone are single reaction processes and that the reactions are ordered, layered, developments with F = 0 at the leading impact wavefront and F = 1 at the end of the reaction zone. All points within the reaction zone reach local thermal equilibrium and the chemical reaction rate at each point is a function of the pressure and rate of reaction, F, at that point. The explosive and products each use different equations of state. In the reaction zone, the equations of state of the mixed material are added up from separately computed pressure components of ratios determined by the rate of reaction from the explosive and product equation state. Moreover, it is believed that the thermal energies of the explosive and of the reaction product which has not yet reacted are equal. In addition, we do not consider here the energy dissipation in the detonation process. The Lagrange fluid dynamics equations which carry this sort of Cochran chemical reaction rate are:

$$\rho \frac{\partial \vec{W}}{\partial t} = - \text{grad}\,(p+q),$$ (3.1)

$$\frac{\partial \vec{R}}{\partial t} = \vec{W},$$ (3.2)

$$\frac{\partial \rho}{\partial t} + \rho \, \text{div}\vec{W} = 0,$$ (3.3)

$$\frac{\partial e}{\partial t} = -(p+q)\frac{\partial\left(\frac{1}{\rho}\right)}{\partial t} + Q\frac{\partial F}{\partial t},$$ (3.4)

$$\frac{\partial F}{\partial t} = (1-F)\,(\omega_1 p^k + F\omega_2 p^m),$$ (3.5)

$$q = \begin{cases} \rho l^2 a^2 (\text{div}\vec{W})^2 & \text{div}\vec{W} < 0 \\ 0 & \text{div}\vec{W} \geqslant 0 \end{cases}$$ (3.6)

$$p = p(\rho, e).$$ (3.7)

In which t is time, $\vec{R}(x,r)$ is the spatial coordinate of the fluid, x is the axis of symmetry, r is radius of revolution, $\vec{W}(u,v)$ is the velocity of the fluid, e is internal energy of a unit mass, ρ is density, p is pressure, g is the artificial cohesiveness pressure, a is a constant, l is the characteristic length, F is the rate of reaction of the explosive, and ω_1, ω_2, k, and m are constants related to properties of the explosive. Equation (3.7) is the equation of state. The equations of state of the explosive are

$$p = (1-F)p_1 + Fp_{2_0}$$ (3.8)

$$p_1 = A_1\sigma^{\varepsilon_1} - B_1\sigma^{f_1} + g_1\rho\, e_T \quad \text{(explosive)} \tag{3.9}$$

$$p_2 = A_2 e^{-\varepsilon_2/\sigma} + B_2 e^{-f_2/\sigma} + g_2\rho e_T \quad \text{(product)} \tag{3.10}$$

in which e_T is the thermal energy of a unit mass and A_i, B_i, ε_i, f_i, and g_i ($i = 1, 2$) are constants related to properties of the explosive. Q in formula (3.4) is the chemical energy of a unit mass of explosive.

We can express the pressure as the sum of the cold pressure, p_x and the hot pressure, p_T.

$$p = p_x + p_{T_o}$$

in which

$$p_x = (1 - F)p_{1X} + Fp_{2x},$$

$$p_T = (1 - F)p_{1T} + Fp_{2T_o}$$

Taking the integral of pressure with respect of density and using e_x to represent the cold energy of a unit mass, we can get a corresponding energy expression. Using these relationships we note that

$$\frac{\partial e_x}{\partial t} = -p_x \frac{\partial}{\partial t}\left(\frac{1}{\rho}\right),$$

and energy equation (3.4) becomes

$$\frac{\partial e_T}{\partial t} (p_T + g)\frac{\partial}{\partial t}\left(\frac{1}{\rho}\right) = Q\frac{\partial F}{\partial t}. \tag{3.11}$$

The differencing scheme of the above equations is set up on a quadrilateral grid. Here R and W are defined at the corners of the grid and ρ, p, g, e, and F are defined at the grid centers. The area, S, volume, V, and mass, m, of the grid are naturally defined at the grid centers.
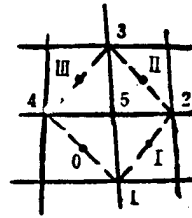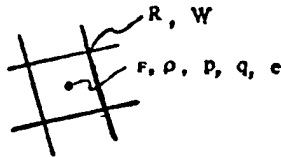
When establishing the difference equations, it is supposed that the relative positions of the grid are invariant. As the above figure shows, the quadrilateral region surrounded by dashed lines is denoted as S. In order to compute the velocity of point 5, equation (3.1) is integrated on S. Supposing that p = p + q has a first order derivative on S, then the right side can use the Green formula

$$\iint_S \text{grad}P dx dr = \phi_T P\, \vec{n}dl$$

61

in which Γ is the boundary of S, and l is arc length. Since $\rho > 0$, $\vec{W}$ is continuous, so

$$\iint\limits_S \rho \frac{\partial \vec{W}^n}{\partial t} dxdr \doteq \frac{1}{\Delta t} (\vec{W}_5^{n+\frac{1}{2}} - \vec{W}_5^{n-\frac{1}{2}}) \iint\limits_S \rho dxdr.$$

From here it is not difficult to obtain the following systems of difference equations

$$u_5^{n+\frac{1}{2}} = u_5^{n+\frac{1}{2}} - \frac{\Delta t}{(\rho S)_5} \{P_0 (r_1 - r_4) + P_I (r_2 - r_1) + P_{I\!I} (r_3 - r_2) + P_{I\!I\!I} (r_4 - r_3)\},$$

$$v_5^{n+\frac{1}{2}} = v_5^{n-\frac{1}{2}} + \frac{\Delta t}{(\rho S)_5} \{P_0 (x_1 - x_4) + P_I (x_2 - x_1) + P_{I\!I} (x_3 - x_2) + P_{I\!I\!I} (x_4 - x_3)\},$$

$$\vec{R}_5^{n+1} = \vec{R}_5^n + \Delta t \, \vec{W}_5^{n+\frac{1}{2}},$$

$$\rho = m/\nabla,$$

$$F^{n+1} = \frac{2F^n + (2 - F^n)\xi\Delta t}{2 + \xi\Delta t},$$

$$e^{n+1} = \frac{2Aq + Q(F^{n+1} - F^n) + (1 + \eta)e^n}{1 - \eta}.$$

in which the superscript n is the time index which represents the instant $t = \sum\limits_{k=1}^{n} \Delta t_k$ and is the time step used in computations.

$$A = \frac{1}{2}\left(\frac{1}{\rho^n} - \frac{1}{\rho^{n+1}}\right)$$

$$\xi = \omega_1 (P^n)^k + F^n\omega_2 (P^n)^m,$$

$$\eta = \frac{1}{2}A (\rho^{n+1} + \rho^n)[g_1 + F^{n+\frac{1}{2}} (g_2 - g_1)].$$

Reference [4] is a special study on a differencing scheme for artificial cohesiveness (3.6). The direction of fluid velocity increase through the grid center, α, makes a straight line and has two intersections with the grid boundaries. With the distance between these two intersections denoted as l and the velocity difference of these two intersections denoted as $\Delta\vec{W}$, the difference scheme for (3.6) is

$$q = \begin{cases} a^2\rho \, (\vec{\alpha} \cdot \Delta\vec{W})^2 & \vec{\alpha} \cdot \Delta\vec{W} < 0, \\ 0 & \vec{\alpha} \cdot \Delta\vec{W} \geqslant 0. \end{cases}$$

Substituting equation (3.3) into (3.6) gives

$$q = \begin{cases} a^2 l^2 \rho \left(\dfrac{\partial \rho}{\rho \partial t} \right)^2 & \dfrac{\partial \rho}{\partial t} > 0, \\ 0 & \dfrac{\partial \rho}{\partial t} \leqslant 0. \end{cases}$$

and its difference scheme is

$$q = \begin{cases} a^2 l^2 (\rho^{n+1} - \rho^n)^2 / \rho \Delta t^2 & \rho^{n+1} > \rho^n, \\ 0 & \rho^{n+1} \leqslant \rho^n. \end{cases}$$

If we employ both of the above forms of a differencing scheme for artificial cohesiveness and take their minimum value, even better computational results can be obtained.

IV.   Examples of Divergent Detonation Processes

1.   Spherical Divergent Detonation Wave

For a divergent detonation wave produced by center point ignition of a spherical explosive, when the radius of curvature of the wavefront is small, the explosion rate and explosion pressure both increase with the increase of the radius of curvature.[5]   In order to reconstruct numerically these sort of indefinite properties for a divergent detonation, we used PBX-9404 explosive and computed the spherical divergent detonation wave. A side of the initial grid was 0.5 mm. At $t = 0$, the given C-J ignition conditions within a certain number of grids in the vicinity of the sphere were: $\rho = \rho_{C-J}$, $u = u_{C-J}$. The computed results are arranged in the table below. For comparison, we used (2.1) and computed the corresponding R location explosion rate, ($D = 8.8$ mm/μs; $\gamma = 2.85$; $l_0 = 0.35$ mm) [Note: The chemical reaction zone breadth, l_0, of a divergent detonation process is variable. During computations it was approximated by the reaction zone breadth of a plane detonation wave, $l_0 = 0.35$ mm.] and the corresponding pressure, P(R), was computed from the explosion rate, D(R). These computations are also included in the table below.

Table 1.   Variation of Explosion Rate and Explosion Pressure of a Spherical Divergent Detonation Wave With Wavefront Radius

Wavefront radius R(mm)	11.248	16.018	20.814	25.619	30.418	25.23	40.106	44.976
$\dfrac{D(R)}{D_J}$ (this paper)	0.691	0.793	0.846	0.876	0.898	0.913	0.924	0.931
P(R) (Gba) (this paper)	17.72	23.34	26.56	28.48	29.93	30.83	31.63	32.37
$\dfrac{D(R)}{D_J}$ (2.1)	0.718	0.801	0.847	0.876	0.896	0.910	0.921	0.929
P(R) (Gba) (2.1)	19.13	23.81	26.62	28.48	29.79	30.73	31.48	32.03

Wavefront radius $R(mm)$	49.747	54.399	58.931	61.885	69.031	75.805	83.136	
$\dfrac{D(R)}{D_j}$ (this paper)	0.938	0.944	0.949	0.952	0.957	0.962	0.968	
$P(R)$ (Gba) (this paper)	32.65	33.07	33.42	33.63	33.99	34.34	34.77	
$\dfrac{D(R)}{D_j}$ (2.1)	0.936	0.942	0.946	0.949	0.954	0.958	0.962	
$P(R)$ (Gba) (2.1)	32.51	32.93	33.21	33.42	33.78	34.06	34.34	

From the table it is evident that the two sets of results are very close. Where R is smaller, due to the effect of the given ignition conditions during computation, the results are slightly different from (2.1) (< 4 percent) but the difference at the other points are all better than 0.5 percent.

2. Ring Detonation Wave

In order to obtain an ultra high pressure detonation wave, in experiments frequently a certain thickness column shaped inert body is buried in the explosive. Then, by diffraction of the detonation wave against the side of the column shaped inert body, a ring shaped detonation wave is produced in the explosion. The ring converges to the axis of symmetry producing Mach reflection to attain the goal of increased pressure.
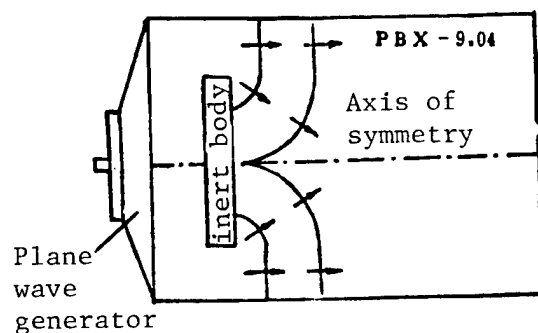
Figure 3. Formation of a ring detonation

In the process of converging to the axis of symmetry, the portion of the ring shaped wave propagated in the horizontal direction is a divergent detonation wave while the portion propagated toward the axis of symmetry is a convergent detonation wave. The other portions of the wave, although divergent waves from the view point of a certain point, also have the influence of convergent factors when looking at the entire wavefront. Therefore, the state of each point on the ring shaped wavefront is different. The explosion rate and explosion pressure of the portion propagated horizontally is lower and higher for the portion propagated toward the axis of symmetry. With the contraction of the ring radius, the explosion rate and explosion pressure of each point on the wavefront gradually increases. After the interactions at the axis of symmetry, it further strengthens the ultra strong detonation wave produced.

The ring detonation process is rather complicated. In theoretical estimates, the above variations in explosion rate and pressure on the ring wavefront are ignored and constants substituted in their place. The results of such computations naturally diverge some from experiments. In order to describe more closely the properties of ring detonations recounted above, we computed the model in Figures 4 and 5. At the place where x = 0, r = 15 mm, given an appropriate size ring ignition zone and C-J ignition conditions, and an initial grid $\Delta x = \Delta r = 0.5$ mm, Figure 5 gives the position of the ring wavefront at the four instants t = 0.5, 1.0, 1.5, and 2.0 µs and gives as well the component propagation conditions of the pressure at the wavefront.
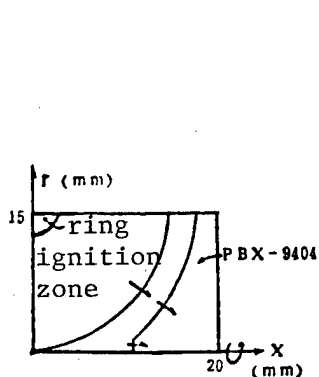
Figure 4. Ring detonation computation model
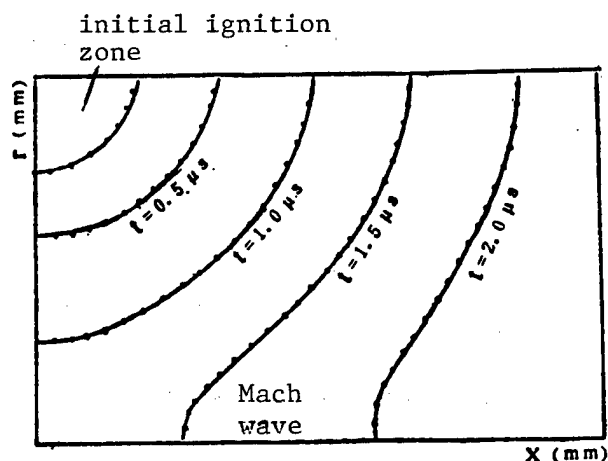
Figure 5. Ring detonation process

Pressure distribution conditions at the wavefront:

t=0.5µs

X (mm)	0.5	2	3	4	5	6	7	7
r(mm)	8.0	8.75	9.25	9.75	10.75	12	13	15
P(10^4 bar)	33.5	33.5	32.5	31.5	32.5	31.5	32.5	32.0

t=1.0µs

X (mm)	0.5	2	3	4	5	6	7	8	9	10	10.3
r (mm)	4.5	4.8	5.0	5.5	6	6.5	7.5	8.5	10	12	15
P(10^4 bar)	38	37	37	36	35.5	34	33	32	32	31	30

t=1.5µs

X (mm)	1.5	4.5	5	6	7	8	9	10	11	12	13	14.0	14.0
r(mm)	0.5	1.0	1.5	2.3	3	3.5	4.5	5.5	6.5	8	10	13	15
P(10^{4}bar)	170	84	50	49	43	40	37	36	35	34	34	32	31

X (mm)	12	13	14	15	16	17	17.5	18
r (mm)	1.0	3.0	4	5.5	7.5	10	12	15
P (10^4 bar)	75	40	37	35.5	34.5	32	32	32

From the results recounted above, we can see the explosion rate of the divergent wave propagated in the horizontal direction, $D_{divergent}$, and the explosion rate of the axially directed convergent wave, $D_{convergent}$ are:

Time interval (µs)	0-0.5	0.5-1.0	1.0-1.5	1.5-2.0
Average explosion rate $\bar{D}_{divergent}$ $\dfrac{mm}{µs}$	6.0	6.5	7.5	8.0
Average explosion rate $\bar{D}_{convergent}$ $\dfrac{mm}{µs}$	6.0	8.0	9.0	

We can also get the variation with time of the explosion pressure in the above two directions:

t (µs)	0.5	1.0	1.5	2.0
Divergent explosion pressure of horizontally directed wave $P_{divergent}$ 10^4 bar	32	30	31	32
Convergent explosion pressure of axially directed wave $P_{convergent}$ 10^4 bar	33.5	38	50	

It is evident that the increase with time of the explosion rate and pressure with time for a divergent detonation propagated in the horizontal direction (the $P_{divergent}$ = 320 kilobar corresponding to 0.5 µs is due to the strength of initial ignition conditions) is more rapid than the increase in explosion rate and pressure of the convergent portion traveling toward the axis. Computations show that when the ring detonation wave is about to collide with the axial, the wavefront pressure of the convergent portion has already reached 500 kilobar. After the interaction, a 1,700 kilobar ultra strong detonation wave has been produced.

3. Interactions and Shaping of a Cylindrical Divergent Detonation Wave

At the external surface of an infinitely thick explosive, when ignition uses two lines, a and b, separated by distance ℓ, the two identical cylindrical divergent detonation waves produced will, after they collide, produce normal reflections and Mach reflections. Since relative energy concentrations are formed at points in the vicinity of the interaction, the explosion rate and explosion pressure will be higher than for a divergent wave. Consequently the trailing Mach wave will gradually overtake the divergent wave.
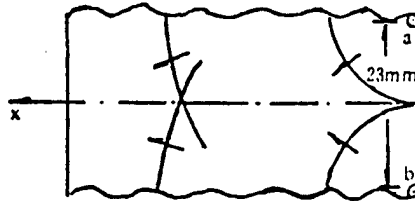
The rough results of this problem can be obtained from theoretical analysis, but can give only the state on the wavefronts at points near the interaction. In order to do comparisons with the after wave state distribution conditions given in reference [1], this paper computes this detonation process, giving the pressure distribution conditions within the flow field for four instants.
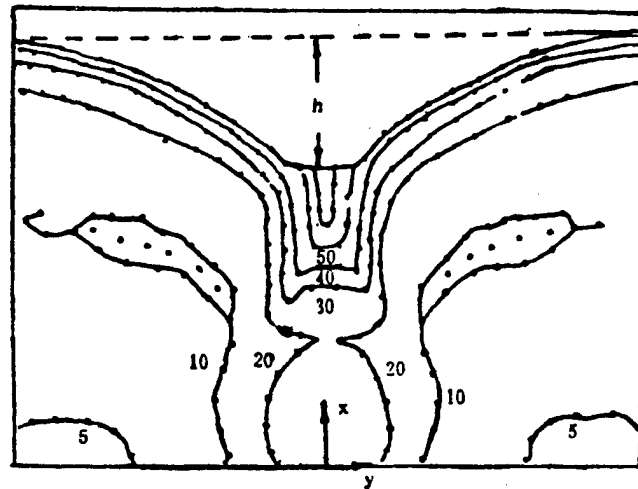
Figure 6. t = 1.5 µs, after wave pressure distribution conditions. Curved lines in the figure are isobars with pressure values noted in units of 10 kilobar. h is the wave form difference in mm.
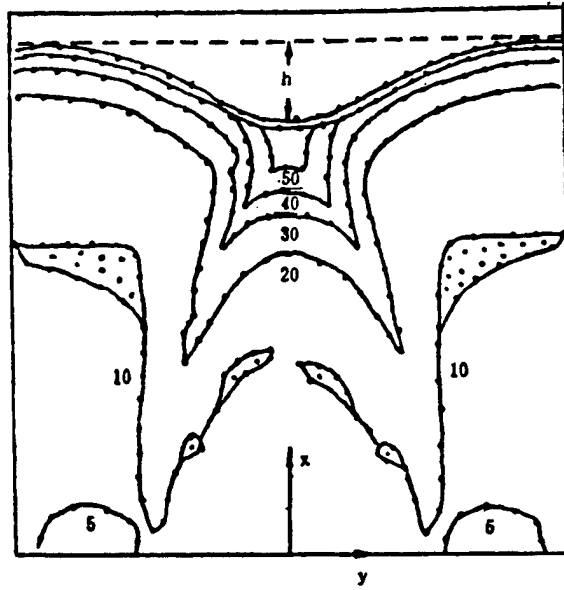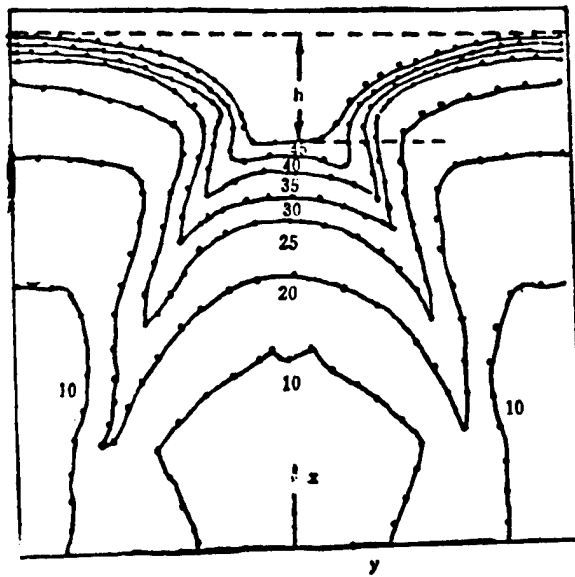
Figure 7.   t = 2.0 μs, after wave pressure distribution conditions

Figure 8.   t = 2.5 μs, after wave pressure distribution conditions

68
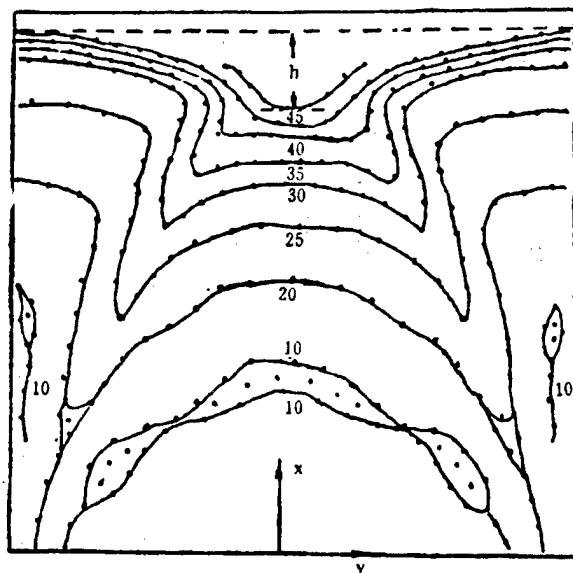
Figure 9.   t = 3.0 μs, after wave pressure distribution conditions

The after wave pressure distribution conditions in Figures 6, 7, 8, and 9 are identical to the results of reference [1]. From the above results, we can also obtain the variation with propagation distance, R, of the wavefront form after interaction:

R(mm)	11.5	12	12.8	13.5	14.6	15.5	16.3	17.0
h (mm)	10.5	8.5	6.8	6.0	5.3	5.0	4.4	4.3
R(mm)	18	19.7	21.5	23	25	26.5	30	
h (mm)	4.0	3.5	30	2.8	2.5	2.2	2.0	

Using the rough methods provided in reference [6], the detonation wavefront shaping conditions obtained are as follows: (Assuming the incident wave is a C-J detonation wave.)   Figure 10 is a comparison between precise computations and the rough analysis results showing very close agreement.

R(mm)	16.55	17.32	18.12	18.95	19.80	21.18	22.77	24.6
h(mm)	4.58	4.29	4.03	3.80	3.59	3.28	2.98	2.68
R(mm)	29.21	32.13	85.6	39.69	44.62	50.56		
h (mm)	2.1	1.82	1.55	1.29	1.05	0.83		

From the above results we see that, using the two dimensional Lagrange method described here and using Cochran reaction rates and JWL equations of state to model explosive initiation processes, not only can better give the shaping conditions of the wavefront after two divergent waves interact but can also better describe the state distribution conditions of the after wave flow field.

69
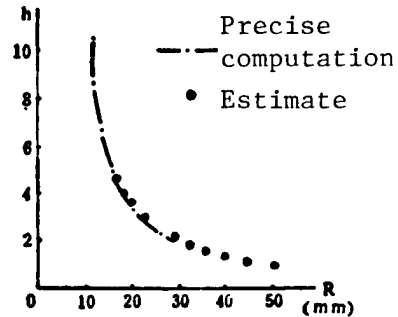
Figure 10. Comparison of detonation wavefront shaping process

4. Oppositely Directed Shock Ignition of Two Waves From a Passive Inductive Explosive

In practical applications, frequently it is necessary to use various means to cause the initiation of passive inductive explosives. For certain safer explosives (like TATB), it is commonly very difficult to cause initiation using a detonator or even projectile impact. In order to increase the shock initiation performance for passive inductive explosives, people commonly used two wave or multiple wave interactions producing high pressure to initiate passive inductive explosives. As a computing example, we used the apparatus of Figure 11 to research the oppositely directed shock initiation problem of two wave interaction on passive inductive explosives.
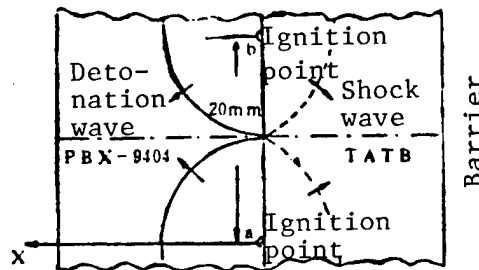
Figure 11. Oppositely directed shock initiation of TATB explosive from the interaction of two cylindrical divergent waves in PBX-9404 explosive

Simultaneously igniting PBX-9404 explosives on lines a and b separated by 20 mm and placed within the explosive plane and on the boundary between the two types of explosives produces two cylindrical detonation waves in the PBX-9404 explosive. Because these divergent detonation waves are insufficient to cause the initiation of the neighboring TATB explosive, what is propagated in the TATB is the shock waves. After the detonation waves in the PBX-9404 collide with each other at point C, there is a possibility this will make the TATB in the vicinity of this point initiate. This question is rather complex so that presently a rigorous analytical solution cannot be obtained. If the assumptions are excessive the true picture will be lost. By using two dimensional numerical methods to study this problem we are capable of obtaining a

clear picture of the process of oppositely directed shock initiation. Computed to t = 1.2 μs, the pressure distribution within the flow field is as shown in Figure 12.
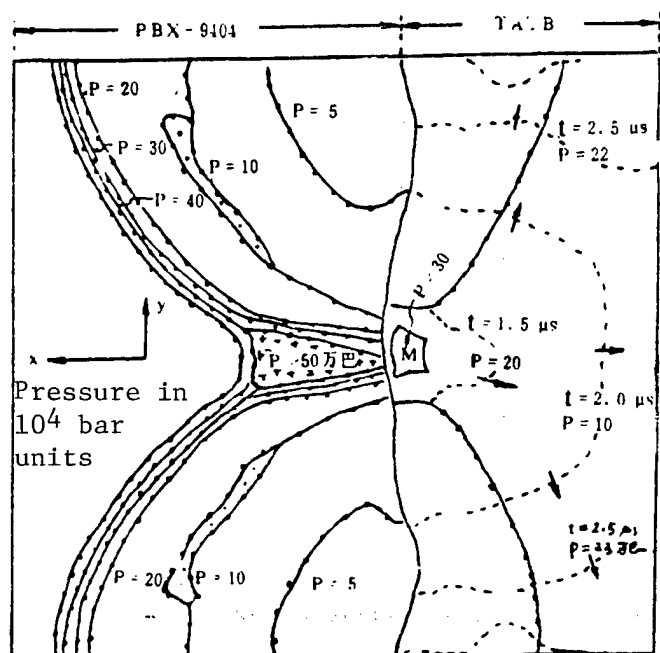
Figure 12. Pressure distribution conditions within the two explosives at t = 1.2 μs

The solid lines in the figure are isobars and the dashed lines in the TATB explosive are pressure variation conditions at the shock wavefront at different times.

From computational results we can see that:

1. In the PBX-9404 explosive, after ignition of point a, the shock wave coming into the TATB along the boundary between the two explosives is certainly incapable of causing TATB initiation.

2. After the high pressure produced by the collision of the detonation waves in the PBX-9404 recoils from the TATB, a P = 300 kilobar high pressure zone is formed at area M in the TATB stimulating a chemical reaction of area M and a C-J bomb pressure of the TATB explosive, P_{C-J} = 315 kilobar.

3. Because the range of area M is rather small, the energy provided is not sufficient to maintain the continued propagation of the divergent wave. With passage of time, the detonation wave attenuates becoming a shock wave and its intensity also gradually attenuates: when t = 1.5 μs, P = 200 kilobar and when t = 2.0 μs, P = 100 kilobar.

4. In the TATB when t = 2.5 μs, the pressure increase near the wall caused by the wall reflection (from 100 kilobar to 220 kilobar) also has difficulty in causing TATB initiation.

Evidently, the oppositely directed shock waves against the TATB from the interaction of two cylindrical waves are not able to start stable detonation. Only if the shock waves are stronger will they make the TATB explosive initiate. For example, if the TATB is placed on the left side of the PBX-9404 and the latter is initiated at a and b forming direct shock waves against the TATB. In this kind of situation, the shock waves against the TATB are much stronger. Computations show that not only is the shock wave from the PBX-9404 into the TATB stronger but also the detonation products will also have an entropic compression process against the TATB. Pre-pressurized TATB under the interaction of two stronger waves is capable of stable detonation.

REFERENCES

1. C.L. Mader, "Detonation Wave Interactions," Seventh International Symposium on Detonation, (1981).

2. S.G. Cochran and John Chan, "Shock Initiation and Detonation Models in One and Two Dimensions," Report 1979.

3. K.E. Gubkin, "The Dependence of the Velocity of a Spherical Detonation Wave on the Radius of Curvature of the Wavefront," Vol 14, No 3 (1978).

4. Liu Bangdi [0491 6721 1717] and Shen Xiuwen [3088 4423 2429], "On Artificial Cohesiveness Pressure," Second International Conference of Fluid Dynamics (1983).

5. R. Cheret and G. Verder, "Divergent Spherical Detonation Wave in a Solid Explosive," Fifth International Symposium on Detonation, (1970).

6. Li Zhiwei [2621 2535 0251], "Interaction and Shaping of Varying Strength Detonation Waves," (internal material) (1982).

7. C.L. Mader, Numerical Modeling of Detonation, London, 1979.

12966/6091

GEOPHYSICAL SURVEYS FOR MANGANESE NODULES CONDUCTED IN PACIFIC

Beijing GUANGMING RIBAO in Chinese 15 Sep 87 p 1

[Summary] The Chinese State Oceanography Bureau survey ship, Xiangyanghong No 16, has successfully finished a manganese nodule investigation in the Pacific Ocean, returning to Shanghai on 14 September 1987.

The Xiangyanghong No 16 set sail on 28 April 1987. During 140 days of oceanographic studies, the ship investigated an area of 500,000 km^2, employing several advanced methods such as trawlnets, multi-frequency probes, deep-sea photography, and remote sampling, etc. The ship successfully finished geophysical studies, sampling from more than 100 survey stations, and collecting the most manganese nodule specimens to date while also appraising areas of nodule concentrations.

A valuable potential strategic material, oceanic manganese nodules are widely distributed on the sea bottom at depths of 3000-6000 meters and contain manganese, copper, cobalt, nickel, and other metals. According to estimates, the manganese nodule reserve in the world's oceans is about 3 trillion tons, about one-half of which is in the Pacific Ocean. Today, many countries are devoting great attentions to the exploration and exploitation of manganese nodules. Since the 1970's, the Chinese State Oceanography Bureau has dispatched oceanographic investigation ships to perform systematic surveys on the distribution of manganese nodule resources in the Pacific Ocean, and has collected first-hand materials and preliminarily obtained significant data on their abundance and grade, as well as the environmental situation of the ocean areas surveyed.

/9604
CSO: 4008/1017

DEVELOPMENT, PROSPECTS OF BIOLOGICAL WEAPONS DISCUSSED

Beijing JIEFANGJUN YIXUE ZAZHI [MEDICAL JOURNAL OF CHINESE PEOPLE'S LIBERATION
ARMY] in Chinese Vol 12, No 1, Feb 87 pp 78-79

[Article by Chen Ningqing [7115 1337 1987]: "Evolution of Biological Weapons
and Prospects for Their Development"]

[Text] The use of biological toxins or infectious diseases by man to subjugate
opponents during war is called biological warfare. Common biological warfare
agents include viruses, Rickettsia, Chlamydia, bacteria, toxins, fungi and so
on. Mankind has been using biological weapons for several decades now, and we
will discuss some related issues to gain an understanding of the evolution of
biological weapons and their developmental prospects.

I. A History of Biological Weapons

The first clearly recorded use of a biological weapon in history was against
the American Indians by the British colonialists. In 1763, Armstrong, commander
of the British Army in North America, ordered his troops to send two blankets
and handkerchiefs used by persons suffering from smallpox to an Indian leader.
Smallpox spread among the Indians and they were subjugated. The first truly
large scale use of biological weapons, however, occurred during the past several
decades. They can be divided into three main developmental stages: 1. During
the first stage, manual application dominated and the main developer was the
German Empire, the wealthiest aggressor at the time and a nation with a rather
higher level of bacteriological and industrial development. The biological
warfare agents were limited to a small number of bacteria dangerous to humans
and animals like anthrax, glanders, meliodosis and others. 2. During the
second stage, from the 1930's to the 1950's, the main developers were Germany
and Japan, followed by England and the United States. Again, most of the
warfare agents were bacterial, but there was greater variety. During the later
part of the period, the United States began to study viral agents and
Rickettsia. The primary method of application was dispersal of the biological
warfare agents using insects as intermediaries, although the United States
undertook studies on aerosol dispersal techniques. Airplanes were the main
means of delivery and there was an obvious expansion in the area of
contamination. The production scale of warfare agents also underwent a
transition from solid medium production to large scale liquid medium
production in fermenting tanks. In addition, biological weapons were tried
out by the Japanese invading army in China and the American invading army in
Korea. 3. The third stage in the development of biological weapons covers

the period from the end of the Korean War to 1972, when the United States, England and the Soviet Union signed treaties banning the use of biological weapons. The main developers were the superpowers. This stage was characterized by: (1) Gradual improvements of aerosol dispersal techniques for biological warfare agents. Experiments on aerosol dispersal, infection, viability and other aspects of aerosol dispersal of warfare agents moved out of the laboratory to on-site field experiments. Experiments on infection made the transition from animal to human experiments. (2) There were continual increases in the variety of viral and poisonous warfare agents used for bilogical warfare agents. Continual discoveries of new viruses were made and technical problems with the cultivation of viruses in large amounts were overcome. (3) Regarding the means of delivery, there was a transition from simply hurling biological bombs to delivery using a variety of guided missiles, which greatly increased the attacking distance of biological weapons and made it possible to use them as true strategic weapons.

II. The Present and Future of Biological Weapons

At present, although treaties have been signed banning biological weapons, the treaties themselves have no restrictive authority. Today there are no real organs for the supervision and inspection of biological weapons, and research on biological weapons can be carried out covertly through common microbiology, genetic engineering and protection research. The situation for the development of biological weapons in the Soviet Union is an example. Strict secrecy means that although the situation is not fully understood, an accident involving aerosol anthrax was reported in Sverdlovsk in April 1974 that caused illness and death in many people in downwind areas. In another example, Bddansky has published a series of articles since 1982 in the renowned English scientific magazine "Nature" which reveal that the United States is utilizing genetic engineering techniques to engage in research on new biological warfare agents. It is apparent from the current situation in biological weapons that weapons of the previous generation have entered a stage of decline and that a new generation of weapons is brewing. Understanding of the military significance of biological weapons also is changing. Before the appearance of nuclear weapons, biological weapons were considered terrible weapons for large scale killing and injury with an enormous ability to create casualties. After the appearance of nuclear weapons, the facts confirmed that the power of nuclear weapons was much more real and enormous than biological weapons. The military specialists' understanding of biological weapons also has changed. The reason is that the effects of biological weapons are strongly subject to the effects of the natural environment, so they cannot be used solely on the basis of military needs. Moreover, biological weapons have encountered resistance from people throughout the world, so their use for less than legitimate military purposes would create an enormous political crisis. The general understanding is that although one cannot ignore the utilization of biological weapons, they can only be used as a sort of auxiliary weapon. It must be noted, however, that biology is advancing rapidly at the molecular level and the multifaceted and enormous influence of biology on human existence and life is becoming more obvious daily. This requires an adequate understanding of the importance of biological factors of death and injury.

III. Developmental Trends for Biological Warfare Agents

1. More viral biological warfare agents are appearing.

Viruses pathogenic to man appear frequently in the natural world today, including examples like the Lasha [2139 3097] virus, the AIDS virus, etc., some of which could become new biological warfare agents. A nine-year survey of the area near the mouth of the Amazon River in Brazil by the United States Rockefeller Foundation's Virus Laboratory led to the discovery of 60 new viruses. According to the "Microbiological and Biomedical Laboratory Safety Handbook" published in 1984 by the United States Center for Disease Control (CDC) and the state-run Institute of Public Health, there were 334 types of insect-intermediary viruses toxic to humans at a second stage of protection. In recent years, the development of hollow fiber and microcarrier technologies has led to basic solutions to many problems in the large-scale cultivation of viruses. As a result, viral warfare agents are sure to account for a greater portion of biological warfare agents in the future. Moreover, the diagnosis and treatment of viral warfare agents is much more difficult compared to biological warfare agents.

2. The utilization of molecular genetics techniques for recombinant DNA has made the possibility of new biological warfare agents a fact. Genetic recombination already has been used successfully in other countries to develop Pasteurella and Tularemia bacteria that are resistant to streptomycin, and they have been able to grow in a rather simple medium. In addition, it is possible that already understood methods to synthesize new genes may generate new types of bacteria with a greater pathogenic capacity in humans and more resistance to the environment. This will bring biological weapons into a new stage, which is the stage of the so-called "genetic weapons." If the structure of the proteins on the exterior surface of viruses is changed, previously effective treatments will lose their protective abilities and formerly exceptional diagnostic methods will lose their distinctiveness. Of course, genetically engineered microorganisms acquire new characteristics and it is not possible to change the basic weaknesses inherent in all microorganisms, facts that can be confirmed.

3. Various biotoxins and low molecular weight poisons may become new warfare agents. All sorts of animals, plants and microorganisms in the natural world produce toxins dangerous to man. Examples include clam [5756 5732] toxin, curare tetrodotoxin, cobravenom, seaweed toxin, Clostridium botulinum toxin, staphylotoxin and various fungal toxins. Moreover, research on low molecular weight toxins is flourishing because of developments in organic chemistry. These materials can cause intense physiological reactions in microdoses, and they affect human behavior and normal functions. Synthetic peptides are considered to be the most likely source of new toxin agents. There also are many types of fungal toxins, including many toxic to humans and animals. Some feel that T-2 toxin, produced by snow mold sickle fungus, is a new type of biological warfare agent—the main constituent of "yellow rain." Although "yellow rain" is the subject of much debate now, some fungal poisons are quite toxic to man and animals, so they may become new biological warfare agents. Because they are easy to produce in large amounts, are more stable than

microorganisms, have a strong resistance to environmental factors and can be stored for long periods, low molecular weight toxins should receive considerable attention from the military. In 1986, a nuclear biochemistry protection magazine in the United States revealed that the Soviet Union is studying genetic engineering techniques to produce snake venom. This biological factor is a biological product that also has certain characteristics of chemical toxins (a short toxicity period and the ability to be artificially synthesized). Some have called these toxins biochemical warfare agents. This is a new developmental direction for biological weapons.

IV. Measures for Countering Biological Warfare

1. Pay close attention to the orientation of research on biological weapons in other countries, particularly to developmental trends of new biological technologies. 2. Strengthen research on comprehensive measures to counter biological warfare. On the basis of medical research on protective techniques for anti-biological warfare and research on concrete methods and equipment in the area of facilities, we also should formulate various advance programs based on different conditions and parameters and store them in computers to prepare for any contingency. 3. Develop microlevel research on biopathogenic factors. This requires research on the structure of all biotoxins and low molecular weight toxins. Basic research in this area could provide new routes for the diagnosis, prevention and treatment of biopathogenic factors. 4. Continue to improve the diagnosis, prevention, treatment and pharmacology of anti-biological warfare. This is particularly important in use of genetic engineering techniques to develop more effective new treatments with fewer reactions, which would be important in both peacetime and war. 5. Propagandize the masses and organize the masses to strengthen national defense.

During an attack by biological weapons, the medical personnel in the contaminated area also may fall ill, and it would be difficult for hospitals to hold large numbers of sick people. In such an instance, those unaffected by illness could care for the sick. Specialized personnel also could provide guidance through inspections, television, broadcasts, newspapers and other means. Better peacetime education and training of all the people to counter biological warfare would lead to better results during wartime.

12539
CSO: 4008/1011

TOOSEDANIN, BOTULINUS TOXIN INTERACTION REPORTED

[Article by Xiong Chunsheng [3574 2504 3932] of the Institute of Microbiology
and Epidemiology, Academy of Military Medical Science, Beijing]

[Text] Since the discovery by Li Peizhong, et al. [1], that toosendanin has
therapeutic value for animals, such as mice and monkeys, poisoned by botulinus
toxin, more research has been conducted on that topic [2,3]. Also, after
administering toosendanin to mice and rats, there are reports regarding
ultrastructural changes, e.g., the reduction in quantity of synaptic vesicles
at neural-muscular junctions [4,5]. In the pre-synaptic cholinergic synapse,
a botulinus toxin's function is similar to that of a transmission interferon.
It interferes with the synaptic transmission at neural muscular junctions,
because it interferes with the release of ACh by the synapses. Toosendanin
provides antitoxic action to botulinus toxin, indicating that the two agents
must react to each other at the neural muscular junction (NMJ). This
experimental study uses the electron microscope to observe the ultra-
structural changes resulting from the interaction between toosendanin and
botulinus toxin.

Materials and Method

Botulinus toxin A concentrate was provided by the Lanzhou Biological Products
Institute (serial No 7192). The concentrate was diluted with 0.2 percent
gelatin buffer (pH 6.5) in preparation for use. Intramuscular injection
of mice in the abdomen was administered at the lethal dosage of 1.7 LD_{50}.

Toosendanin--The industrial grade product was purchased from Sichuan Yibin
Pharmaceutical Factory, and purified by our chemical laboratory. The purity
of sample was 98 percent or higher. Toosendanin was dissolved in 60 percent
propylene glycol (5 mg/ml), and pre-distilled water was used to dilute it
to 1 mg/ml. Mice were given spinal intramuscular injection at the therapeutic
dosage of 9 mg/kg.

Observation material--Left diaphragm, obtained from male mice with body weights of approximately 20 g.

Experimental groups--Mice were given toosendanin and botulinus toxin at different times. In addition, a treatment group, toxin group and solution control group were set up.

Preparation of electron microscopic specimens--The same method by the same author as reported in [5] was used. Ultra-thin sections were observed under JEM-6c and EM-400T electron microscope lenses.

NMJ measurement--Using Hally's [6] theory of micro-measurements, self-designed microscopic measurements were used to measure under the dissecting microscope, the negatives from which showed the density and size of the synaptic vesicles and other ultrastructures at the synaptic junction equivalent to the area within 2500 A of the anterior membrane of the synapse ('synaptic area').

Results

(1) Ultrastructures of NMJ of mice diaphragm in solution control group (Figure 1) [not reproduced]:

The NMJ ultrastructure and measured values of the mice control group resembled those reported by Andersson-Cedergren [7] and those reported by the author on rats. There were a large number of synaptic vesicles at the synapses, mostly round or oblong in shape, with diameters approximately 350 $\sim$ 400 A. Other commonly-occurring features included empty vesicles, tubular vesicles (vesicles longer than 600 A were called "elongated vesicles") and neurofilaments. There were many mitochondria, mostly at the center, synaptic clefts were of even width, approximately 500 A. There were also numerous junction folds, with branching. In neighboring myoplasm, there were many mitrochondria, particulate reticulum, ribosomes and glycogen. Golgi bodies and myocyte nucleii, myofibrils and striations were very clear.

(2) Ultrastructures of NMJ of mice diaphragm injected with botulinus toxin (Figure 2) [not reproduced]:

Nine and twenty-eight hours after injection of botulinus toxin, the diaphragm NMJ of mice showed obvious ultrastructural changes. The results are identical to those of Harris, et al [8]. The densities of synaptic vesicles and other structures were similar to those of the solution control group. However, NMJs exhibiting structures similar to myeloid structures and phagosomes were relatively higher (8.3 percent versus 4.4 percent).

(3) Ultrastructural changes of mice diaphragm NMJ after injection of toosendanin (Figures 3, 4) [not reproduced]:

Approximately 3-4 hours after the injection of toosendanin, the anterior part of the mice diaphragm NMJ showed obvious changes. The results were identical to those of rat NMJs as studied by the author [5]. The main features included the reduction of synaptic vesicles inside the synapses, with about 60 percent of the NMJs showing a significant reduction in the number of vesicles. Vesicles in the synaptic region were at a density of $68 \pm 14/\mu^2$, the reduction being 60 percent that of the solution control group. Another feature was the relative abundance of elongated vesicles. The average density of elongated vesicles in the synaptic region was $5.2 \pm 1.0/\mu^2$, which was twice as many as that of the control group at $2.0 \pm 1/\mu^2$ (P $<$ 0.001). Another fairly obvious change was the relative common appearance of myeloid and phagosome-like structures at the synapses. About 13.8 percent of the NMJs showed these structures, which was three times as many as those of the control group (4.4 percent). Furthermore, a small number of NMJs (about 7 percent) also showed slightly or partially widened synaptic clefts (600 $\sim$ 800 A). There were also a small number of NMJs (approximately 2.5 percent) which showed Schwann cells protruding into the synaptic clefts.

(4) Ultrastructural NMJ changes when mice were given toosendanin followed by botulinus toxin immediately or after one hour (Figure 5, 6) [not reproduced]:

Botulinus toxin was given immediately or one hour after the injection of toosendanin, and specimens were obtained after four hours. Ultrastructural changes of the diaphragm NMJ were identical to those of mice that were given only toosendanin.

(5) Ultrastructural changes of diaphragm NMJ when mice poisoned with botulinus toxin were given toosendanin (Figures 7, 8) [not reproduced]:

When mice were given toosendanin 5 hours after having been poisoned by botulinus toxin, the density of synaptic vesicles of the NMJ synaptic region was $137 \pm 18/\mu^2$, while approximately 10 percent of the NMJs showed obvious reductions. When mice were given toosendanin 24 hours after having been poisoned by botulinus toxin, the average vesicle density was $130 \pm 26/\mu^2$, with NMJs showing obvious vesicle reduction approximately 19 percent. The results showed that for these two groups of mice, NMJ vesicle densities were about 90 percent higher (P $<$ 0.001) than those of mice that had been given only toosendanin.

Other NMJ structural changes in these two groups of mice were similar to those in mice that were given only toosendanin. Neither did these two groups differ significantly in other respects. The only observed difference was that mice that were given treatment 24 hours after poisoning showed relatively more slight or partial widening of the junction fold, about 17 percent. The other group was at 8 percent, which resembled that of the toosendanin only group.

80

Discussion

It is observed in this study that when normal mice were given toosendanin, there was an obvious reduction of NMJ synaptic vesicles. On the other hand, mice poisoned by botulinus toxin did not show obvious reduction of NMJ vesicles when given toosendanin. This seems to show that when botulinus toxin acts on NMJs, there is an inhibitory effect on the vesicle reduction action of toosendanin. This is to say that perhaps botulinus toxin has an inhibitory effect on the sequential quantum release process. Koa, et al., [9] observed similar phenomena in the study of the botulinus toxin action mechanism.

According to the dynamic model proposed by Simpson [10], botulinus toxin interacts with NMJ and causes a delay in the synaptic transmission. This process has three stages, i.e., combination, transfer and paralysis. Botulinus toxin in the combination stage can be counteracted by antidotes. On the other hand, botulinus toxin in the paralysis stage cannot be counteracted by antidotes. Under the present experimental conditions, when mice poisoned with botulinus toxin were given toosendanin within 1 ~ 6 hours, the treatment was effective. At 24 hours the treatment was ineffective [1]. Therefore, 5 hours after poisoning was probably the end of the combination stage, and 24 hours was perhaps the paralysis stage. However, according to our observations, the degree of reduction of NMJ vesicles of these two groups of mice was roughly the same, which may be because botulinus toxin, at the end of the combination stage and in the paralysis stage, is at the same inhibitory effect level involving the release of the vesicles. Simpson observed that the botulinus toxin could inhibit the increase in frequency of the electropotential caused by batrachotoxin at the diaphragm's neuro- muscular end-plates. He also proved that only at the paralysis stage was botulinus toxin effective against batrachotoxin, while botulinus toxin did not affect such changes during the combination stage [11].

It is also evident from this study that when botulinus toxin is given immediately or with one hour following the administration of toosendanin, the changes in the NMJ ultrastructure are characteristic of those of toosendanin alone, and there is no indication that botulinus toxin has any inhibitory effects on toosendanin. This may be because the molecular weight of toosendanin (574) is much lower than that of botulinus toxin (150,000), and, therefore, is able to react much faster with presynaptic membranes. Only when botulinus toxin had had prior interactions with presynaptic membranes did it successfully inhibit the action of toosendanin. This is identical to the reported interaction between toosendanin and botulinus toxin in causing the paralysis of the in vitro diaphragm nerve and muscle specimens [3].

Because the mechanism of botulinus toxin is still not well understood, further research on toosendanin should be conducted. Our study only provides an inroad to the understanding of the interaction between toosendanin and botulinus toxin.

BIBLIOGRAPHY

1. Li Peizhong [2621 1014 1813]. Results of Toosedanin Treatment on
   Botulinus Toxin-Poisoned Animals. CHINESE HERBAL MEDICINE [0022
   5430 5673] 1982; 13:28.

2. Shi Yuliang [2457 3768 2856]. Toosedanin--A Blocker on Transmission
   of Nerve/Muscle Connection. JOURNAL OF PHYSIOLOGY 1980;
   32:293.

3. Li Peizhong [2621 1014 1813] and Sun Guozhang [1327 0948 4545].
   Anti-Botulinus Toxin Action of Toosedanin on Mice. JOURNAL OF
   PHYSIOLOGY 1983; 35:480.

4. Huang Shikai [7806 0013 2818]. Effect of Toosedanin on Super
   Microstructure of Mice' Nerve/Muscle Connection. JOURNAL OF PHYSIOLOGY
   1980; 32:385.

5. Xiong Chunsheng [3574 2504 3932]. Effect of Toosedanin on Rats'
   Nerve/Muscle Connection. JOURNAL OF PHARMACOLOGY 1982; 17:407.

6. Hally A.D. A Counting Method for Measuring Volumes of Tissue Components
   in Microscopical Sections. QUART J MICROSCOP SCI 1964; 105:503.

7. Andersson-Cedergren E. Ultrastructure of Motor End Plate and Sarcoplasmic
   Components of Mouse Skeletal Muscle Fiber. J ULTRASTRUCT RES SUPPL 1, 1959.

8. Harris A.J. and Miledi R. The Effect of Type D Bolutinum Toxin on Frog
   Neuromuscular Junction. J PHYSIOL 1971; 217:497.

9. Kao I, et al. Botulinum Toxin: Mechanism of Presynaptic Blockade.
   SCIENCE 1976; 193:1256.

10. Simpson, L.L. Kinetic Studies on the Interaction Between Botulinum
    Toxin Type A and the Cholinergic Neuromuscular Junction. J PHARMACOL
    EXPR THER 1980; 212:16.

11. Simpson, L.L. Pharmacological Studies on the Subcellular Size of
    Botulinum Toxin Type A. J PHARMACOL EXP THER 1978; 206:661.

12996/8309
CSO: 40081043

FUTURE TRENDS, GOALS OF MEDICAL RESEARCH REPORTED

[Article by Wang Rukuan [3769 3067 1401], Deputy Director and Research
Associate, Institute of Medical Information, Chinese Academy of Medical
Sciences]

[Text] Changing the Almost Blank Picture in Medical Research

After New China was established, a number of new scientific research
organizations in medicine and health were set up--from the central government
level down to the local level. Of particular note was the establishment of
the Chinese Academy of Medical Sciences, the Institute of Traditional Chinese
Medicine, the Institute of Military Medicine, and various specialized research
institutions. This has allowed a basic change in China's medical research
program to emerge from a practically blank situation. By 1985, there was a
total of 323 medical research institutions in China, and more than 400
medical research subsidiaries. The number of scientific research personnel
totalled more than 330,000. Various medical science interest groups sprung
up throughout China, initiating numerous scholarship activities. In 1981, the
Ministry of Public Health invited 1,190 medical specialists to form a Medical
Science Council.

In the early 50's, China's medical research emphasized treatment and prevention
of various infectious and parasitic diseases that seriously threaten the life
and health of the people. Diseases such as cholera, plague, smallpox,
relapsing fever, typhoid, measles, blackwater fever, and venereal disease
were gradually or basically eliminated within a short period after New China
was founded. The incidence and mortality of various parasitic diseases also
showed a marked drop.

An Institute of Biological Products was established to research and manufacture
vaccines. A free nationwide program to immunize the population was carried
out, and the incidence of infectious diseases such as measles, encephalitis,
etc. was greatly reduced. After large-scale epidemiological studies, the
incidence and scourge of endemic diseases such as brucellosis, Keshan disease,
Kaschin-Beck disease, endemic goiter, etc. were largely controlled. The use
of sodium selenite to prevent Keshan disease, and research application of a

brucellosis vaccine have both scientific and economic value. Much progress has also been made in leprosy research--the numbers of those suffering from this disease has dropped from 500,000 cases in the 50's to less than 150,000 at the present time.

Progress in Applied Research and Basic Research

Beginning in the late 50's and early 60's, China made research breakthroughs in the treatment of large area burns, reattachment of severed limbs, and treatment of chorionic carcinoma. These accomplishments made China a leader internationally, in theory and practice.

In strengthening and developing the foundation derived from the fruits of prevention and treatment of infectious and parasitic diseases, massive survey studies were initiated on the epidemiology, etiology, and prevention and treatment of malignant tumors, cardiovascular diseases, diabetes, viral hepatitis, etc. In particular, a study of malignant tumors and a retroactive statistical survey of mortality statistics was done, from which a tumor incidence map was compiled. As a result, significant progress was made in understanding the occurrence of some serious tumors, particularly esophageal carcinoma, carcinoma of the liver and nasopharyngeal carcinoma, the etiological mechanism in cancer occurrence and early cancer treatment and prevention. At present, China is participating in international research by carrying out a large-scale experiment involving chemotherapy and immunotherapy projects to study esophageal carcinoma in Linxian County in Henan Province, and in Qidong County in Jiangsu Province. These projects have attracted close attention from medical circles abroad. Important progress has also been made in research on the oncogenes, monoclonal antibodies, and transfer mechanisms.

China is also using modern scientific techniques and methods to study the theory and clinical practice of traditional Chinese medicine, particularly the principles of treatment in traditional Chinese medicine, the nature of the spleen [sometimes interpreted as the stomach in traditional Chinese medicine]-kidney (pishen) linkage, the principle of acupuncture anesthesia, and other combined traditional Chinese and Western medicine approaches to treating emergency abdominal conditions, small-splint treatment of fractures, etc., which have attracted much attention at home and abroad. The combined use of Chinese herbs with Western and traditional Chinese medicine to treat cancer and cardiovascular diseases has also yielded significant results.

The successful research and production of qinghaosu, [7230 5548 4790] an extract from the Chinese herb Artemesia apiacea to treat malaria, diphenyl diester to treat hepatitis, a series of herbal preparations and pharmaceuticals to treat cancer, and drugs to treat cardiovascular disease were rated highly by medical specialists in China and abroad. The synthesis of alkaloids from Cephalotaxus fortunei and Camptotheca acuminata (camptothecine) places China on an advanced level worldwide. Successful synthesis of the extremely difficult to produce anticancer drug maytansine has placed China in the advanced ranks of the international pharmaceutical field. Use of modern

biological techniques to study and produce new drugs has shown encouraging developments. Experimental manufacture of research tools such as the computed temography unit, the linear accelerator, the B-model ultrasound, and the diagnostic laser has been successful, and they are now put into use. Research on various contraceptive drugs has also yielded notable results.

At the same time that China is emphasizing applied research, our country also realizes the importance of basic research. In the early 60's, basic studies in the fields of biophysics, pathophysiology, biochemistry, virology, etc. developed. Later on, progress in fields of cytobiology, molecular biology, immunology, genetics, and the new fields of biomedical engineering and social medicine filled in the gaps in many fields. This, in turn, stimulated overall development in Chinese medicine.

Outlook for Future Developments in the Medical Sciences

Analysis of scientific development trends in medicine in China and abroad and China's present condition, shows that development in the following aspects will assume increasing importance:

-- Changes in medical models. That is, change from the "biomedical" model to the "socio-psycho-biomedical" model will be stepped up. Medicine studies the life of people regarding disease and health, their biomedical and social aspects, covering their physiological and psychologicals activity. Research from the perspective of biology only, is found increasingly unable to adapt and meet the needs of people for disease prevention and treatment, and that of society to service these medical care and health needs. At present, various socio-psychological factors are affecting the physical and emotional health of people more and more, and are becoming the important causes of diseases of body and mind. Therefore, the need for change is urgent. Social medicine will undergo great development, and the medical care system, the hospital system, disease prevention concepts, etc. will see rather large reforms, and society's medical care and health maintenance services will grow.

-- A stronger trend for in-depth departmental studies, multidepartmental coordination and socialization of scientific research. In-depth research will lead to detailed branching and requires detailed analytical studies of various life activities microscopically, from the molecular to quantum levels, to explain total body function, the nature of life, and the phenomenon of disease. However, resolution of this problem must consider macroscopically, the total body mechanism and its environment. As the result, it needs multi-departmental coordination and multi-sector collaboration, from the perspective of social medicine, group medicine, environmental medicine, and even as far as cosmic medicine, to investigate the influence of society and natural factors on the human body. This coordination and collaboration can lead to the emergence of a great modern science.

The focus of medical care research, in accordance with changes in the disease spectrum and mortality, must be transferred from infectious diseases, etc.

to cardiovascular disease and cancer--diseases that threaten the life and health of the people. Research on these diseases must be strengthened for clinical and certain basic breakthroughs to be realized on the etiology, disease mechanism, and prevention and treatment of some of these cancers.

-- New progress in research in herbal medicine, and combined Western and traditional Chinese medicine. By using modern scientific techniques and methods to study traditional Chinese medicine theory, particularly that pertaining to principles of treatment, principles of acupuncture use, certain breakthroughs will be made. The four [techniques of] diagnosis, the eight rules, and principles of treatment will take on more objectivity gradually. The clinical application of traditional Chinese medicine and herbal medicine will become even more popular, and it will be possible for it to treat tumors and certain new diseases with astounding success.

-- Fairly rapid developments in geriatrics research and the study of gerontology. Aging in the Chinese population is becoming more obvious by the day. It is predicted that the aging population will rise to 11 percent of the present total by the year 2000. Old-age related illnesses, geriatric health, and various services for the aging population will become immediate problems. These concerns are enough to stimulate research in geriatrics and old-age related illnesses.

-- Comparatively broader use of new techniques. The use of new techniques, particularly the broad use of modern biological techniques in medicine, will reap important results, especially breakthroughs in research and manufacture of new drugs to counter tumors, cardiovascular disease, and hepatitis. "Biological missiles" will be widely used in the diagnosis and treatment of tumors.

-- Comparatively great development in the basic sciences, particularly molecular biology. Basic research will be stimulated, for there is an urgent need for a large amount of experience to move from theoretical levels to some conclusion and be improved upon, for any prevention and treatment problem to be resolved through basic research. A look at Nobel prizes awarded in medicine and physics over the past 40 years shows that most of them were for research done in the field of molecular biology.

-- Importance of family planning and control of excessive population growth. Closely tied to national prosperity and strength, family planning and control of population growth are still focal points getting much attention. Even safer contraceptive drugs and devices will be produced, as will be more acceptable contraceptive measures. Important progress will be seen in the study of reproductive physiology and research in eugenics.

-- Great progress in research into medical information retrieval, and establishment and construction of a Chinese Clearinghouse of Biomedical Information. Progress in medicine, and growth of medical knowledge and its accompanying literature have resulted in a shortened cycle between research results and their application. Individuals working in science and technology fields will be able to locate all or most of the data they want from a sea of biomedical literature, to create their own research after digesting and absorbing this information. Therefore, medical information retrieval and its research will receive increasing attention for further development.

5292/12851

RESEARCH IN DISEASE PREVENTION, TRANSITION IN TRADITIONAL MEDICINE

40081085c Hongkong LIAOWANG [OUTLOOK] OVERSEAS EDITION in Chinese No 18,
4 May 87 pp 10-12

[Article by Wen Xiao [5113 2556]]

[Text] Beginning in the 80's, scientific research in Chinese medicine has
been going through a period of acute transition. This is closely related to
reforms in China and an open policy. From the overall standpoint of scientific
research in medicine, there is a wide gap between China and the advanced
countries. But scientific development in Chinese medicine has its own
characteristics, and has shown a capability for breakthroughs in certain
fields.

In the Service of Disease Prevention and Treatment

In recent years, the three diseases causing the greatest mortality are
cardiovascular disease, cerebrovascular disease, and cancer. Their incidence
is similar to that prevailing in more developed countries. In the early 50's,
diseases with the greatest mortality rates were infectious diseases, tubercu-
losis, and endemic diseases. This transition must necessarily cause changes
in the disease prevention and treatment aspects of scientific research in
Chinese medicine, and large numbers of medical workers and scientific
personnel would quite naturally direct their attention toward these three
diseases. In the Sixth Five-Year Plan (1981-1985), and during the "Seven-Five"
period, the etiology, and prevention and treatment of these three diseases has
become the focal point of scientific research in Chinese medicine. After
several years of concentrated effort, China has made research progress into
the prevention and treatment of these three diseases. For example, coopera-
tive studies into the prevention and treatment of myocardial infarction by all
the large hospitals in Beijing resulted in a drop in the myocardial infarction
mortality rate from 40 percent to the present rate of about 10 percent.
Medical workers at Shanghai's Huashan Hospital used a special reconstruction
technique to restore patency in blocked cerebrovascular vessels, and treated
over 30 hard-to-treat intracranial hemangiomas with no surgical casualties.
The post-surgical prognosis was favorable in more than 90 percent of the
cases treated, thereby allowing this treatment to meet advanced international
standards.

The incidence and mortality rate of stomach cancer are the highest of all cancers in China. To attack this problem, scientific research personnel at the Beijing Municipal Institute of Cancer Prevention and Treatment studied the disease mechanism of stomach cancer from its genetic aspects. They used genetic engineering and gene transfer techniques to clone and isolate the oncogene Ha-ras from stomach cancer cell strains, analyzed its DNA sequence, and studied the mechanism of cancer development in depth. This exploration which used the Ha-ras oncogene as a probe adopted molecular hybridizing methods to diagnose cancerous tumors, with certain results.

The oncogene (gene which causes cancer) is one of the important focuses of basic cancer research at present. Not only is it extremely valuable for clarifying the basic nature of malignant change, it also opens up new vistas in cancer diagnosis and treatment for now and the future. On the international level, the existence of more than ten actively viable oncogenes have been isolated or confirmed from soft tissue cancers of the bladder, lung, or colon, and from tumors in the hemopoietic system, but such reports concerned with primary carcinoma in humans have not been formally reported.

At the Shanghai Municipal Institute of Cancer Research, high-molecule DNA stain-transfer techniques used on 7,402 primary liver carcinoma and liver cancer cell strains demonstrated that the oncogene inducing malignant change in mouse cells (NIH3T3) is the human N-ras oncogene. At the same time, excessive MRNA expression of N-ras was discovered in six of nine cases of human liver cancer, and it was possible to prove, from the transformed cell, the excessive expression of the oncogene product P21. This is the first time that N-ras has been proven internationally to be the chief oncogene in human liver cancer on the DMA, MRNA, and protein levels.

The incidence of nasopharyngeal cancer is rather high in certain areas of southern China. Professor Zeng Yi [2582 3015] of the Virology Institute, Chinese Academy of Preventive Medicine, and colleagues used a sensitivity-specific method to determine the immunoglobulin A antibody for the EB (Epstein-Barr) virus, to check the blood serum of over 300,000 people around Cangwu and Wuzhou in Guangxi Province. It yielded an early diagnosis rate for nasopharyngeal cancer that exceeded 92 percent. They based their study on characteristics of the Chinese village and discovered a very simple examination technique: they simply placed drops of the blood to be examined on filter paper which was sent, after drying, by mail to the laboratory for examination. This way, patients living in areas without laboratory facilities were able to participate in a serological determination/screening test for nasopharyngeal cancer. The results of this research approach places it in the international forefront.

Scientific workers in the field of medical care in China also did not let up on their research into the prevention and treatment of some life-threatening endemic diseases. Among items that received 1986 Ministry of Public Health, Science and Technology Achievement Awards are many results culminating from research into the prevention and treatment of endemic diseases. For example,

viral hepatitis is a fairly prevalent endemic disease in China. For this reason, prevention and treatment of viral hepatitis is an important research topic in Chinese medicine. Professor Liu Chongbai [0491 1504 2672] and colleagues at the Virology Institute collaborated with related organizations and groups to conduct an extensive survey, beginning in 1979, of epidemic hepatitis among 270,000 persons nationwide. They obtained a large amount of firsthand data, and in 1985 produced the results of their research with a report entitled "Transmission and Interception of Hepatitis B Between Mother and Infant." This provided scientific data for widescale promotion and use of a henatogenous vaccine.

Under the leadership of Professors Zhu Jiming [4281 2478 2494] and Ren Guifang [0117 6311 2455], breakthroughs were also obtained in the research and experimental production of genetically engineered hepatitis B vaccine from mammalian cells.

"Research into a Hematogenous Vaccine for Hepatitis B and Its Experimental Production," a project which received a Class A Research Award from the Ministry of Public Health, was conducted by units at the Beijing Institute of Biological Products and the Ministry of Public Health during the Sixth 5-Year Plan period. This vaccine is safe and effective, and shows an antigen-positive reaction in more than 95 percent of the cases vaccinated, a successful interception rate between 80-90 percent in mother-to-infant transmission, and vaccine quality achieving that of advanced international levels. The Ministry of Public Health has decreed that the 3 million vaccine doses produced in 1987 by the related groups should be diverted first for mother-to-infant transmission cases.

As for research into the prevention and treatment of other endemic diseases such as diarrhea, Keshan disease, malaria, and filariasis, great progress has also been made.

The basic national policy for serving China is the important direction being taken by the medical sciences in China. The practice of population planning and eugenics in China has also received considerable attention and effort from medical research workers. In the past, China did not pay enough attention to this matter. In the early 80's, the number of mongoloids in China was found to be over one million, about 2-4 percent of the children born. During the last few years, noticeable progress has been made in the prevention and treatment of this hereditary disease. In 1980, Zhou Xianting [0719 2009 1656] and Sun Nianhu [1327 1819 1833] of Beijing began to use amniocentesis to obtain amniotic cells for study and determination of hereditary disease in the fetus. Later, others checked for the presence of congenital diseases such as brain deformity or spinal bifida in the fetus, as determined by the levels of alpha fetoprotein or acetylcholine in biochemical examination of the amniotic fluid. In recent years, China has been the first internationally to use examination of chorionic cells extensively to check for genetic disorders in the fetus.

Gradual Progress Toward Disease Prevention

While medical work in China adopted a policy of prevention first early on and numerous medical workers exerted much effort in this direction, the tendency has always been more attention to treatment and less to prevention, possibly because of economic conditions in China and a lag in scientific progress behind the West, whether in clinical medicine or medical research. To change this situation, the Ministry of Public Health has directed the focus of research topics to factors such as nutrition and the environment that affect human health. This includes studies in occupational diseases, smoking, and other physico-chemical factors that affect people. A project "An Epidemiological Survey of Occupation-Related Cancers in China," in which agencies such as the Institute of Hygiene and Health and the Chinese Academy of Preventive Medicine are collaborating, is one such important topic. This study has analyzed the incidence and mortality data on more than 10 types of cancer from more than 1,505,000 cases. After the survey, the possibility of occupational cancers arising after contact with an appropriate amount of certain compounds was clarified. The quality of this survey attained international levels for similar research topics.

Among projects recognized by the 1986 Science and Technology Achievement Awards from the Ministry of Public Health is a survey on pulmonary silicosis. Health workers who observed and studied coal mining conditions over a 20-year period clarified the role of dangerous occupational factors existent in the mine. These included temperature and humidity conditions in the mine, and presence of coal dust, noise, radiation, microelements etc. This has definite practical significance and theoretical value in preventing and treating many occupational diseases among coal miners.

Since 1972, He Fengsheng [0149 7685 3932], Lu Boqin [0712 0130 2953] and others at the Institute of Hygiene and Health of the Chinese Preventive Medicine Center have been conducting an in-depth systematic study of multiple neurologic diseases among workers in the chloroethylene industry from clinical, toxicolgic, and neuropathologic aspects. They discovered and proved the toxic effect of chloroethylene on the peripheral nervous system, and suggested singly arrived at opinion on the pathological characteristics of nervous system damage caused by chloroethylene. In 1984, Ho et al received the "Xi-beiang Kaguli Award" from the Labor Medical Foundation of Italy. This award was established by Italy to encourage creative research in fields of occupational medicine, physical medicine, and hygiene.

Strengthening Basic Research

Basic theoretical research has always been the weak link in China's research effort in medicine. Before this, some Chinese medical scholars made some exploratory efforts in this direction, but they did not lead to forming an organizational force. In recent years, related agencies in the Ministry of Public Health included basic research in their plans and increased manpower resources. Certain results were achieved in scientific fields such as

91

biogenetic engineering, cell engineering, molecular biology, etc. that were rarely touched in the past. The Hematology Institute of the Chinese Academy of Medical Sciences was the first in the world to discover monoclonal antibodies from T-4 cells. This achievement has been certified recently and won an award at the Third International Conference on Human Lymphocyte-Differentiating Antigens held at Oxford, England. In this experiment, mouse cells immunized by fetal T-cells and mouse myeloma cells were fused to obtain a group of six human anti-thymus monoclonal antibodies, described respectively as T-cell monoclonal antibodies 1, 2, 3, 4, 5, and 6. T-cell monoclonal antibody can be used to identify chronic lymphocytic leukemia of the T-cell typetype, a feature which makes it highly significant in diagnosis, treatment, and prognosis of the disease. T-cell monoclonal antibodies 1, 2, and 3 are important tools used to study T-cell differentiation, etiology of lymphocyte proliferation, and nature of the hemapoietic stem cell. The Hematology Institute used these monoclonal antibodies to check 76 cases of leukemia of different types, and classified 104 cases of lymphocytic leukemia epidemiologically. This clearly raises the levels of clinical diagnosis and treatment for leukemia. Moreover, T-cell monoclonal antibodies 1 and 2 can help differentiate the stages of dermo-lymphoma to make a prognosis.

At the Xinjiang Medical College located in China's border region, China's first research effort in analyzing fetal hemoglobin structure was quite successful. Furthermore, this technique was used to identify, in the umbilical cord, three Y-chain mutations which were confirmed by the International Hemoglobin Information Clearinghouse as new entities, and were named hemoglobin F urumchi, hemoglobin F xinjiang, and hemoglobin xin--su.

Fetal hemoglobin is formed from four peptide chains, of which the Y peptide chain contains 146 amino acids. A substitution in any one of these amino acids will result in an unusual fetal hemoglobin--that is, a Y-chain mutation. The technique for analyzing the structure of fetal hemoglobin is rather difficult, and the number of top laboratories worldwide engaged in such study can be counted on one's fingers. Persistence of fetal hemoglobin is a genetic problem which could lead to serious disease. Such studies greatly enrich China's hemoglobin data bank, and the information they provide is highly useful in family planning and improving the quality of national and racial traits.

Attention to Research Studies in China's Traditional Medicine

China's traditional medicine is a precious treasure house waiting to be explored. Besides the traditional medicine of the Han people, there are the traditional medicine heritages of the Tibetans, the Mongolians, and other national minorities. In the last several thousand years, China's traditional medicine has accumulated a rich amount of clinical experience for its unusual theory of medicine. This human-oriented body of knowledge dwelling on the relationship between man and his environment also emphasizes a continually evolving view of the medical theory concerned with the human mechanism and the pathological changes it experiences, which corresponds unintentionally

with modern medicine and science. At present, some diseases such as cancer, cardiovascular disease, endocrine diseases etc. that western practitioners consider difficult to treat, are treated with traditional Chinese medicine methods, which frequently are quite effective. However, many of the traditional Chinese medicine theories are quite simple and cannot be explained by the reasoning of modern science. To establish traditional Chinese medicine theory on a modern scientific footing will require much effort from scientific workers in Chinese medicine over a long period of time. However, a positive note is the fact that many Western medicine practitioners in China pay considerable attention to studying traditional medicine, and some of them have been using a combined Western and traditional Chinese medicine approach to treating disease, with good results. In many areas, the traditional Chinese medicine herbalists and workers in the natural sciences find themselves leaning toward a combined approach. The Ministry of Public Health has also emphatically encouraged collaborative research in many fields. This situation should be very beneficial to research in traditional Chinese medicine.

A more proper regard that is accorded traditional Chinese medicine at present is due largely to the collected revolutionary and counter-revolutionary experiences of the past 30 some years. In the early 50's, the central people's government encouraged the combined practice of Western and traditional Chinese medicine, but authorities at the Ministry of Public Health then emphasized Western medicine only. By requiring traditional Chinese medicine practitioners to learn from Western medicine, they were actually trying to eliminate traditional Chinese medicine. This erroneous approach was corrected later on by the central government, who required the existing 500,000 traditional Chinese medicine practitioners to take on 500,000 apprentices so that China's traditional medicine could be continued and undergo further development under the new China. Traditional Chinese medicine colleges and hospitals were established in numerous localities, and the practice of traditional Chinese medicine went forward.

However, during ten years of unrest (1966-1976), traditional Chinese medicine became one of the "Four Old's" and many practitioners were thrown into "buffalo pens." It was only after efforts of the last ten years that traditional Chinese medicine was able to pick up its pace to move forward again. In 1986, to activate developments in traditional Chinese medicine, the central government established the National Bureau of Traditional Chinese Medicine to coordinate work in traditional Chinese medicine (including scientific research). This indicates a new phase in the evolution of traditional Chinese medicine.

Tracking the World's Medical Science Advances

The general new trend for China's medical sciences and clinical medicine is to track advances in the medical sciences worldwide so our own weaknesses can be corrected. Many new medical sciences have appeared in time. For example, nuclear medicine which appeared only 40-50 years ago is making new headway in China now. At present, over 700 medical care units throughout

China are using nuclear medicine techniques to treat disease, and scientific research into its use to diagnose heart disease, cancer, brain disorders, etc. approach that of advanced international levels. The CAT scan is a new nuclear medicine visualization technique used in the 1980's for diagnostic purposes. Nuclear medicine researchers in China have also introduced this new technique for use in China now.

Because of the relationship between actual economic conditions in China and its scientific base, any effort to follow and cover the whole field of medicine worldwide, and to put into use all the new and advanced medical techniques is not possible at this time. For research to proceed in a stable and healthy manner, the Ministry of Public Health has adopted some new measures. Chen Minzhang, the Minister of Public Health, says: "I do not approve of a policy of conducting research in the medical sciences on an overall scale, but would advocate concentrating our economic and material resources to establish a complex of laboratories with the best equipment in certain locations to attract scientific personnel from inside and outside China to conduct research on focal topics. It is understood that five research bases will be established in the near future. Their gradual expansion will follow progress in economic development and a rise in the level of scientific expertise.

"Specialists think that developments in the medical sciences must correspond with developments in other medical fields as well as with the model is the same as that worldwide. However, medicine has progressed from a simple biomedical model toward a more complex bio-, psycho- and socio-medical model, that is, a biomedical model which includes psychological and socio-logic factors as part of medicine. Now that Chinese medicine is further developing, it is also in transition to an adaptation to this worldwide medical model."

5292/12851

RECENT DEVELOPMENTS IN TRADITIONAL MEDICINE OUTLINED

40081085d Hongkong LIAOWANG [OUTLOOK] OVERSEAS EDITION in Chinese No 18,
4 May 87 pp 13, 14

[Article by Wang Xiangli [3769 0078 5439]]

[Text] Since the late 1970's, traditional Chinese medicine, which has had a
long history in China, has been making great strides, whether in clinical
practice or in theoretical research. Its singularly unusual body of theory
and wealth of clinical experience are becoming the increasing focus of
medicine worldwide.

Theory and Practice of a Singularly Unusual Traditional Chinese Medicine

Where it is different from Western medicine, traditional Chinese medicine
considers the body as a whole, where the relationship between man and his
natural environment is linked in a state of continuous motion, in its
treatment of the human body and the pathological changes it encounters. Its
principles of treatment emphasize supporting the proper (increasing the
body's resistance to disease) and driving off the bad (eliminating the cause
of disease), with the chief focus on supporting the proper.

At present, diseases considered by medical specialists worldwide as
difficult to treat, e.g., cancer, cerebrocardiovascular disease, endocrine
disorders, aging, geriatric diseases, aplastic anemia, etc. have been
treated by traditional Chinese medicine with good results on many occasions.
For cases of severe chronic renal failure, besides renal dialysis and renal
transplantation, Western medicine has no effective treatment. But in the
1950's, traditional Chinese medicine came up with an effective prescription
of herbs.

The theory and clinical practice of traditional Chinese medicine go back
several thousand years in an unbroken tradition. Early during the Zhou
Dynasty (1122-247 B.C.), an official departmentalized medical care system
headed by physicians was established. At present, there are 115 libraries
within China housing over 31,000 volumes of ancient medical texts in over
13,000 categories.

The voluminous "Yellow Emperor's Classic of Internal Medicine" propounds a simple materialistic theory on yin and yang, and the five elements, and describes the causes of disease in the human body, their mechanisms of action, pathology, diagnosis, treatment and prevention, thereby building the foundation for traditional Chinese medicine theory. During the Eastern Han era in the 2nd and 3rd Century, Zhang Zhongjing [1728 0112 2529] drafted his "Treatise on Various Kinds of Fevers," which established for traditional Chinese medicine a basic therapeutic approach in concepts such as discriminative therapy and a theory of clinical medicine.

The world's oldest national pharmacopoiae was issued by China in the 7th Century during the Tang Dynasty. "The New Revised Herbal Reference" listed 850 medicinal herbs and agents. In the 16th Century, the "Pharmacopoiae" complied by Li Shizhen [2621 2514 3791] contained 1892 listings, the most comprehensive work of its kind at the time. It has been translated into more than ten languages, and is found on every continent.

New Accomplishments of China's Traditional Medicine

Ever since the open policy has been effected, not only has China not abandoned research into its traditional medicine, it has further strengthened work in this area, for the development pace of traditional Chinese medicine to be stepped up.

From 1980 on, the awards traditional medicine has received from the Ministry of Public Health for research efforts have totalled 149, of which 38 were received in 1986.

Research on an extract from the antimalarial Chinese herb Artemesia apiacea which received a National Second Class Discovery Award is a new breakthrough in the history of China's antimalaria effort. It was found to show break-through effectiveness against the chloroquine-resistant parasites of falciparum malaria. Xiaozhi Ling [3194 4023 7227], a Chinese herbal concoction for injection use, which received a National Science and Technology Progress Award, proved particularly effective for treating 3rd stage internal hemorrhoids and mixed hemorrhoids. Last year, it also won two gold medals at two international discovery/invention exhibits held in Yugoslavia and Belgium.

In areas of dermatology, oncology, gynecology, etc. traditional Chinese medicine has shown some outstanding results. For example, traditional Chinese medicine practitioner Zhou Mingci [0719 7686 1477] of Liaoning Province prepared a fish-scale concoction for treating "ichthyosis." He based his remedy on a principle of traditional medicine which theorizes that when the liver and kidneys are yin-deficient, the stomach/spleen are also weak, so that the blood becomes weak to general wind, which in turn induces dryness, thereby leading to loss of nutritional balance in the skin. The efficacy of this preparation is 93.17 percent.

96

By adhering to a policy of combined practice for Western and traditional Chinese medicine, China proceeds from objective practical conditions where both traditional Chinese medicine and Western medicine are already in China. Furthermore, their practice has always been based on the disease prevention and treatment needs of the people.

Since 1955, when the Ministry of Public Health developed the first course in traditional Chinese medicine for Western medicine practitioners, over 4,500 have been trained in traditional Chinese medicine. In recent years, research in this combined medical discipline has progressed from clinical to basic studies. At the same time that traditional Chinese medicine theory is developed, it is also making a certain contribution to modern medicine. For example, when Western and traditional Chinese medicine are used jointly to treat fractures, the theory of traditional medicine and the splint are used together with Western medicine's X-ray examination. By following the principle of "combined activity and inactivity," the time for bone healing is reduced one-third, and function is restored in one-fourth--with an effectiveness greater than either Western medicine or traditional Chinese medicine alone. Again, take acupuncture studies on the principle of pain relief, which delve into the neuron, electrophysiology and neural mediators (such as brain peptides, etc), on a molecular biology level. These studies have attracted the wide attention of neurophysiologists and neuropharmacologists.

With respect to acute serious illnesses, the present use in China of traditional Chinese medicine, alone or in combination with acupuncture, or jointly with Western medicine, has been quite satisfactory; for treating many acute infections, shock, DIC (diffusive intravascular coagulation) of various etiologies, various acute abdominal conditions, etc. The treatment efficacy for some diseases is higher than that when Western medicine alone is used. For some other diseases, the efficacy may be similar to that for Western medicine, but traditional Chinese medicine often does not have the serious side effects resulting from Western medicine. Basic research into theories on the nature of the meridians, the concept of yin and yang, circulatory stasis, "deficiencies," etc., and on the integration of singularly unusual treatment specialties also made some new strides forward.

At the same time, use of modern scientific approaches to uncover the mystery of traditional Chinese medicine also confirms the fact that research studies in Chinese medicine have begun.

Beginning this year, the Chinese Academy of Academic Sciences, the Institute of High-Energy Physics of the Chinese Academy of Sciences, and the Anhui College of Traditional Chinese Medicine are collaborating in research to study the true nature of the meridians, using nuclear medicine techniques. They have confirmed the transmission of matter and signals along meridian pathways, and found this transmission follows a set direction and speed, a phenomenon that coincides with meridian theory (arriving at the same conclusion) as described in traditional medicine writings.

Again, take acupuncture studies into the principle of acupuncture anesthesia, using strict scientific techniques such as those used in modern physiology, biochemistry, microbiology, epidemiology, and in recent years, laser needle therapy which clarified the principle of acupuncture treatment, and provided acupuncture therapy with a scientific base. Organizations for Chinese medicine also experienced development in recent years. At present, there are a total of 54 institutes of traditional Chinese medicine in China. Seven more have been completed or almost completed. More than half of all counties in China have established colleges of traditional Chinese medicine.

Worldwide "Wave of Traditional Chinese Medicine"

The influence of traditional Chinese medicine worldwide increases by the day, particularly after China declared an open policy. Because of the incidence of drug-caused illnesses and other not easily resolved ailments, many countries who were attempting to find solutions through natural remedies or non-drug therapies, placed their hopes in Chinese herbal medicines.

A joint China-Europe medical conference was held this April in France in Strasbourg. Some traditional Chinese medicine herbal specialists and representatives from many European nations explored means to further collaborate and promote the use of traditional Chinese medicine. Discussions covered the use of modern Western European techniques and China's experiences in assaying crude product quality and assessing finished product efficacy in joint efforts to produce Chinese medicinal herbs of high quality.

The United States and the USSR have also strengthened their efforts in research and application of Chinese herbal medicine.

Traditional Chinese medicine specialists have been invited abroad in scholarly exchanges and lecture tours, and the numbers of foreign scholars who come specifically to study this topic increases by the day. At present, of topics selected by foreign students studying the natural sciences in China, traditional Chinese medicine has top preference.

In recent years, the international acupuncture courses conducted in China have trained over 1,000 acupuncture specialists from over 116 nations. In October, a joint international meeting will be held in Beijing to conduct scholarly exchanges in the field of traditional Chinese medicine, and to announce the establishment of an international acupuncture association. Over 1,000 scholars representing more than 100 countries are expected to participate.

International health agencies have set up six collaborative centers in China on traditional Chinese medicine. In October 1985, at the regional conference on "The Role of Traditional Chinese Medicine in Primary Health Maintenance" called by China, more than 20 foreign countries sent representatives to the meeting.

Outlook for Developments in Traditional Chinese Medicine

In recent years, the three great miracle drugs of Western medicine--antibiotics, hormone preparations, and anti-cancer drugs--have saved numerous lives, and are given great credit for promoting human health. However, the side effects accompanying their use is the greatest deficiency. Because traditional Chinese medicine places great emphasis on natural remedies and non-drug therapies (e.g., acupuncture, breathing exercises, massage, etc.), not only is it not harmful in the treatment of disease, it can also reduce or eliminate any side effects caused by Western medications. Sometimes traditional Chinese medicine can even increase the body's immunological defenses to maintain health, strengthen the body, and delay the aging process--all of which causes it to be well received by the Chinese people. For illnesses where Western and Chinese medicine are similarly effective, Chinese medicine is frequently the medication of choice because of side effects inherent in Western medicine. Where drug therapy and non-drug therapy offer a choice, non-drug therapy is frequently the option. A few years ago, the Institute of Traditional Chinese Medicine assisted Japan in treating several patient groups suffering from ill effects caused by chloroform. Because they were able to maximize the beneficial effect of acupuncture and Chinese medicines, favorable results were obtained.

The theory of holistic balance in traditional Chinese medicine in recent years is becoming the focus of increased attention by international scientists who regard it as a form of thought of a higher order. The content of traditional Chinese medicine is very similar to that in the latest modern scientific theories, such as systematics. For example, the well-known physicist F. Karpel, one of the pioneers of modern scientific thinking said: "If the theory of Chinese medicine which regards the human body as a composite of inter-related parts in an indivisible system approximates the classical Descartes model, we might as well say it is even closer to the modern systematics model." Again, to quote the Japanese scholar Bmarugama, "Taking an organic, holistic, and balanced view of the body's internal parts, its mind and body, and its body and the environment is the true value of Chinese medicine with its several-thousand-year tradition."

In keeping with the revolutionary developments of modern science, the scientific nature of traditional Chinese medicine theory must be proven further. In other words, in-depth study and development of traditional Chinese medicine theory and Western medicine must complement each other. This, in turn, may set in motion greater advances for medicine in the future.

The capital outlay needed by traditional Chinese medicine to treat disease is much lower than that needed by Western medicine. This is acceptable, not only to Third World countries, but also for developing nations. During the early 1980's, China conducted a survey comparing health maintenance costs and social benefits of two similar cities, one in China (Shanghai environs), and one in the United States (a city in California). Results of the survey

showed that the benefits in both cities were comparable, but the health maintenance costs in China were much lower. Even when certain special factors were considered, the difference was still scores of times lower. The result of promoting traditional Chinese medicine will help realize the goal of "health care maintenance for all by the year 2000."

From what has been discussed, it can be seen that traditional Chinese medicine has great development potential, not only in China, but throughout the world.

5292/12851

NEW MINISTER OF PUBLIC HEALTH INTERVIEWED

40081085a Hongkong LIAOWANG [OUTLOOK] OVERSEAS EDITION in Chinese No 18,
4 May 87 pp 8, 9

[Article by Yang Chaoling [2799 2556 7812] and Wang Xiaoli [3769 2556 7812]]

[Excerpts] On the morning of April 22, we visited the new Minister of Public
Health Chen Minzhang [7115 2404 4545] in his office, and interviewed him on
the status of research in the medical sciences in China today and the problem
of reform in this area.

Chen, who is of medium build, is a physician with more than 20 years of
clinical experience. He graduated from the Shanghai Medical College in 1955,
and became Deputy Minister of Health in 1984, with responsibility for medical
research.

A New Picture of Scientific Research and Development in Chinese Medicine
Undergoing Reform

In discussing the present status of scientific research in Chinese medicine
today, Chen very enthusiastically declared: "Scientific research in Chinese
medicine has embarked on a stable path of development, and various important
research topics are now on a planned track. This situation is closely related
to the recognition since 1979 that the past tendency to oscillate between
left and right must be corrected." He further stated that because of the
mass approach to scientific research, propounded since 1958, which yielded few
results, and the negative attitude of the Cultural Revolution for 10 years,
the cadre of scientific research workers have been dispersed.

Minister Chen also said: "Since the 1980's, in order to stimulate the
positive nature of a large number of medical researchers, we have established
a system of recognition and awards. The state has established the Inventor's
Award and a Science and Technology Progress Award. The Ministry of Public
Health has established the Medicine and Health Achievement Awards, which
large numbers of medical and scientific researchers find quite encouraging."

Minister Chen mentioned that besides the various awards in this recognition
system, the Ministry of Public Health has further concentrated its energy on
restructuring the system of medical research in medicine. In light of causes

101

of disease that threaten the people's health, the Ministry of Public Health has called specialists in related fields together, to set down some focal topics of national concern for further study.

At the same time, the research funding mechanism also needed restructuring. Originally, research funding was appropriated and distributed evenly on the basis of research personnel head count. Beginning in 1986, 60 percent of the research funds was used on announced focal topics, and 40 percent of the money was for policy-based research. The Ministry of Public Health included publicly announced focal research topics in the Seventh 5-Year Plan, while other non-focal topics such as traditional topics studied over several decades, certain special topics such as high-altitude medicine pertaining to the high plateaus of Qinghai and Tibet, and other items of an exploratory nature were funded by policy-based appropriations.

"This does not mean we only pay attention to a few focal items and forget the others," Chen explained. "Most units emphasize the application and promotion of the fruits of research. We feel this approach is suited to national conditions in China today."

The Ministry of Public Health pays a great deal of attention to encouraging the active participation of young people in scientific research. It has designated 500,000 yuan annually as scholarships for young people, to encourage outstanding young medical research workers. At the same time, it is also encouraging local authorities to set up similar scholarships. "While such scholarships are only symbolic awards, they do affect the young people in a positive way," commented Chen.

Plans for Developing Medical Research in China

Minister Chen stated some of his plans very simply and clearly. This famous "specialist-researcher model," internationally known for a greater than 90 percent success rate with bile and pancreatic duct imaging techniques, gives considerable thought and definite plans for those problems of a macroscopic nature.

"The overall direction of medical research should go from one emphasizing treatment to one emphasizing prevention. After prevention work becomes effective, the benefits will be great and the quality of health care for the people will be greatly improved."

Minister Chen also said: "Traditional Chinese science must be fully studied. The field of traditional Chinese medicine encompasses not only traditional Chinese herbal medicine, it also includes traditional Tibetan and Mongolian medicine. These are uniquely Chinese treasures that have great promise for scientific research."

There are some new scientific research areas that need to be explored. Minister Chen said: "Our national policy is to expand scientific research to assure the health of the average population, in endeavors such as family

102

planning. This is tied in closely with economic and social development. For better family planning, we must improve prenatal and postnatal health care, and improve on genetic and immunologic studies to develop and practice eugenics for improving our national character." He continued, "Economic conditions in China at present are vastly improved over those in the past, but surveys show that the incidence of anemia among the young is quite high. That is due to an unscientific approach to childhood nutrition. In the future, we must initiate studies on nutrition and diseases caused by nutritional factors."

Statistics have shown that by the year 2000, the aging population will comprise of 11 percent of the total population. To adapt to this change in the population makeup, geriatric studies must be initiated now to fully employ the anticipated effect of scientific research.

Projects which Minister Chen feels need to be implemented are quite numerous.

"Take the number of research topics, for instance. Those having a direct application that determine the direction for all the present and the future comprise 60-70 percent, while those concerned with basic studies comprise 15-20 percent. Besides these 15 percent is allotted to exploratory topics given policy consideration. Scientific research organization structures are tied in with institutions of higher learning and hospitals, and wherever possible, no new independent scientific research organization need be built."

"Strengthening international exchanges, enriching and stimulating scientific research in Chinese medicine are quite important," Minister Chen emphasized. "Scientific research in Chinese medicine has been more active in recent years, a benefit of the open policy. When communication is good, the initial research threshhold is high. Advanced techniques from abroad are quickly grasped by research scholars we send abroad, and these techniques return with them. Furthermore, use of research equipment and protocols from abroad has also hastened fruition of some of our research results."

Imminent Difficulties and Problems

The new Minister of Public Health did not evade difficulties and problems inherent in scientific research in Chinese medicine. For example, inadequate funding, a need for medical science information specialists, and the fact that only 30 percent of the total scientific research results are being promoted and used. Scholars sent abroad and not able to learn and progress on the basis of China's needs often find what they have learned is not consistent with the nation's needs, and a paradox exists. Problems involving experimental animals, standardization and national production of testing agents also need urgent attention.

On these existing difficulties and problems, Minister Chen says, "We are actively looking for ways to solve them. As long as we devote ourselves wholeheartedly to this task, the problems can always be solved one step at a time."

5292/12851

DEVELOPMENT OF TELEVISION INDUSTRY DISCUSSED

40080049e Beijing ZHONGGUO DIANZI BAO in Chinese 31 Mar 87 p 2

[Article by Zhou Xiaobing [0719 2556 0365] and Xu Jiahua [1776 0857 5478]: "China's Television Receiver Industry Developing a Beneficial Direction"]

[Text] China's TV industry is developing in a beneficial direction. In 1986, of 60 plants designated for the manufacture of TV receivers, 20 showed profits which surpassed 10 million yuan, while 11 plants had profits of more than 20 million yuan.

In 1986, many TV receiver plants practiced the plant manager responsibility system, and all gave a prominent position to enhancement of economic benefits. In this way, they strongly developed lateral economic links, and began to emphasize revision of the economic structure.

After the Jijinxing Economic Alliance, the TJ Alliance, and the Peony Television Group, the Chinese TV industry established the Changhong Television Group and the Huanyu Export Group. With these key enterprises as the nucleus, there are now groups that cut across regional and industrial lines, completing the chain for accomplishing our goal of having TV receivers that are wholly manufactured in this country. This will improve the quality of TV sets and by linking the separate parts into a whole will further open up new routes for developing color TV sets that are wholly manufactured in China. The Guizhou Television Receiver Plant and the province's Five Metals Power Company formed the Guizhou Home Appliance Joint Company; the Hunan Television Receiver Plant adopted the stock system along with several other units, such as that province's Five Metals Power Company, the provincial Television Broadcasting Corporation, and the Changsha Power Station to form the "Hunan Shaofeng Home Electronics Management Group." This joint arrangement borke away from the existing commercial-industrial pattern of doing things separately. In such aspects as decreasing sales links, mediating merchandising channels, cutting down on the amount of warehouse space occupied, and speeding up the withdrawal of currency, etc., there have been advantages gained in varying degrees.

In 1986, many TV receiver plants began to develop a variety of types and models of products. According to incomplete statistics, because of the efforts last year to develop new products suited to the demands of the

market, the new products on the market this year include: 51 types of black-and-white TV sets in a variety of models, including ones that can be operated on AC or DC or are multifunctional; and 48 kinds of color TV sets, including double frame picture and stereo sound. There are also radio products, community antenna TV systems, cameras, electronics musical instruments, games, monitors, projectors and satellite receiving equipment.

The year 1986 was also a better year for the export of TV sets. Due to the reliablility of product quality, attractiveness of appearance, and the adoption of various kinds of and forms of trade partnerships, Chinese TV sets have received favorable comment in such overseas markets as the United States, Great Britain, Finland, Hungary, Korea, Mali and Southeast Asia. Such enterprises as the Tianjin Radio Plant, the Nanjing Radio Plant and the Suzhou Television Plant have become the foundation for the nation's export of electromechanical products.

According to survey data furnished by the Chinese Television Industry Association's Economic Information Center, four enterprises in the TV industry are still operating at a deficit, and many are still low in their economic benefits, however a greater many still have the potential to increase these benefits. Therefore, future efforts should go in the following several directions:

--Above all, expenditur and waste should be cut. In 1986 there was an obvious increase in expenditure; for example, in regard to the 44-cm, black-and-white, all-channel, integrated circuit, imported kinescope TV set: last year, the industrywide outlay for workshop and enterprise management averaged 38.1 yuan per set. This was 49.71 percent higher than the year before, and represented an industrywide total increase for the year of 16.66 million yuan. In addition, the losses in waste material for the same set last year averaged 1.73 yuan per set, a 32.1 percent increase over 1985, and an industrywide total expenditure of 55.3 million yuan for the entire year. The prospects for economizing on expenditures are obvious.

--Various channels should be opened for supplying funds, and their circulation should be speeded up. Last year the shortest period of time for circulation of funds in the TV industry was 52 days. In large-scale Shanghai No 18 Radio Plant, Shanghai No 4 Radio Plant, and medium-scale Shanghai No 11 Television Plant, a higher standard of management was reflected not only in the value of output and profits, but also in use of funds. It would be worthwhile to summarize and draw upon the lessons of their experience.

--There should be active circulation between localities. In 1986 sales of black-and-white TV sets slumped for a time, with a sales rate of only 85.01 percent for the first half of the year's manufacturing output. Moreover, in the enterprises a top-quality system should be developed for providing good marketing according to the needs of the market, developing sales, maintenance, training and service. After vigorously opening the rural markets, the production and sales rate for output at the end of the year had increased to 140.66 percent, with the average for the entire year amounting to 94.43 percent. This year there are still some good prospects for opening up the rural markets.

12625/9835

ELECTRONICS RESEARCH TO SERVE TECHNOLOGICAL TRANSFORMATION

40080049d Beijing ZHONGGUO DIANZI BAO in Chinese 31 Mar 87 p 1

[Article by Shen Yao [3947 3852]: "The Major Battlefields For Electronics Research Lie in Serving the Technological Transformation of Engineering and Traditional Industries"]

[Text] During the period of the Seventh 5-Year Plan, as China's electronics industry develops, the Ministry of Electronics Industry will concentrate the majority of its research strength on two major battlefields; in those major engineering topics and traditional industries which are of decided significance for the national economy, it will serve to carry out technological transformation. This was proposed at the conclusion of the ministry's 23 March working conference on electronics industry technology.

The first major battlefield lies in the important engineering fields such as computers, integrated circuits and communications. Tackling these key engineering technologies, shaping them into a complete whole and forming a regulated economy, electronics research will take a leadership role in our national economy at a very early stage, and will exert a decisive influence. In these newly emerging technological fields, leading high technology industries will certainly be formed through research and development. These are the new heights that China's current electronics industry must scale.

The second major battlefield lies in serving the technological progress of new fields for the national economy. It is characterized by research and development comprised of the entire process of design, manufacture and application of products, as well as opening up markets for them. The key today is the selection of correct policies and strong measures to transfer as quickly as possible the existing military-industrial research system to the system of technological transformation of traditional industries.

In addition, due to the output value of color TV receivers and their compatible parts, these constitute approximately one-third of the total output value of the electronics industry. This then is the mainstream product of the entire electronics industry, as well as the mainstream product of our foreign trade. So there also should be a strengthening here, with a certain amount of research results put into it.

106

Deployment of research teams in the electronics industry's development battlefields means that research and development work will for a time be lodged in industrial development. Various categories of research institutes can find their own place on these two major battlefields, and in this way make their own contributions.

12625/9835

WAYS TO EXPAND MARKETS FOR ELECTRONIC PRODUCTS EXAMINED

40084009g Beijing ZHONGGUO DIANZI BAO in Chinese 5 Apr 87 p 1

[Article by Wang Dianfu [3769 3013 3940] of the Beijing Broadcast Equipment Plant: "An Inquiry Into Several Ways To Open Up Markets for Investment Class Electronic Products"]

[Text] Opening up markets for investment class electronic products is an urgent task facing the electronics industry. Although the task is enormously difficult, the prospects are extremely attractive.

By the end of 1985, China had imported $270 million in medical electronic equipment and more than $400 million in cameras and video recording equipment for commercial use. This latter figure does not include video recorders imported for home use. The amount of electronic equipment imported by other industrial departments was also considerable. This demonstrates that the domestic market capacity for investment class electronic products is very large. Based on our experiences over several years at the Beijing Broadcast Equipment Plant, I intend here to offer my opinions on ways of opening up the market for investment class electronics.

1. Organize sales units throughout the entire industry; listen earnestly and sincerely to consumers' views; help consumers to fulfill their plans.

There is a fundamental difference between investment class products and consumer class products: those units that manufacture and use investment class products basically are publicly owned. So these usually come under a 5-year plan and a medium- or short-term program. To satisfy the needs of development plans of this sort for the units that will use the products generally requires that three conditions be fulfilled: first, we must explain to the consumer the level of electronic products, both foreign and domestic, and our program, while making service the guiding principle; second, we must understand the consumer's manufacturing situation, problems and plans, while listening to his views; third, we must conduct joint research on how to select the best equipment while economizing on investment, helping the units that will use the product to accomplish their development plans. Making contacts of this sort can often product unexpected results. For example, we held a service meeting in one province which brought more than 17 million yuan in orders.

2. Organize complete production and supply for total service to the consumer.

The second characteristic of the development of investment class products
is that the consumer demands total service, which is often a systematic
process. Therefore, we must organize for systematic design, production,
compatibility, installation and debugging. It is very difficult for one
plant alone to fulfill consumer demands. Therefore over the past several
years we have organized three types of joint operations: the first is for
antenna cable and parts that are compatible with transmitters; the second is
for monitoring instruments and central apparatuses that are compatible with
transmitters; the third is a plant for small-scale compatible spare parts.
These joint efforts which focus on the whole transmitter are very practical,
with each plant voluntarily engaged in mutual benefit, and planning for the
long term. Uniting for joint progress in this way is a group company. The
consumer is totally satisfied with the systematic compatibility and the full
service. This also makes for a superior electronic industry.

3. Organizing first-rate technical service is the key to opening up
markets for investment class electronic products.

The three characteristics of investment class electronic products are: the
technology is complex; the technology is concentrated, so the consumer does
not grasp it readily; and a high degree of equipment reliability is called
for. So, if a problem should arise, it can have a major effect. Therefore
it is essential that in marketing, there be a good service system from first
to last. This is done chiefly by accomplishing two things. First, prior to
the sale there should be consultation with the consumer, so that the system
design; definitely will assure systematic stability and reliability. Second,
the technical personnel should be trained for the consumer, and especially
the key technical staff: these should definitely be brought to the manu-
facturing plant to participate in equipment debugging, so that in the case
of routine breakdowns they can carry out their own repairs. Over the last
6 years, out plant has trained over 50,000 technical applications personnel
from throughout the nation. Third, complete technical manuals and informa-
tion should be provided on applications safety, as well as product instruc-
tional literature and a variety of special teaching materials. Fourth,
spare parts for maintenance should be supplied: emergency parts and
medium- and long-term parts, assuring the consumer of emergency, medium-
and long-term maintenance. Fifth, installation, debugging and periodic
maintenance checks should be explained so that the equipment can always
be maintained in good condition, and a system should be established for
quality exchange.

4. Apply the value process for consumer service.

The fourth characteristic of investment class products is that the focus
must be on their benefits to society. Above all, product quality must be
at a high level. The consumers of the 1980's demand 1980's-standard
products; if we continue to give them 1960's or 1970's service, it will
be very hard to gain consumer acceptance. Today, it is necessary to go to
high-level products, guided by the market, revising the product structure and

developing new products, so that the products will satisfy the requirements of the society, "suiting the needs of the market." Doing this will bring good results. During the period of the Sixth 5-Year Plan, out plant developed and mass-produced metric wave band (channels 1-12) color TV transmitters and relay transmitters. The electronic performance of these products was up to the international standard of the time for similar products, so they were the choice of consumers. We installed 2,000 sets of equipment nationally. Other than a foreign part which we had to purchase, the equipment was totally Chinese-manufactured, and consumers were pleased.

Second, the total cost of the product should be kept low in order to save the consumer as much money as possible. Not only should the manufacturing costs be held down and the product competitively priced, but special attention should be given to keeping the consumer's maintenance costs as low as possible in the course of using the product, by making the product simple, reliable, and convenient to service. The consistent reliability of products is a key problem with regard to current electronic products which must be solved. When this problem is resolved, consumers will be reassured and will use our products without hesitation.

Third, the technical service must be of a high standard. Service must be rendered promptly and satisfactorily; the consumer's concerns and thinking must be shared.

All of China's applications units speak often of practicality. As long as we can really carry out the above three points, there is no need to "give dinners or send gifts," because the consumer will show a definite preference for our products, enabling us not only to seize the domestic market, but to penetrate the international market as well.

5. Spread out from a point to an area, expanding from one breakthrough to an entire area. This is the best way of developing investment class electronic products.

Besides being technologically concentrated, investment class electronic products require a considerable one-time investment, and consumers have misgivings about electronic products manufactured in China. Therefore, in developing investment class products, it is best to put the initial emphasis on testing, joining with the consumer to build cooperatively. After successful testing, on-site conferences to which the consumers are invited should be held in order to familiarize them with the products and provide experience in using the products. This is the best "advertisement" of all.

In 1980, Heilongjiang's Television Department retained us to test its county-operated TV station. The Nenjiang county leadership assumed personal responsibility for raising the necessary funds, in the amount of 600,000 yuan. Our plant was responsible for the installation and debugging of the entire system's equipment while concurrently training the county's technical force. In less than half a year, we had set up China first county-operated 1 kW TV station. This color station officially went on the air on 13 May 1980, and when the people of the great northern wilderness saw the color, it created

a sensation throughout the county. The common people reacted to it with drums, goings and firecrackers. As they happily expressed it, "Like the thousand-year-old iron tree bursting into blossom, Beijing television has come to our homes." This experience with Nenjiang county's TV station told us three things. First, a county can not only run a TV station, but can do it well once the "mystery" is taken out of it. Second, after the county was operating the station, 70 percent of all the people in the county could watch TV, and in less than 3 months the countywide sales of TV sets totaled more than 11,000, with business profits of more than 700,000 yuan. Third, and even more important, through TV the people of the county can now watch news from the central authorities, as well as entertainment programs and they can acquire culture. TV has become a modernized tool for establishing a spirit of civilization among the people of frontier areas. Consequently, we held more than 80 on-site meetings in Nenjiang with other Heilongjiang counties, disseminating the experiences of Nenjiang. By 1983, TV coverage in Heilongjiang had expanded from 16 to 80 percent, and the number of TV sets had grown from 200,000 to 2 million. One billion yuan in currency reverted to the nation, and our plant recorded 10 million yuan in sales of transmitting equipment.

After Heilongjiang's experiences were known throughout the nation, national TV coverage grew from 30 percent to 69 percent during the final year of the Sixth 5-Year Plan. Thus, it is essential in the development of investment class electronic products to expend time on all aspects, because a breakthrough in one aspect can bring many more along with it.

12625/9835

DEVELOPMENT OF LANZHOU ELECTRONICS INSTITUTE DESCRIBED

40080049f Beijing ZHONGGUO DIANZI BAO in Chinese 31 Mar 87 p 2

[Article by Tian Jingying [3944 7231 3841] and Zheng Shilong [6774 0013 7127]: "An Inspiring 'Mini' Institute--Notes on the Lanzhou Weixing Electronics Technology Research Institute"]

[Text] Everyone says that the vast northwest is lacking in manpower, but in actuality, a "sleeping giant" is often at its side. The question has been how best to mobilize electronic research personnel, creating the conditions that will put their talents to best use. Recently, these reporters paid a visit to Lanzhou's Weixing Electronics Technology Research Institute, which is situated beneath Mount Nielan in that beautiful region south of Lanzhou beside the Mount Yushan Park. We learned quite a bit from this.

Nourishing the Seedlings From Strong Roots

This institute's predecessor was the Lanzhou Radio Plant's Satellite TV Receiver Development Group. When it was founded, it had only four people on its staff. It is a collective unit, responsible for its own fund-raising and its own profits and losses. In 1983, when China's TV education was still not too well developed, the Development Group undertook a market survey, which forecast that there were vast prospects for the development of satellite TV technology. Working with simple and crude plant equipment and a shortage of funds, they developed an I-wave band satellite TV receiver, and after obtaining initial results, carried on from there. Continuing, they accepted the mission of developing a K-wave band satellite TV receiver from the provincial S&T commission. In 1984, it took only half a year to finish a prototype for trial manufacture. In the intense heat of summer, the development group led by Wang Tiantai [3769 1131 1132], Xu Damin [6079 1129 3046] and Sun Boyuan [1327 0590 3220], set out from Lanzhou and headed straight for Fuzhou to conduct an on-site test. In the end, they successfully received the "Lily Blossom" program broadcast by satellite from Japan. In the group's appraisal of the on-site receiving test, the conclusion was that in regard to the picture received, background noise, clarity and color saturation, results were on the average up to those of color TV sets in China's major cities. The picture was evaluated as being of grade 3.5. For a very small research institute from the frontier regions, where "generals" are few and "soldiers" scattered, to succeed in accomplishment of something close to the national standard was considered incredible!

In 1985, just as the developmental group was preparing to climb to even higher goals, a cutback in research funding confronted them with a deteriorating situation. It was just at this time that the central government announced the decision to reform the S&T system. Wang Tiantai and several other comrades talked it over and made plans to assume responsibility for their own fund-raising and their own profits and losses, and they applied to contract as an integrated research unit. This approach was supported by the leadership of their provincial and municipal science commissions. These bodies decided to lend material support, and they also extended to the group preferential treatment in the form of a 3-year tax exemption. So, in May 1985, the Lanzhou Weixing Electronic Technology Research Institute was born, the first integrated research unit in Gansu. After this four-person "mini-institute" was set up, it very quickly completed developmental work on the K-wave band (12 GHz) satellite TV receiver, and constructed a functional K-wave band satellite ground station for the Fujian Television University. Moving on, they imported from Canda's Mai Kang [phonetic] Corporation C-wave band satellite TV receiver technology which they matched with a 3 meter antenna to successfully receive programs from the Central Television Station transmitted via international satellite. Moreover, they assumed a position of competitive superiority in both technological and economical quotas. Today, many units in Xinjiang, Qinghai, Gansu and Xian are placing orders with them. At the same time, this "mini-institute" has gradually begun to develop.

"Handyman" and "Point Man"

This institute has a strong capacity for handling emergency situations, and can respond promptly according to market needs. When selecting research topics it pays close attention to the close links between research and production. It has been using the management tactic of filling in the "cracks" by taking on those research projects characterized by small-batch production, an urgent deadline, a high degree of difficulty, and that some large units do not want. In this regard, it is starting to function as a "handyman." For example, in June 1985 the Shanghai Jinshan Petrification Plant was in urgent need of electronic equipment for extracting salt; the plant sent someone to the institute especially to request that the institute assume responsibility for development. In only 3 months, the institute had successfully developed and delivered what was wanted. In addition, it improved the engineering for the Loyang Oil Refinery and the Panjin Asphalt Plant, and supplied salt extraction equipment for such key national companies as the Liaoyang Refinery and the Nanjing Yangzi Ethylene Plant. Today, it is developing a third generation of micro controls, to solve a pressing need for large enterprises. This will also raise the institute's technological level to a new height.

Unity Strengthens a Dominant Position

Taking the route of unity has given the institute more competitive strength, not only allowing it to evade the frontal assaults of the large enterprises, but also giving this small institute exuberant vitality.

113

In the work of developing a satellite ground station, the institute lacked the processing capability to manufacture antennas. It reached an agreement with the Xian Aircraft Company to jointly manufacture the entire system. In manufacturing, it had difficulty in making the housing, so combined with the Lanzhou Oil Pump and Accessory Plant. This gradually changed this tiny institute from the status of "leaning against a big tree enjoying the cool shade," to an opposite position of dominance. Recently, it also concluded agreements with the Ministry of Railways Design Academy No 1 for joint development of microinstruments; with the Lanzhou Petrifaction Institute for development of equipment used in electrostatic dust removal and salt extraction; and with the British Development Corporation in Hong Kong for joint development of electronic equipment, seizing the initiative in product development.

Today, the Weixing Electronics Research Institute is starting to expand, with a current total annual output value of 550,000 yuan, and profits of 250,000 yuan. It not only declined to take even 1 fen of the nation's money, but each person has annually turned over 1,000 yuan in management expenses to the original organization. The institute's staff not only enjoys a salary equal to that of personnel of equal rank nationally, but each person can also rise to the next class in salary.

The institute's development growth has been a "mini" inspiration for electronics research units throughout the northwest region, as it has accumulated some useful experience that can be "produced, assembled and applied."

12625/9835

NEW INFRARED IMAGING DEVICES SUCCESSFULLY EVALUATED

40080049b Beijing DIANZI SHICHANG in Chinese 26 Mar 87 p 1

[Article by Yu Ruming [0151 3067 2494]: "Monolithic Infrared Charge-Coupled Imaging Device Fills a National Gap; Two New Products From the Ministry of Electronic Industry's No 44 Institute Passes Department-Level Evaluation"]

[Text] The Ministry of Electronic Industry's No 44 Research Institute has developed the model GZ313 monolithic chip 3-to-5 micrometer, 64 bit PSi Schottky barrier diode infrared charge-coupled imaging device; the GT322 model all-metallic coupled, sealed, InGaAs, surface PIN optoelectronic diode recently passed departmental level evaluation.

The GZ313 has important applications in the fields of remote sensing from space, infrared guidance systems, early-warning detectors, medicine and public health, night vision, prospecting, forest resources, etc. This monolithic chip, 3-to-5 micrometer, 64 bit, PSi Schottky barrier diode infrared charge-coupled imaging device has the best prospects of all the new infrared and middle infrared devices. It has a rational design and advanced composition. This device uses a 64 Schottky barrier diode display, multi-channel infrared detector and charge-coupled multicircuit transmission apparatus, which is employed with large-scale integrated circuit technology. It is completed with an infrared imaging detector, a signal integrator and automatic scanning function. The entire unit's 64 analog sampling signals, starting from the same point on a surface, diffuse throughout the diode sensor output, overcoming those difficulties that the cold-type of multi-channel infrared detectors have problems with. In representative random sample checks, the device's parameters have been consistently good: its heterogeneous distribution, response rate, degree of detection and scanning area in general are all up to the international standard for the start of the 1980's. Appraisal has shown that its successful development has been a major breakthough in China's development of a new generation of infrared detectors. It fills a gap in this country, and may have important further applications for national defense and national economic construction.

At the same time, the GT322 model metallic InGaAs/PSi surface PIN opto-electronic diode which has been evaluated is for use in long wavelength,

115

large capacity, fiber optical communications detection, high-speed light pulse measurements and optical signal optoelectronic transformers. This new type of instrument uses surface passivation, increased permeable film [6631 5229] and represents the first use in this country of all-metallic, coupled, sealing technology. The product's chief parameters are comparable to the 1985 laboratory standard of the U.S. Bell Labs and Japan's Fujitsu. China has realized satisfactory results when the fiber optical communications system was used three or four times.

12625/9835

CHANGJIANG COMPUTER COMPANY FOUNDED IN SHANGHAI

40080049c Beijing ZHONGGUO DIANZI BAO in Chinese 3 Apr 87 p 1

[Article by Lao Chengxin [0525 6134 0207] and Wang Longji [3769 7893 1015]: "Changjian Computer Company Founded at Shanghai"]

[Text] The Changjiang Computer Company was officially founded in Shanghai on 23 March. In compliance with the reform of the economic system, it was founded in order to revise the structure of the computer industry, accelerate the use of electronic computer technology to transform traditional industries, and advance the orderly development of the computer industry and its product structure. The new corporation will be based on the Shanghai computer and electronic industries, and will be supported by the Shanghai Economic Zone. The Changjiang Computer (Group) Company will cut across localities and businesses, and will have as its principle nucleus nine enterprise units, including the Ministry of Electronic Industry's No 32 Research Institute and the Shanghai Computer Plant. Inall, it will join together 47 enterprise units and major academic institutions related to eight businesses in Shanghai and the provinces of Jiangsu, Zhejiang, Anhui and Hunan.

Its combined staff will be in excess of 41,000, of whom 12,000 will be S&T personnel. Through technical superiority, it will develop research and production, production and application, and will build the group into an intensified, fundamental and regulated base for the computer industry.

The Changjiang Computer (Group) Company will implement a comprehensive management responsibility system under the leadership of a board of directors. It will be an economic entity with independent management and accounting, as well as sole responsibility for its profits and losses, giving it legal entity status. For the principle units involved and the products which they will cooperatively develop and manage, it will carry out unified planning, development, distribution and accounting.

The group will fill an applications gap by serving the technological transformation and progress of traditional industry. Making wider use of the application system, it will develop the computer and information industries by advancing the evolution and development of chief products and giving impetus to the software, systems and manpower training cycle. By developing

the separate stages of research, development, production, application, marketing and service, it will advance the development of reputable products.

The group has already taken the first steps toward the evolution of a computer industry base. It has imported products and technology, and has organized production lines for microcomputers single-circuit regulators, Winchester disk and floppy disk drives, and multilevel print plates. It has developed the 8030 and 8060 intermediate-type computers, the Donghai series of micro- computers, and the DJK series industrial control computers, and corresponding peripheral equipment. These have been widely applied to control functions in posts and telecommunications, railways, banking and manufacturing processes, with excellent economic benefits. On the base they have now, the group will concentrate the strengths of each member to maximize the group's superiority, and by means of the application system it will spur the development and manufacture of major products. On the eve of the group's founding, each member unit drew up group goals for the short term, with specific projects for development. They then held serious discussions on these projects in order to clarify the division of labor and set the specifics for implementa- tion. This was an encouraging step forward in the establishment and develop- ment of the group.

12625/9835

BRIEFS

8060 INTERMEDIATE-TYPE COMPUTER--There has been another major breakthrough in China's computer science research. An 8060 intermediate type computer system with even greater capabilities has been developed successfully in Shanghai, and has undergone national level evaluation in that city. The 8060 computer system is compatible with international mainstream computers, and can work with IBM 4300 system software and the various kinds of program products that it controls. It can also be utilized in communications networks, has Chinese character capabilities, etc. The system was designed and developed by the Ministry of Electronic Industries No 32 Research Institute. It took 3 years of effort, and is based on imported technology and adoption of compatible technology and efforts. The 8060 computer system is an important development, as it includes a mainframe system, comparable systems' software and communications networks. This gives the system a higher technological level for numerous products and practical applications. [By Lao Changxin [0525 6134 0207]] [Text] [40080049a Beijing DIANZI SHICHANG in Chinese 26 Mar 87 p 1] 12625/9835

END

119